Fall 2023 InSAR Survey of Ground Displacement and Subsidence Monitoring Report

Sulphur Mines Salt Dome

ANNUAL SURVEY

Prepared for:

Westlake US 2, LLC

Prepared by:

Lonquist & Co., LLC
12912 Hill Country Blvd. / Suite F-200
Austin, TX 78738

Louisiana Firm License Number EF-5937

April 2024

Fall 2023 InSAR Survey of Ground Displacement and Subsidence Monitoring Report

Sulphur Mines Salt Dome

ANNUAL SURVEY

CERTIFIED BY:
Lonquist & Co., LLC
Louisiana Registration No. EF5937

Teresa H. Rougon, P.G.

Date Signed: April 30, 2024
Baton Rouge, LA

Teresa H. Rougon, P.G.
Principal Geologist
Louisiana License No. 330

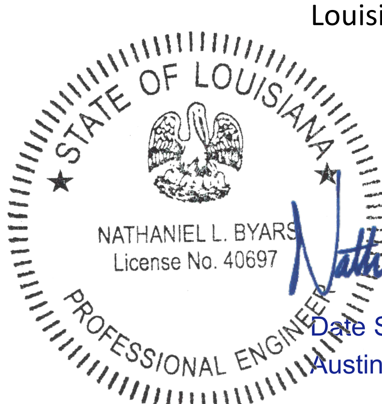

Nathaniel L. Byars

Date Signed: April 30, 2024
Austin, TX

Nathaniel L. Byars, P.E.
Principal Engineer
Louisiana License No. 40697

Executive Summary

Lonquist and Co., LLC ("Lonquist") was contracted by the three (3) operators at the Sulphur Mines Salt Dome to prepare a subsidence monitoring plan that utilizes InSAR (Interferometric Synthetic Aperture Radar) data to detect ground displacement. TRE Altamira ("TREA") was contracted by Lonquist to collect, process, and analyze the data across the dome and surrounding area. Upon completion of the InSAR subsidence analysis by TREA, Lonquist is providing the Louisiana Department of Natural Resources ("LA DNR"), Injection Mining Division ("IMD"), with a detailed review of the reported data and a supplementary evaluation of the subsidence trends that have been observed over the dome.

Statewide Order 29-M-3 and Statewide Order 29-M (Rev. 3), require that both brine mining operators and hydrocarbon storage operators conduct subsidence monitoring surveys on an annual basis during the same period. Monitoring at Sulphur Mines is carried out in the fall of each year. The analysis performed by TREA serves as the Fall 2023 subsidence survey for the dome.

The evaluation discussed herein details ground displacement measurements as captured from two satellite orbits over the time spans of October 2016 - December 2023 and January 2023 - December 2023, respectively. True vertical displacement and east-west displacement were identified via triangulation of the two satellite datasets during the January 2023 - December 2023 timeframe when data was collected from both satellite orbits.

The methodology of subsidence evaluation follows guidance provided by the IMD in 2019 for estimation of subsidence rate trends and apparent rate changes for survey monuments over the dome. The charts provided within this report illustrate the historical ground displacement and subsidence trends within areas of interest (AOIs) in lieu of survey monument locations. The contour maps generated from this data depict the spatial distribution and present condition of vertical and east-west ground displacement across the dome.

<u>No anomalous subsidence trends or regions have been identified in the Fall 2023 survey.</u> This indicates that rates of cavern closure and other factors of influence are continuing to act in a consistent manner at this time.

As the second annual survey performed with InSAR data, this report is also intended to provide evaluation and clarification of the following: 1) Discussion of InSAR technology and modifications to the subsidence evaluation methodology over the dome, 2) Comparison of current and prior annual subsidence rates indicated by InSAR, 3) Review of the 7-year 1-D SNT dataset to confirm historical rate consistency, and 4) Identification of 2-D data gaps over caverns and supplementary evaluation of 1-D data in those areas.

Table of Contents

APPENDICES

Acronyms and Abbreviations

1-D	1-Dimensional - Line of Site
2-D	2-Dimensional – Vertical and East-West
AOI	Area of Interest
IMD	Injection and Mining Division
InSAR	Interferometric Synthetic Aperture Radar
LA DNR	Louisiana Department of Natural Resources
LOS	Line of Sight
SNT	Sentinel 1 Satellite
SPR	Strategic Petroleum Reserve
TREA	TRE-Altamira
TSX	TerraSAR-X Satellite
TSX/PAZ	TerraSAR-X and PAZ Satellite Constellation

1.0 Background

Salt caverns are created through a process called solution mining. This is achieved by drilling into a salt formation and circulating water into the drilled hole to dissolve the salt. This process forms a brine-filled cavern within the salt body. Salt caverns can then be used to store various fluids such as natural gas and refined hydrocarbon products. Salt domes have been known to experience deformation due to gradual closure of the mined spaces within the salt formation or other geological processes related to the salt and overlying caprock. The gradual closure of cavern space is formally known as salt creep and stops only when the cavern has reached a geostatic equilibrium with the surrounding rock. Factors such as cavern depth, ground temperature, salt properties, regional stresses, overburden density, operating pressures, and the geometry of and proximity to neighboring caverns affect the magnitude of salt creep.

Due to salt creep, the overburden rock layers begin to move downward towards the caverns. This can be seen on the surface as subsidence (or ground displacement) vertically and to a lesser extent horizontally toward the center of the subsidence basin. Consequently, it is anticipated that surface subsidence will transpire over all solution-mined caverns in domal and bedded salt to varying extents. The vertical displacement rate over a solution-mined cavern generally ranges from less than ¼ inch annually to several inches per year. Pursuant to the provisions of Statewide Order 29-M (LAC 43: XVII. Subpart 3) and Statewide Order 29-M-3 (LAC 43: XVII. Subpart 5), subsidence must be measured annually over all solution-mining and storage caverns.

1.1 Monitoring History

Subsidence monitoring over salt caverns allows operators and regulators to prepare for and respond to potential stability issues in a proactive manner. Monitoring of surface elevations has been undertaken for a number of years by individual companies operating on the Sulphur Mines Salt Dome. The data provided to Lonquist & Co., LLC ("Lonquist") indicates level surveying for subsidence monitoring was initiated in 1993 by Westlake US 2, LLC ("Westlake") (formerly Eagle US 2, LLC and PPG Ind., Inc. – Ind. Chem. Div.) and was generally conducted on a two-year basis. These elevation surveys were conducted internally by a PPG staff surveyor. In addition to the surveys being performed by Westlake, surveys were also conducted by American Surveyors, LLC, on behalf of Liberty Gas Storage, LLC ("Liberty") and Boardwalk Louisiana Midstream, LLC ("Boardwalk").

In 2015, an agreement was reached between all three (3) operators to conduct a coordinated precision level survey across the Sulphur Mines Salt Dome utilizing a common set of benchmarks and monuments. Hydro Consultants, Inc. ("Hydro Consultants"), a professional land surveying company, was subcontracted by Lonquist to conduct the survey. A survey plan was created, and a set of benchmarks and monitoring stations were selected to be surveyed. Level surveys were performed in accordance with this plan through the Fall 2021 survey. Following that survey, the decision was made to transition to InSAR subsidence monitoring for the next annual survey in Fall 2022 and subsequent surveys going forward.

Since the coordinated monitoring effort began in 2015, continual and relatively consistent ground displacement has been observed. The greatest subsidence rates have been identified over the central portion of the dome with a gradual tapering toward the dome flank.

1.2 Sulfur Extraction

Although the current monitoring program is affiliated with cavern operations on the dome, the primary source of subsidence has been attributed to past sulfur extraction from the overlying caprock. Between 1902 and 1924, the caprock was heavily drilled and molten sulfur was mined through wellbores resulting in a total production of 10.5 million US tons of sulfur. This tonnage equates to 28 million barrels or 3,600 acre-feet of extracted volume. Over the approximately 75 acres of caprock extent, an average 48-foot thickness of sulfur is estimated to have been removed. By the time mining was completed in the late 1920's, the collapse of voids left by the sulfur extraction had resulted in subsidence in excess of 20 feet. This led to the creation of a lake extending across the mined area, surrounding the present-day salt cavern locations.

Subsidence continued at lesser rates over the following century and large sections of the lake were backfilled to support infrastructure and well pads. Dredging of the surrounding area to provide fill material is what led to the creation of the large lakes that surround the site. A study performed in 1965 comparing data from wells drilled before and after the sulfur mining operations, resulted in the development of a caprock collapse map identifying changes in caprock thickness below ground. Large collapses up to 163 feet were identified in some places, but most values ranged between 25 and 50 feet across the mined area.

In a 1980 study commissioned by the Strategic Petroleum Reserve ("SPR"), subsidence was estimated from level survey data to be occurring at an average rate of about 1.2 inches/year above the existing SPR cavern locations (PPG Nos. 2, 4, 5, 6, and 7). The study noted that this rate of subsidence had been occurring for some time and was likely to continue into the foreseeable future. These subsidence rates agree with current survey data, indicating that the trend has remained consistent to present day. The study concluded that subsidence over the dome was the result of the following factors: 1)

Continual closure of caprock voids from the past sulfur mining, 2) Consolidation of soils used to fill subsided regions, and 3) Natural dissolution of evaporite layers and collapse of preexisting voids from groundwater flow within the caprock.[1] Although not acknowledged as a factor in the report, creep closure in the Sulphur Mines salt caverns may have been contributing in some degree to the rates of observed subsidence.

1.3 Westlake US 2, LLC

Westlake US 2, LLC operates only Class III Solution-Mining caverns which are regulated by SWO 29-M-3. The statutory compliance requirements found therein mandate that Westlake perform an annual survey as part of the ongoing monitoring program established at the dome. The InSAR survey and this supplementary evaluation report are being submitted to fulfill the annual monitoring effort for the Fall of 2023.

2.0 Fall 2023 InSAR Survey

Beginning with the Fall 2022 subsidence evaluation, the decision was made to employ an alternative survey method known as Interferometric Synthetic Aperture Radar, or "InSAR". This method of data collection relies on satellite-based ground displacement readings calculated from radar imagery. Compared to traditional level surveys, data resolution is improved both spatially and temporally, allowing for the analysis of thousands of ground locations on regular, multi-day intervals. InSAR is a high-accuracy, remote sensing technology that effectively provides an updated level survey of a target area with each successive pass of an orbiting satellite. Spatial density of the measurement points varies, but in areas of non-vegetated ground cover, a substantial number of ground targets can be surveyed on a regular basis. The Fall 2023 survey is the second annual survey to employ InSAR data for subsidence monitoring.

TRE-Altamira ("TREA"), a global leader in InSAR ground displacement monitoring, was contracted by Lonquist to collect, process, and analyze ground displacement data over the Sulphur Mines site. TREA utilizes an advanced, proprietary form of InSAR data processing that tracks ground movement by analyzing a stack of radar images collected over time. This technology, termed "SqueeSAR®", provides a collection of spatially distributed measurement points that each contain a time series of ground deformation measurements reported to a 0.1 mm (0.004 inch) scale. Measurement accuracy is on par with traditional rod and level surveys in terms of error range with vertical displacement rate precision being estimated at ±0.02 in/yr. The analysis report prepared by TREA has

[1] **Whiting, G H. 1980.** "Strategic Petroleum Reserve (SPR) geological site characterization report, Sulphur Mines Salt Dome: Section I, Section II, and Section III". United States.

been provided for reference as Appendix E. The report contains a general description of subsidence related observations over the analysis area as well as a detailed description of the InSAR monitoring system and data processing method.

2.1 Data Properties

Imagery collected via satellites over successive orbital passes is used to identify and define measurement points on the ground. Objects or ground features providing a stable reflection of radar energy such as buildings, roads, and infrastructure produce the highest quality of measurement points. Measurement points can be generated in some areas with vegetation, but data quality is affected by changing ground characteristics over time, leading to data gaps in areas with dense vegetation, farming or wetlands. In the absence of stable reflectors, additional datapoints can sometimes be generated in areas with lower but homogenous signal return by averaging groups of readings into a single measurement point.

InSAR uses phase and amplitude in the radar signal images to measure the distance between the satellite sensor and the measurement points on the ground. The data generated from the InSAR technique results in a time series of displacement values at each measurement point. These displacement values are reported in relation to the original distance measured for each point in the dataset.

When a measurement point on the ground moves, whether that be vertically or laterally, the phase value detected by the sensor on the satellite is impacted due to a change in the distance between the sensor and ground target. Displacement values generated in this way are referred to as 1-D Line-of-sight (“LOS”) measurements, referring to the line-of-sight of the satellite to the ground target. Data collected in this manner is understood to convey a movement distance that is not purely vertical. This distinction only affects the assignment of a precise direction to the movement identified. As the primary component of the observed displacement is often vertical, InSAR analyses based on 1-D data are regularly used to identify and monitor the consistency of movement trends related to ground subsidence.

If precise delineation of vertical movement is required, datasets from a pair of satellite orbits can be utilized to calculate the vertical component of ground displacement via triangulation. Data generated from a pair of 1-D LOS datasets processed in this manner are referred to as 2-D measurements. These datasets identify vertical and horizontal ground displacement. Due to the orbital direction of the satellites, radar images are always captured from an eastern or western direction relative to the target area. Therefore, horizontal ground movement identified via InSAR is defined as east-west displacement. The north-south component of ground movement is unknown in 2-D datasets, and cannot be identified via InSAR due to the viewing direction of the satellites. Analysis of an InSAR dataset allows for the identification of displacement velocity in inches/year and acceleration in inches/year^2. Measurement precision is affected by the satellite sensor resolution and the timeframe of the dataset. Average accuracy ranges for individual measurements can vary between ±0.20 inches for a low-resolution satellite and ±0.03 inches for a high-resolution satellite. With time, velocity trends can be measured with high accuracy yielding standard deviations in the range of ±0.01 inches/year.

2.2 Reference Point

The InSAR survey method relies on the selection of a local reference point from among the measured ground targets. The reference point is represented as static in order to produce calculations of relative movement at all other measurement points. In this way the reference point is similar to the off-dome, deep-rod benchmark monuments used in past level surveys at the site. However, unlike benchmark monuments, the reference point is chosen more for its motion behavior and radar properties than its location and construction. The reference point used for the evaluation of each dataset must exhibit high-quality signal return and not be affected by fluctuating ground movement within the time period evaluated.

Movement, if present at the reference point, is confirmed to be linear and assumed to be representative of broad regional displacement that extends beyond the analysis area. Once this movement is zeroed out at the reference point, regional movement is assumed to be excluded from the displacement rates calculated at other measurement points. This is similar to historical ground surveys that relied on relative measurements from benchmark monuments. Ideally, the reference point will not change between surveys, but subsequent non-linear movement or increased signal noise may require selection of a new location.

As discussed in the following sections, two InSAR datasets were collected from a pair of satellite orbits which were used to triangulate vertical and east-west 2-D data. The reference points for each 1-D LOS dataset are located near to each other, 1.68 miles to the southeast of the approximate dome center. The reference point for the calculated 2-D data is located 1.96 miles to the east of the approximate dome center. The off-dome benchmark used in past surveys was located at a similar distance from the site at 1.79 miles to the south-southwest of the dome center.

Discussions were had with TREA to understand why the 2-D reference point was positioned at a different location than the 1-D data reference points. It was explained that the 2-D measurement points generated in the subsampling of the 1-D data each possess individual characteristics of quality and motion behavior following the generation of the 2-D grid. Although the 2-D displacement appears relatively stable at the location of the 1-D reference points the 2-D cell with the highest data quality and stability was ultimately identified at an alternate location and was thus selected as the 2-D reference point for this analysis.

2.3 Satellite Data Sources

Two satellite datasets were used in the InSAR analysis which were acquired from satellites on both ascending and descending orbits. An ascending orbit denotes the satellite's longitudinal course from south to north as it passes over the site and radar images from ascending orbits are captured in an eastward direction. In descending orbits, the satellite moves from north to south and images are captured with a westward viewing direction.

The first 1-D LOS dataset was captured from a Sentinel 1 (“SNT”) low-resolution satellite on an ascending orbit. The dataset timeframe covers a 7-year period from October 4, 2016 to December 15, 2023 with a 12-day image capture frequency. Data from this satellite was originally processed and evaluated in May 2022. Given the availability of a multi-year data span from the SNT satellite, the objective at that time was to compare subsidence trends identified via InSAR to the historical level surveys, and to establish historical baseline trends for future InSAR surveys. That evaluation led to the following conclusions: 1) Trends were identified as matching historical level surveys in the degree of consistency of linear ground movement observed, 2) Horizontal ground displacement was evident necessitating the use of a second satellite in future surveys to triangulate the vertical and lateral components, and 3) Due to data gaps in vegetated and marshy areas, the second dataset would need to come from a high-resolution satellite to maximize the spatial density of data point capture.

For the Fall 2022 survey, the second 1-D LOS dataset was gathered via a TerraSAR-X (“TSX”) high-resolution satellite on a descending orbit with an 11-day revisit frequency. The dataset timeframe covered a 6-month period from June 16, 2022 to December 20, 2022. High-resolution commercial satellites must be tasked for these purposes so historical data preceding the selection of the satellite for monitoring was not available.

In January 2023, the decision was made to transition to a new source for high-resolution satellite data to better satisfy a continuous InSAR monitoring effort that is currently active over the dome. This dataset is gathered from a pair of satellites, a TerraSAR-X satellite and the PAZ satellite, which share the same descending orbit and capture with a westward viewing direction. Both satellites orbit with an 11-day revisit frequency but their imaging periods are offset which provides the benefit of more frequent data collection. This data source is referred to as the TSX/PAZ Constellation (“TSX/PAZ”). The

PAZ satellite passes over the site 4 days after the TSX satellite which results in a combined image frequency that transitions between 4- and 7-day intervals. This dataset provides the second 1-D LOS dataset for use in this evaluation and covers an 11-month period from January 24, 2023 to December 31, 2023.

Table 1 below provides additional information on the satellite data parameters. Figure 1 provides a diagram of the orbital paths in relation to the Sulphur Mines site and Figure 2 depicts the data capture timeline.

Table 1 – Satellite Data Parameters, Data Timeline, and Orbit Visualization

Analysis Characteristics	Sentinel-1 (SNT)	TSX/PAZ Constellation
Satellite Properties		
Band (Wavelength)	C-band (2.32 in)	X-band (1.22 in)
Track	T136	T67 & T120
Pixel resolution	65 x 16 ft	3 x 3 ft
Revisit frequency	12 days	4 & 7 days
Orbit (LOS Angle, θ)	Ascending (42.45°)	Descending (37.06°)
Data Properties		
Period covered	10/04/2016 - 12/15/2023	01/24/2023 - 12/31/2023
No. of images processed	193	62
Reference Point location - *WGS 84*	Lat: 30.235765 Long: -93.392750	Lat: 30.235718 Long: -93.392146
No. of measurement points	25,747	54,269
Average point density	1,880 pts/mi^2	3,963 pts/mi^2
Average displacement rate standard deviation	< ± 0.04 in/yr	± 0.05 in/yr
Average time series measurement error bar	± 0.20 in	± 0.07 in

Figure 1 – Satellite Orbit Visualization

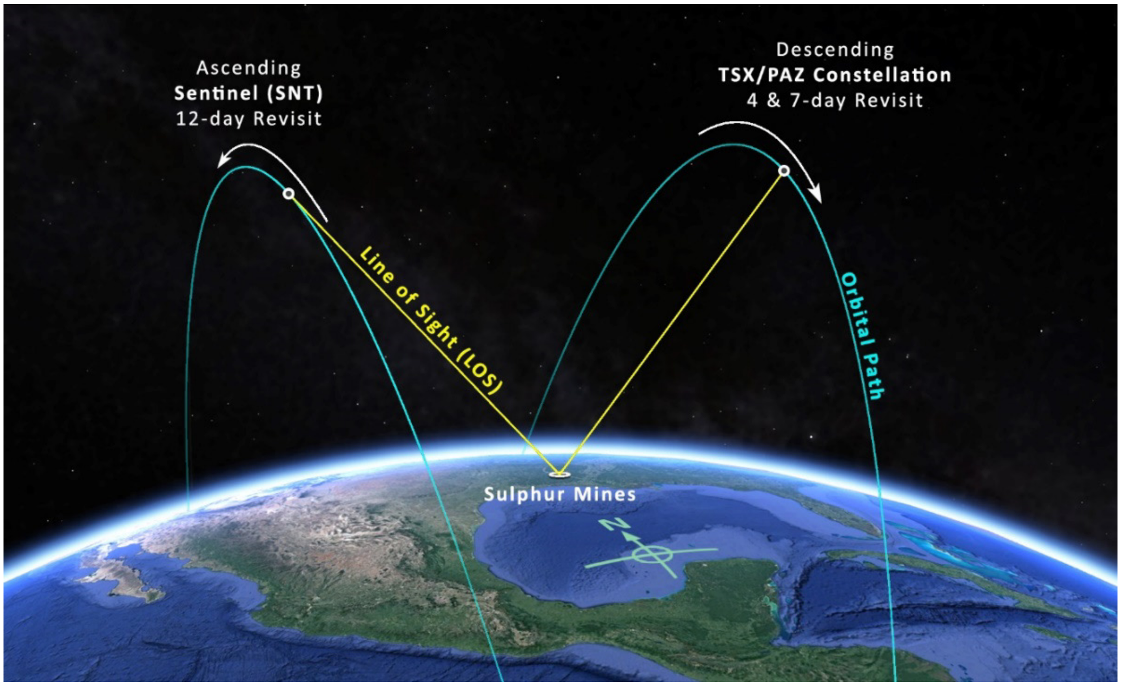

Figure 2 – Satellite Data Timeline

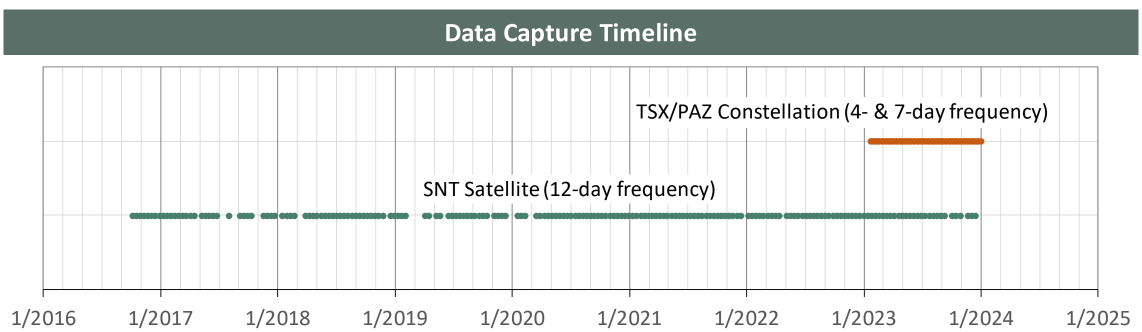

The 1-D LOS InSAR datasets generated from the two satellite orbits each cover a 13.7-square mile area that extends roughly 1.85 miles out from the center of the Sulphur Mines Salt Dome. Figure 3 below depicts the measurement point locations, reference points, and data extent for the SNT and TSX datasets in relation to the dome structure contours. Areas of dense data capture are situated over roadways and infrastructure associated with dome operations and the city of Sulphur, Louisiana to the southeast. Areas showing farmland, forests, and water bodies can be seen to lack measurement data.

Figure 3 – SNT and TSX/PAZ 1-D LOS Measurement Points

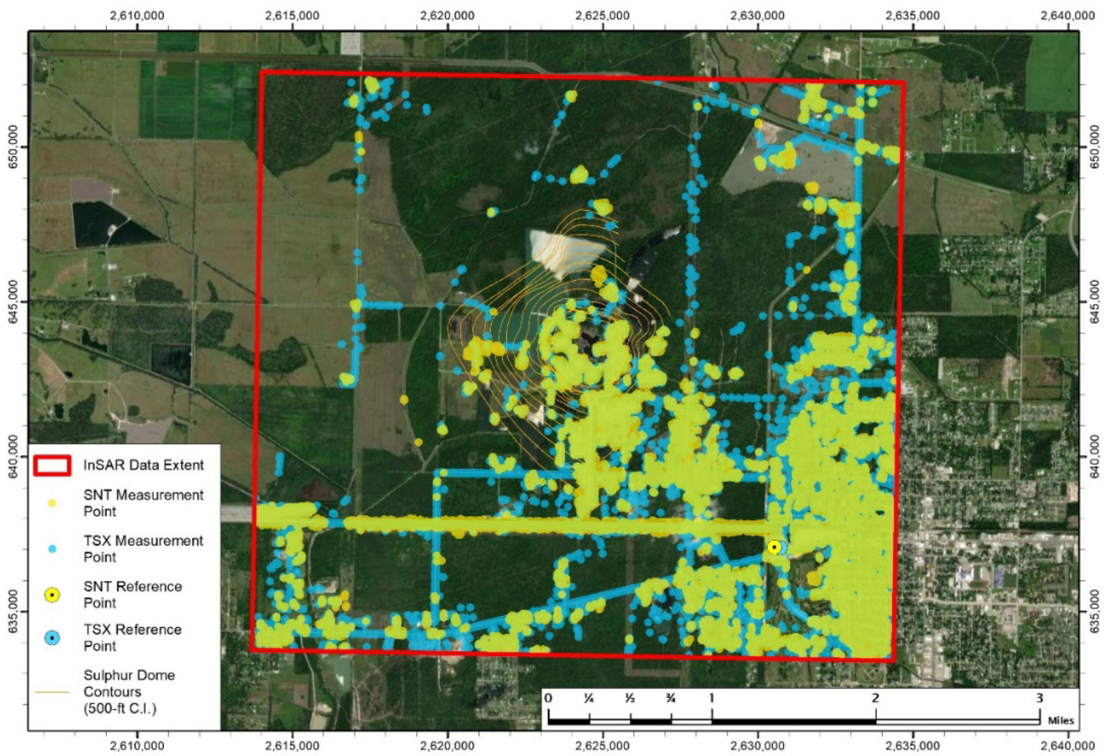

2.4 Vertical and East-West Data

In order to generate the 2-D dataset from the 1-D LOS data, a grid of cells measuring 82 x 82 feet was created across the 13.7 square mile data extent. For cells that contained at least one measurement point from each of ascending and descending 1-D datasets, a vertical and east-west displacement value was calculated by triangulation of the 1-D displacement values. If multiple 1-D measurement points from the same dataset were present within a particular cell, those values were averaged to produce a single 1-D time series of displacement values prior to the calculation. The 2-D measurement points are located within the center of each cell for which the calculation was performed.

Two datasets were generated from this process, a vertical displacement and an east-west displacement dataset, with a time series of displacement values for each calculated measurement point. The time series for these two datasets span the 11-month overlap of the data, January 24, 2023 to December 13, 2023. Interpolation of the data in time allows for a displacement value to be calculated for each date of data capture from either satellite. The resulting displacement time series display a higher frequency of displacement values than the source data frequencies. Table 2 below provides additional information on the 2-D parameters. Figure 4 shows a diagram of the calculated displacement components in relation to the Sulphur Mines site and Figure 5 displays the calculated data timeline.

Table 2 – 2-D Data Parameters, Data Timeline, and Displacement Visualization

Analysis Characteristics	Vertical	East-West
Period covered	01/24/2023 - 12/13/2023	
No. of images processed	79	
Reference Point location - *WGS 84*	Lat: 30.249700 Long: -93.379668	
No. of measurement cells	3,895	
Cell size	82 x 82 ft	
Average displacement rate standard deviation	± 0.02 in/yr	± 0.02 in/yr

Figure 4 – 2-D Displacement Visualization

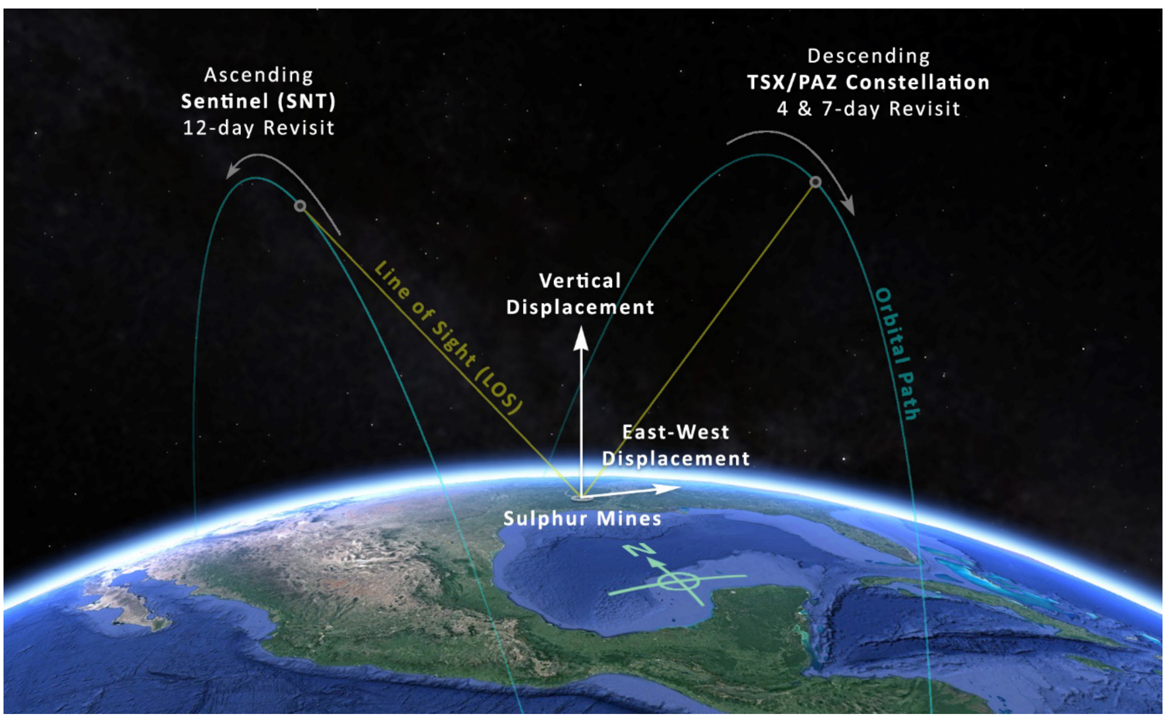

Figure 5 – 2-D Data Timeline

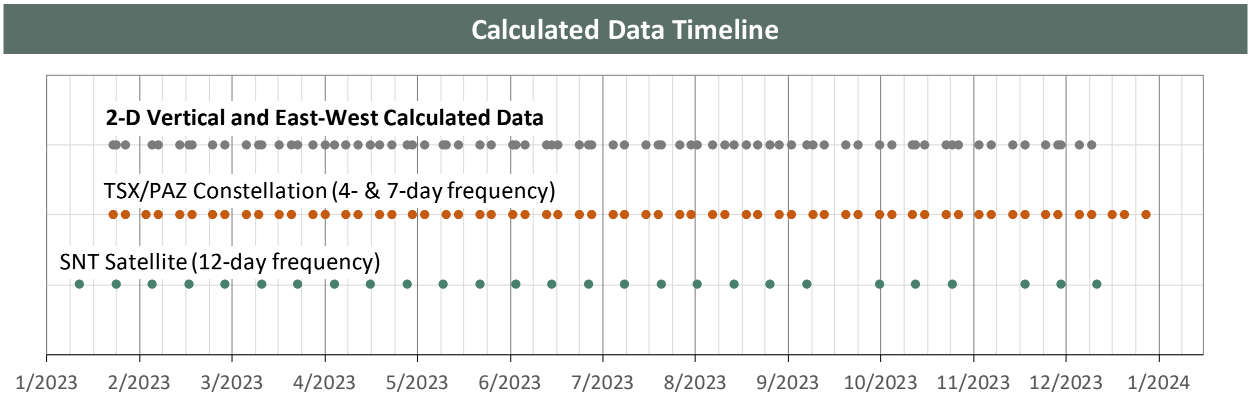

The vertical and east-west 2-D datasets generated from the 1D LOS data cover the same 13.7-square mile area. Figure 6 below depicts the grid cell positions with calculated measurement points in relation to the dome structure contours. Data coverage indicates areas where both SNT and TSX/PAZ data were present within the data extent.

Figure 6 – 2-D Vertical and East-West Measurement Points

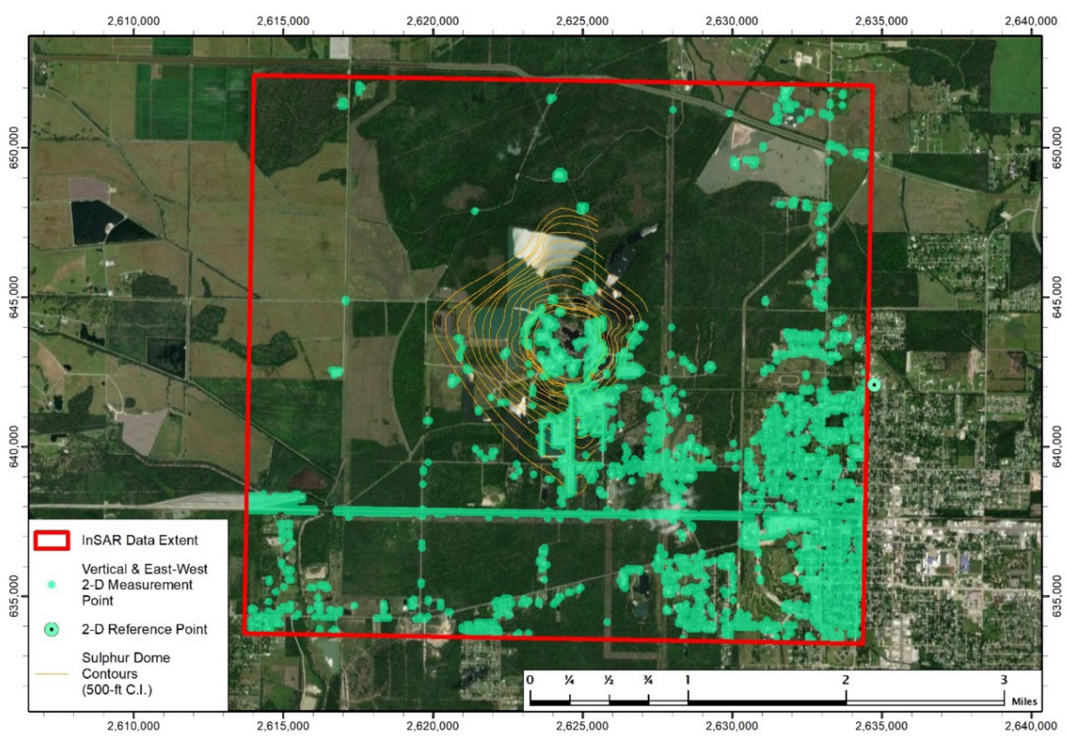

3.0 Areas of Interest

Past level surveys were performed on a set of thirty-six (36) physical monuments located on cavern wellheads, abandoned cavern well caps, and additional monuments positioned over and around the dome. Of this total, there were two (2) off-dome benchmark deep-rod monuments, twelve (12) additional rod monuments, and twenty-two (22) wells. Fifteen (15) of the wells are owned by Westlake, five (5) wells by Boardwalk, and two (2) by Liberty.

This system was designed to provide comprehensive monitoring for any areas that may be subject to subsidence as a result of current or past cavern operations. Survey measurements of these monument elevations were used to develop time series charts of the elevation changes and movement trends as well as contour maps of the interpolated subsidence velocity and acceleration across the dome.

With InSAR data, the displacement values for each measurement point can similarly be used to generate contour maps of displacement velocity and acceleration, indicating the spatial distribution of subsidence magnitudes. Velocity and acceleration rates are determined via trend analysis of the displacement time series for each individual measurement point. In total, 3,895 calculated measurement points are available in the 2-D dataset for generation of contour maps. Roughly 300 of the points are located in close proximity to the dome top and cavern locations.

Given this number of measurement locations, a data reduction method must be considered to visually convey and evaluate trend consistency in displacement time series charts. This can be achieved by the grouping of measurement points to generate time series of the averaged displacement values for each group. Averaging of the displacement data within point groups also allows for the reduction of scatter (noise) in the plotted displacement values associated with individual measurement accuracy.

3.1 AOI Boundary Definition

Past level surveys measured elevations at cavern wellheads and at supplemental monuments over the dome. In an effort to maintain a similar mode of reporting and analysis, Areas of Interest (AOIs) were drawn to group measurement points over individual cavern extents and to encompass the dome-wide coverage achieved in prior monitoring.

In total, twenty-one (21) AOIs were created to evaluate displacement trend consistency across the dome. The AOIs were numbered and eighteen (18) of the AOIs which encompass cavern extents were additionally labeled with acronyms denoting the associated cavern. One of the AOIs was found to lack 2-D measurement data – AOI 14 (PPG 16). This resulted from a lack of overlap between SNT and TSX/PAZ measurement locations within the AOI boundary. 1-D LOS data is present, however, allowing for confirmation of trend consistency within this AOI. This is discussed further in Section 6.2 along with planned measures that will be taken to ensure future 2-D data acquisition where needed across the dome.

Table 3 below provides a list of the AOIs and 2-D measurement point counts. Figure 7 depicts the AOI boundaries in relation to the historical maximum cavern extents and past level survey monuments.

Table 3 – InSAR Point Group Parameters

AOI Name	Area (Acres)	2-D Point Count
AOI 1 (LGS 1)	3.75	2
AOI 2	2.71	4
AOI 3	3.01	5
AOI 4	4.71	9
AOI 5 (PPG 21)	5.92	5
AOI 6 (PPG 6)	9.49	21
AOI 7 (PPG 7)	6.35	23
AOI 8 (PPG 22)	5.46	7
AOI 9 (SMS A1)	5.92	5
AOI 10 (PPG 2)	8.18	33
AOI 11 (PPG 5)	4.43	9
AOI 12 (PPG 4)	9.74	15
AOI 13 (PPG 18)	8.24	4
AOI 14 (PPG 16)	8.83	0
AOI 15 (PPG 20)	7.51	12
AOI 16 (LGS 2)	8.71	9
AOI 17 (SS 4)	5.40	21
AOI 18 (SS 2)	3.23	12
AOI 19 (SS 5)	2.86	15
AOI 20 (SS 1)	4.20	13
AOI 21 (SS 3)	3.10	13

Figure 7 – InSAR Point Group AOI Boundaries

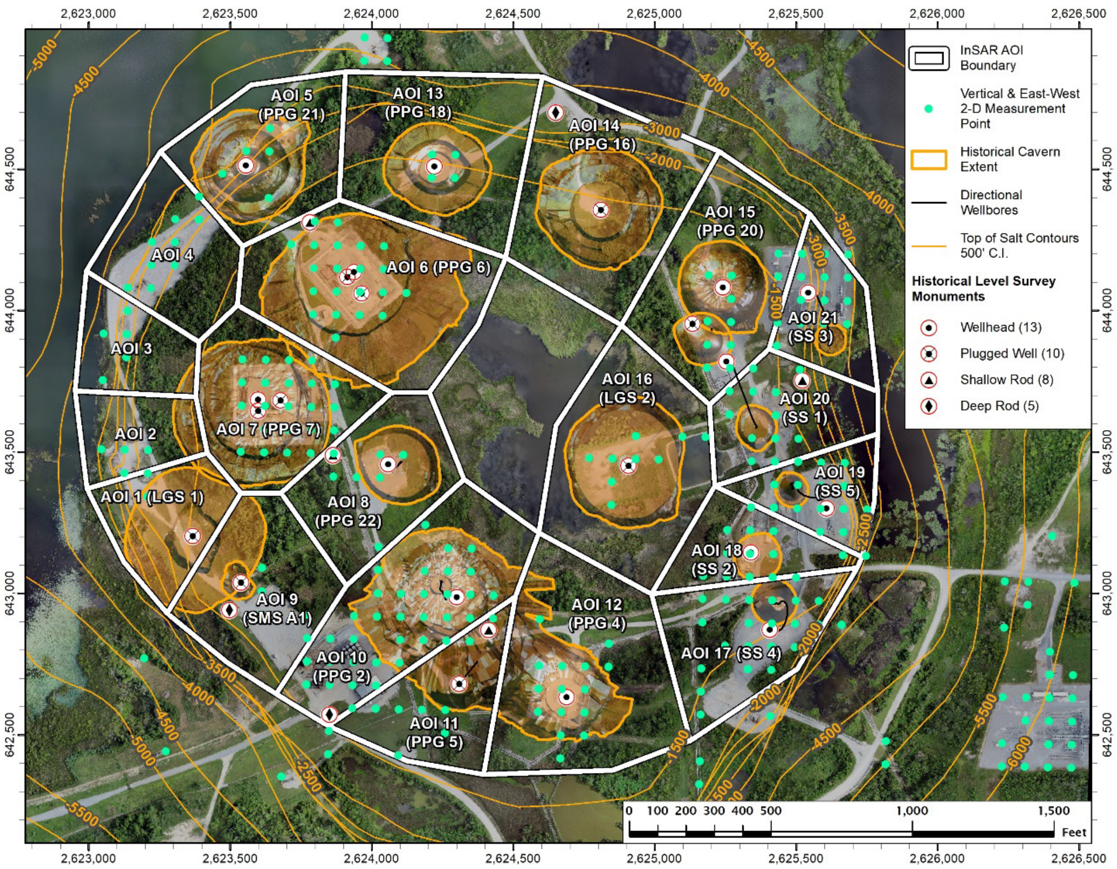

A larger format map has been included as Appendix A that depicts the AOI regions in relation to the 2-D measurement point locations. The map also depicts the surface locations of cavern wells along with well names, serial numbers, and statuses.

4.0 Subsidence Rate Determination

Per guidance issued by the Injection and Mining Division of the LA DNR in 2019, a determination of the current rate of subsidence over each survey point is to be evaluated. This is considered the "velocity" of ground displacement at each monument. Additionally, the guidance requests that the rate at which this "velocity" is changing be determined if non-linear movement trends are identified. This rate of change is considered the "acceleration" of ground displacement at each monument. In place of monument elevations, the displacement values associated with each measurement point in the InSAR survey are used. The historical displacement data provides the basis for determining these ground movement rates through analysis of the long-term trends.

4.1 Selection of Trend Equation

Trend analysis data was generated by plotting average displacement values over time for the measurement point groups within the AOI regions. The use of non-linear trend equations was evaluated which could yield acceleration estimates in addition to velocity. However, due to the relatively short 11-month timeframe of the data in combination with the accuracy range of the measurements, calculated accelerations varied dramatically and were found to lack statistical significance.

Knowledge of the subsidence behavior over the site from past level surveys and evaluation of the 6-year SNT data provides evidence of nearly linear subsidence trends that contradict the acceleration values calculated for the 11-month 2-D data. The decision was made to calculate subsidence values using linear trend equations and to postpone evaluation of vertical and east-west acceleration across the site until longer-term datasets can be generated. For the time being, notable deviation from the calculated linear trends will be evident, if present, in the AOI time-series charts provided with this report, but the associated acceleration rates cannot be accurately estimated using the timeframe of the 2-D dataset.

Figure 8 below shows sample point groups from the SNT 1-D data that have been plotted to convey the discrepancy in accelerations identified using the 11-month timeframe. The charts provide examples of the acceleration rates, represented by the magnitude of curve in the trend lines, if a multi-year timeframe is used relative to an 11-month timeframe.

Figure 8 – Non-linear Trend Estimation for Multi-year vs. 11-Month Datasets

SNT 1-D LOS Point Group – AOI 12 (PPG 4) – Point Count: 121

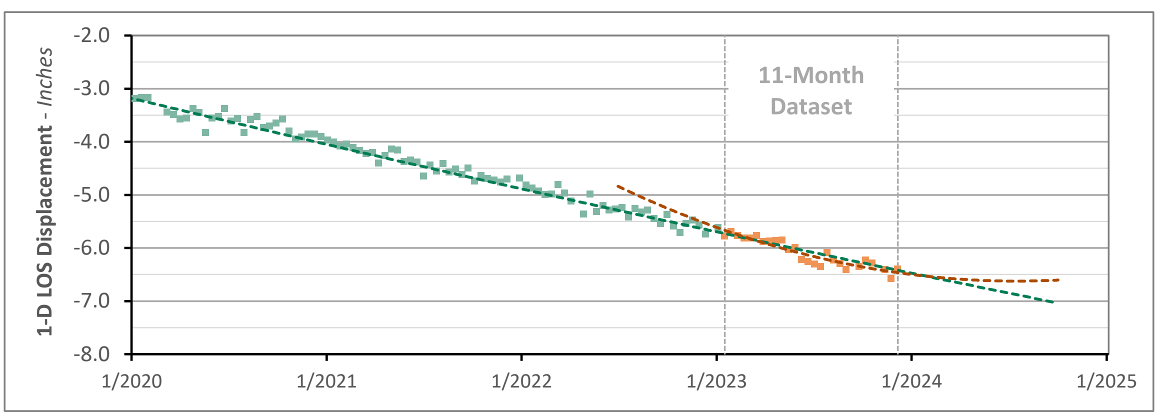

SNT 1-D LOS Point Group – AOI 15 (PPG 20) – Point Count: 69

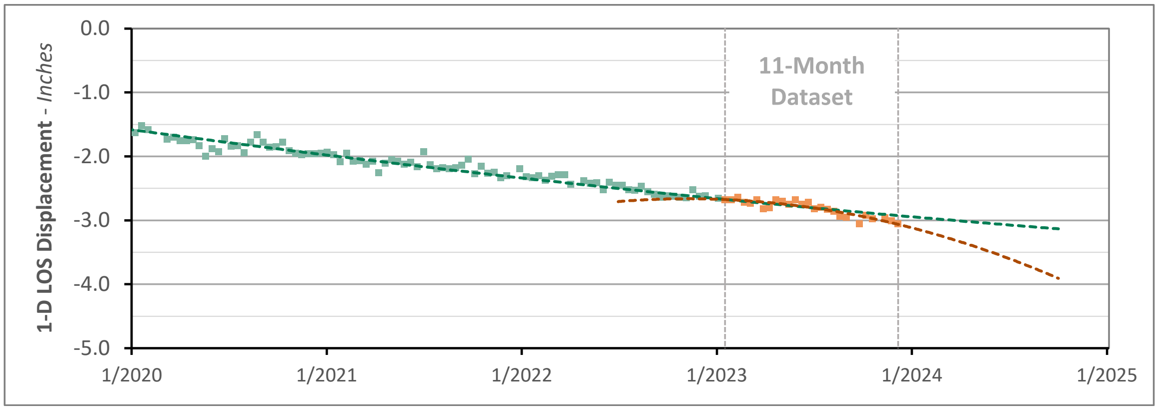

4.1 *Linear Regression Analysis*

To evaluate subsidence trends in the 2-D displacement data, a linear least squares regression analysis was performed to define trend variables for each AOI dataset. In least squares regression analysis, the sum of the squared difference between model-predicted and actual data is minimized by a computationally derived set of model variables. The model formula is shown below in Equation 1.

$$D(t) = \beta_0 + \beta_1 t \qquad \text{Equation 1}$$

where $D(t)$ is the predicted displacement at time (t), and β_0, and β_1, are fit parameters determined by the regression analysis performed on the historical dataset for each AOI.

Once this model has been defined, the predicted rate of displacement can be calculated by taking the derivative of the model equation with respect to time. The formula used to approximate the rate of displacement is provided below in Equation 2.

$$d/dt\ [D(t)] = \beta_1 \qquad \text{Equation 2}$$

where $d/dt\ [D(t)]$ is the predicted rate of displacement. This value represents the velocity of ground displacement estimated by the model for each AOI. Velocity is calculated irrespective of time (t) in linear regressions. In the vertical data, negative velocity values represent downward rates of ground displacement and positive values represent upward displacement. In the east-west data, negative values are associated with westward displacement rates, and positive values are eastward.

5.0 Data Analysis

5.1 Time Series Plots

Averaged displacement values for vertical and east-west movement were plotted for each AOI with respect to time. The resulting time series charts provide a visual depiction of the calculated trends and associated data. These plots are shown for reference in Appendix B. The modeled trends for each AOI are shown by the dashed lines that overlay the displacement measurements on each plot. No divergence was seen between the data and the linear trend lines that would imply material acceleration of displacement rates is occurring within any of the plotted AOI datasets. Overall, the data exhibited relatively low scatter and consistent near-linear trends in all AOIs evaluated.

AOIs with higher point counts were generally found to exhibit less fluctuation and scatter in the plotted data, indicating that the accuracy limitations in individual measurement point values were mitigated through data averaging. The properties of the 1-D SNT and TSX/PAZ source data likely also play a role in the relative measurement precision depicted in the charts. The specific number and distribution of the 1-D measurement points and the quality of the radar targets within each AOI region will lead to variation in measurement quality for the averaged 2-D displacement data.

The trend models generated for each AOI were used to identify the velocity of vertical and east-west displacement in inches/year. These calculated values are provided in Table 4 below. Average displacement rate standard deviations for both the vertical and horizontal data were calculated as ±0.02 inches/year.

5.2 Displacement Velocity Maps

The same process that was followed to generate trend equations for the AOI point groups was also performed on each individual measurement point in the 2-D dataset. The velocity values calculated for each point were used to generate contours to illustrate the spatial distribution of displacement velocities across the surveyed region. Vertical and east-west velocity contours are provided on maps in Appendices C and D, respectively, for reference.

Table 4 – InSAR Point Group Vertical and East-West Displacement Velocities

AOI Name	Vertical Displacement		East-West Displacement	
	Velocity *(Inches/Year)*	Direction	Velocity *(Inches/Year)*	Direction
AOI 1 (LGS 1)	-0.96	Downward	0.96	Eastward
AOI 2	-0.80	Downward	0.77	Eastward
AOI 3	-0.73	Downward	0.87	Eastward
AOI 4	-0.71	Downward	0.68	Eastward
AOI 5 (PPG 21)	-0.55	Downward	0.21	Eastward
AOI 6 (PPG 6)	-1.08	Downward	0.49	Eastward
AOI 7 (PPG 7)	-1.14	Downward	0.80	Eastward
AOI 8 (PPG 22)	-1.42	Downward	0.66	Eastward
AOI 9 (SMS A1)	-1.33	Downward	0.64	Eastward
AOI 10 (PPG 2)	-1.34	Downward	0.45	Eastward
AOI 11 (PPG 5)	-1.27	Downward	0.47	Eastward
AOI 12 (PPG 4)	-1.36	Downward	0.02	Eastward
AOI 13 (PPG 18)	-0.95	Downward	0.26	Eastward
AOI 14 (PPG 16)	N/A	N/A	N/A	N/A
AOI 15 (PPG 20)	-1.19	Downward	-0.44	Westward
AOI 16 (LGS 2)	-1.90	Downward	-0.25	Westward
AOI 17 (SS 4)	-1.43	Downward	-0.44	Westward
AOI 18 (SS 2)	-1.43	Downward	-0.48	Westward
AOI 19 (SS 5)	-1.18	Downward	-0.59	Westward
AOI 20 (SS 1)	-1.27	Downward	-0.63	Westward
AOI 21 (SS 3)	-0.93	Downward	-0.42	Westward

5.3 Comparison to Fall 2022 Survey

This review will summarize a few notable observations in relation to the prior Fall 2022 InSAR survey. For the sake of clarification and to qualify these comparisons a few variables are noted below that differ between the current and prior 2022 analysis:

1) A modified approach was used in the drawing of the AOI boundaries for this evaluation to improve inclusion and averaging of the available datapoints over the dome. This leads to minor differences in the assignment of datapoints to the cavern-specific AOI regions and may influence direct comparisons to the prior survey's calculated AOI displacement velocities.

2) The Fall 2022 survey was performed on a 6-month time span of 2-D InSAR data due to a limited overlap of the available 1-D LOS datasets utilized in that evaluation. This introduces the potential for seasonal ground movement to affect an imbalance in the velocity trends identified between the two datasets.
3) Measurement accuracy is improved with the number of radar images utilized by TREA in their processing algorithm. The 11-month data span and the higher image collection frequency of the TSX/PAZ dataset may be considered to provide improved accuracy in the current analysis.
4) The Fall 2022 survey utilized a descending satellite source with a steeper viewing angle from the east of 17.18 degrees relative to the current TSX/PAZ constellation with a viewing angle of 37.06 degrees. Shallower viewing angles such as the one utilized currently are more sensitive to horizontal movement. This should improve accuracy in the resolved vertical and horizontal components of the 1-D displacement measurements.
5) Moreover, the current evaluation employs an alternate descending InSAR dataset with a new grid of natural radar targets. Minor variations should be expected between interpreted data from different InSAR data sources.

5.4 Observations

In general, the subsidence rate is greatest over the eastern-central portion of the dome with a gradual tapering toward the dome edges. Subsidence rates continue to slow at further distances from the dome, but the slowing trend is less uniform as evidenced to the south and southeast of the dome where data coverage is more densely present. Regions of near-zero subsidence were noted near the perimeter of the data extent at distances of roughly 1.5 to 2 miles from the dome center.

The AOI point groups with the highest rates of calculated subsidence were AOI 8 (PPG 22), AOI 16 (LGS 2), AOI 17 (SS 4), and AOI 18 (SS 2). The maximum rate of subsidence was -1.90 inches/year at AOI 16 which overlies the plugged and abandoned Liberty Gas Storage No. 002 cavern. This is consistent with the subsidence rate of -1.91 inches/year identified for the analogous AOI region in the prior Fall 2022 InSAR evaluation. The Fall 2021 evaluation performed with ground survey data additionally showed the highest rate of subsidence at this position based on surveying of the cavern well cap monument. The rate identified in the Fall 2021 evaluation was also -1.91 inches/year. None of the AOI point groups exhibited upward movement in the Fall 2023 calculated trends.

The mapped geometry of the vertical velocity contours shows general agreement with prior annual monitoring maps generated from analysis of ground survey data. Additionally, the mapped geometry of the subsidence velocity contours and the calculated velocities of the AOI point groups in the present evaluation were found to agree substantially with the results of the Fall 2022 InSAR analysis.

Analogous AOI regions between the two surveys were compared and subsidence velocities were found to mostly fall within ± 0.15 inches/year of the 2022 calculated rates. The only notable increases in subsidence rates were observed at AOI 9 which overlies the plugged and abandoned Sulphur Mines Storage No. A-1 cavern and AOI 17 which overlies the active Sulphur Storage No. 004 cavern. For AOI 9 (SMS A1) and AOI 17 (SS 4), the 2023 calculated subsidence rates were -1.33 and -1.43 inches/year, respectively. The rates calculated for the analogous AOIs in the prior 2022 survey were -0.96 and -1.21 inches/year, respectively. Both of the vertical displacement time series charts for these AOIs exhibit consistent linear motion throughout the 11-month evaluation period. A separate review of the historical multi-year SNT data additionally showed consistent near-linear ground movement trends within these AOIs from 2016 to present. It is assumed for the current reporting period that the observed differences in the calculated annual rates are not indicative of changing ground movement conditions in these areas of the dome.

East-west displacement velocities in the present analysis were seen to generally indicate that lateral ground displacement is occurring toward the center of the dome. Lateral ground displacement can be expected to coincide with vertical displacement in this way. Sub-surface soils will tend to compact and settle into the void created by a subsiding area, causing horizontal movement toward the center of the subsidence basin. The phenomenon is akin to lateral soil creep that occurs over time on shallow slopes due to gravity. Although the dataset is limited to east-west displacement, it can be assumed that north-south movement is occurring in a similar fashion toward the dome center in accordance with the shape of the subsidence basin.

The region of zero horizontal movement in the east-west velocity contours divides the dome from north to south and passes near to the area of greatest vertical subsidence. On the western side of the dome, horizontal east-west velocities are seen to be generally greater than velocities on the eastern side of the dome. This may be related to the eastern offset of the subsidence basin center relative to the dome center.

Additionally, it appears that horizontal displacement exhibits more spatial irregularity than vertical displacement across the AOI regions. Similar magnitudes of east-west displacement observed within the dome footprint are also observed sporadically across the full analysis area.

The AOI point groups with the highest rates of eastward movement were AOI 1 (LGS 1), AOI 2, AOI 3, and AOI 7 (PPG 7). The highest east-west displacement rate was calculated as +0.96 inches/year at AOI 1 which overlies the plugged and abandoned Liberty Gas

Storage No. 001 cavern. All four of these AOIs are centrally located on the western edge of the dome and encompass the region with the greatest calculated rates of eastward movement in the 2-D dataset. The AOI point groups with the highest rates of westward movement were AOI 19 (SS 5) and AOI 20 (SS 1). The highest rate of westward movement was calculated as -0.63 inches/year at AOI 20 which overlies the active Sulphur Storage No. 001 cavern. These two AOIs are centrally located on the eastern edge of the dome and encompass the region with the greatest calculated rates of eastward movement in the 2-D dataset.

The general division of eastward and westward movement remained consistent over the dome relative to the Fall 2022 analysis. However, direct comparisons between AOI regions were not possible due to some broadly apparent differences between the 2022 and 2023 horizontal datasets. The main difference was noted as a general eastward shift of all rates in the AOI regions. The prior 2022 evaluation of east-west movement observed that data scatter in the 6-month time series plots was significant relative to the vertical data. The average standard deviation in the calculated horizontal displacement rates was 2.5 times greater than in the vertical rates in the 2022 analysis. The lower data precision may have influenced mapped east-west displacement rates in the 2022 analysis. With the noted eastward shift and the improved sensitivity to horizontal movement in the TSX/PAZ satellite viewing angle utilized in the current survey, it is assumed that comparisons between the two analyses would not be statistically meaningful in this evaluation.

6.0 Supplementary Discussion

A few additional reviews were performed using the 1-D LOS data to supplement the observations made in the 2-D data evaluation. The results of these reviews are described in this section.

6.1 Sentinel 1 (SNT) 7-Year InSAR Dataset

A 5.5-year dataset from the Sentinel 1 (SNT) low-resolution satellite was originally processed and evaluated in May 2022. A supplementary evaluation of the updated 6-year dataset was then presented in the Fall 2022 annual report. Both reviews revealed consistent near-linear subsidence in all areas of the dome and provided a link to past level survey monitoring results.

The updated 7-year SNT dataset was evaluated again as part of this review. The primary objective was to confirm general continuation of ground displacement trends from 2016 to present. Time series charts were generated for each of the current AOI regions and reviewed for recent trend consistency. This was done to confirm that the subsidence trends identified using the 11-month 2-D data could be considered continuations of the historical trends within each AOI. Figure 9 below provides two examples of the AOI time series that were reviewed as part of the historical evaluation of the SNT 1-D LOS data.

No acute deviations from the historical trends were observed during the 2023 timeframe that warranted further investigation. Overall, the subsidence rates identified through linear regression of the 11-month 2-D dataset are believed to generally agree with historical trends and to provide a reasonably accurate portrayal of ground displacement rates within the AOI regions.

Figure 9 – Sample SNT 1-D Displacement Time Series of AOI Regions

SNT 1-D LOS Point Group – AOI 6 (PPG 6) – Point Count: 135

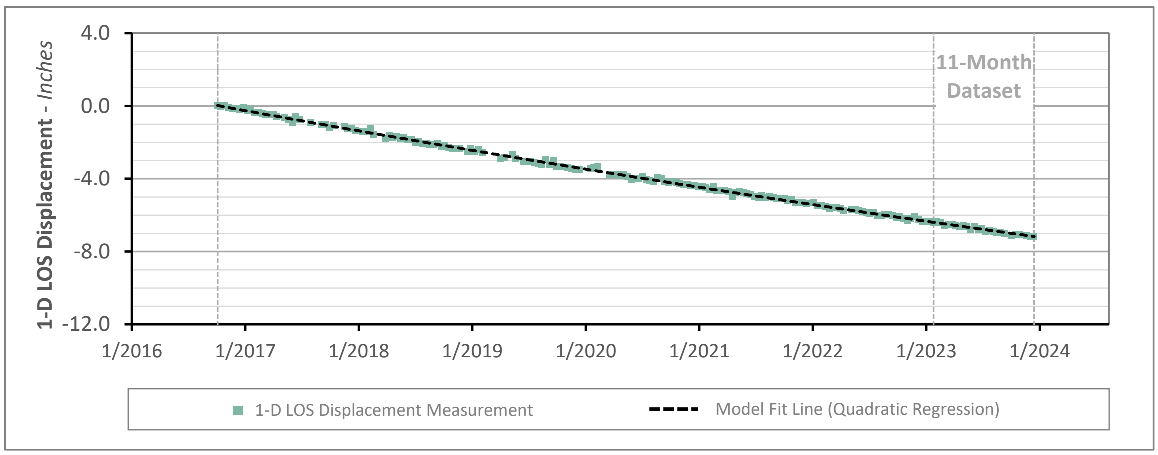

SNT 1-D LOS Point Group – AOI 9 (SMS A1) – Point Count: 58

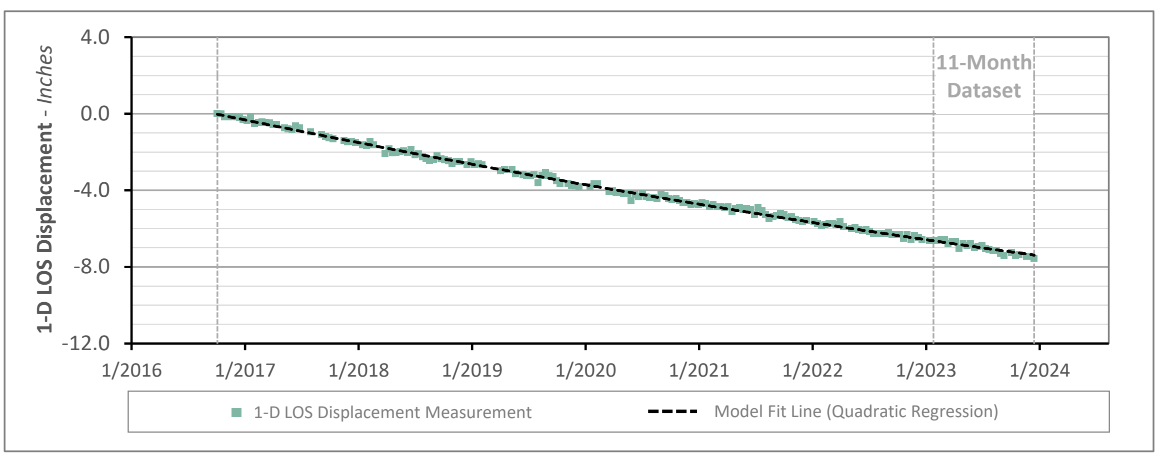

6.2 Evaluation of Data Gaps

AOI 14, which overlies the plugged and abandoned PPG No. 016 cavern, was not able to be evaluated for vertical and east-west displacement due to a lack of 2-D measurement data within the boundary. 2-D data was not available due to a lack of overlap between SNT and TSX measurement locations within the 2-D grid cells. 1-D LOS data is present within the AOI region, however, allowing for an evaluation of trend consistency over the 1-D data timeframes. AOI 14 contains eleven (11) measurement points in the 11-month TSX/PAZ dataset and one (1) measurement point in the 7-year SNT dataset. The time series of the averaged 1-D displacement data are provided below in Figure 9 with trendlines overlaid.

Overall displacement rates can be seen to be consistent over the available data timeframes. Due to the presence of a single SNT measurement point in AOI 14, the associated chart displays a significant amount of data scatter. Trend consistency still appears to be generally present throughout the 2023 timeframe.

Figure 9 – 1-D Displacement Time Series of AOIs with No 2-D Data

TSX/PAZ 1-D LOS Point Group – AOI 14 (PPG 16) – Point Count: 11

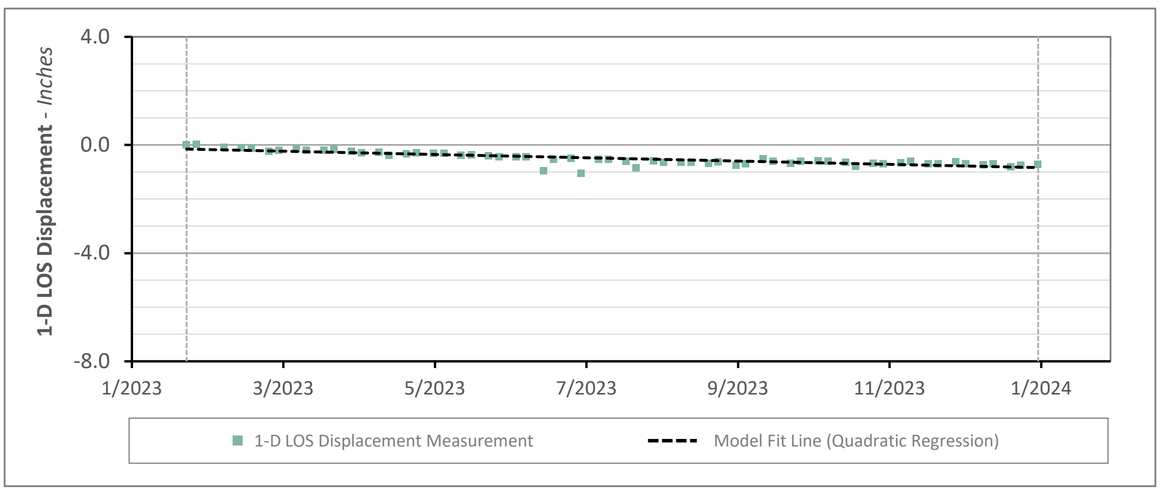

SNT 1-D LOS Point Group – AOI 14 (PPG 16) – Point Count: 1

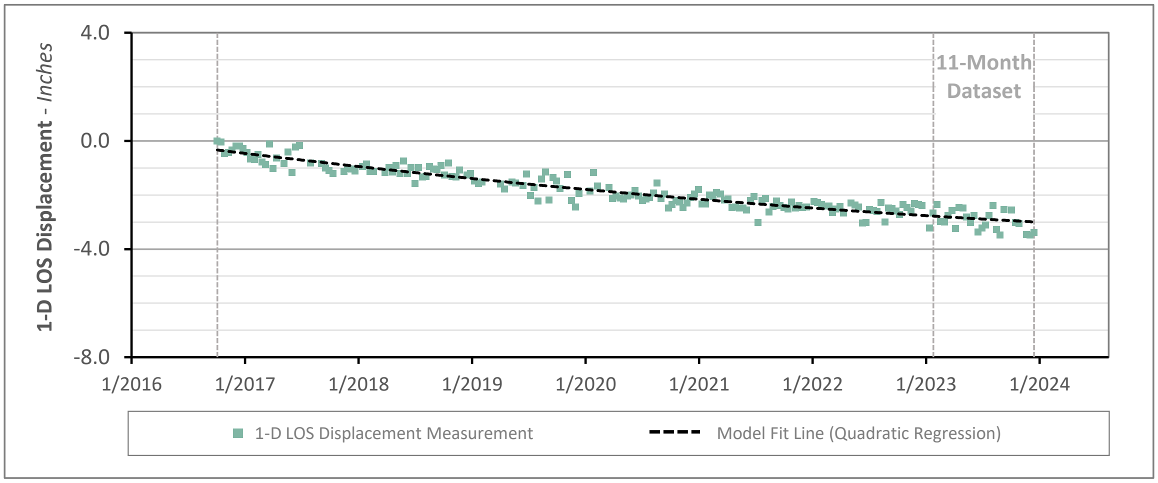

A network of corner reflectors is planned to be installed in 2024 in various areas of the dome including AOI 14 to improve InSAR data coverage in future analyses. Corner reflectors are metallic angular structures that can be erected at specific positions to ensure reliable InSAR data capture. Corner reflectors provide ground targets with the highest amplitude of signal return in radar imagery.

6.3 Fall 2023 Trend Consistency

Based on the supplementary review of the 1-D LOS datasets and the evaluation of the calculated 2-D data, subsidence trends appear to be continuing as observed in the multi-year SNT data and as historically defined in past level surveys. This indicates that rates of cavern closure and other local factors of influence are continuing to act in a consistent manner at this time.

7.0 Conclusions

1. The second annual InSAR survey of the Sulphur Mines Salt Dome showed sustained trend continuity and geometry of the subsidence basin, with potential enhancements in the calculated lateral displacement.

2. In general, the subsidence rate is greatest over the eastern-central portion of the dome with a gradual tapering toward the dome edges. At further distances from the dome, subsidence rates continue to slow but exhibit more variability in the mapped

contours. The greatest subsidence rates were identified at AOI 8 (PPG 22), AOI 16 (LGS 2), AOI 17 (SS 4), and AOI 18 (SS 2), with the maximum rate being -1.90 inches/year at AOI 16 which overlies the plugged and abandoned Liberty Gas Storage No. 002 cavern.

3. East-west displacement velocities were seen to generally indicate that lateral ground displacement is occurring toward the center of the dome. The highest eastern displacement rate was calculated as +0.96 inches/year at AOI 1 (LGS 1) and the highest westward movement was calculated as -0.63 inches/year at AOI 20 (SS 1). Both AOIs were located respectively near the western and eastern edges of the dome where the highest rates of lateral displacement were observed.

4. AOI 14 (PPG 16) was not able to be evaluated for vertical and east-west displacement due to a lack of 2-D measurement data within the AOI boundary. An evaluation of the 1-D LOS data within the AOI showed consistency of the subsidence trend over the available data timeframes. A network of corner reflectors is planned to be installed in 2024 to improve InSAR data coverage in future surveys.

5. Subsidence rates identified in the InSAR analysis agree well with the trends established through past monitoring surveys of the site. Based on the evaluation of the calculated 2-D data and the supplementary review of the 1-D LOS datasets, subsidence trends appear to be progressing as historically defined. This indicates that rates of cavern closure and other local factors of influence are continuing to act in a consistent manner at this time.

Appendix A – Map of 2-D InSAR Measurement Points and AOI Boundaries

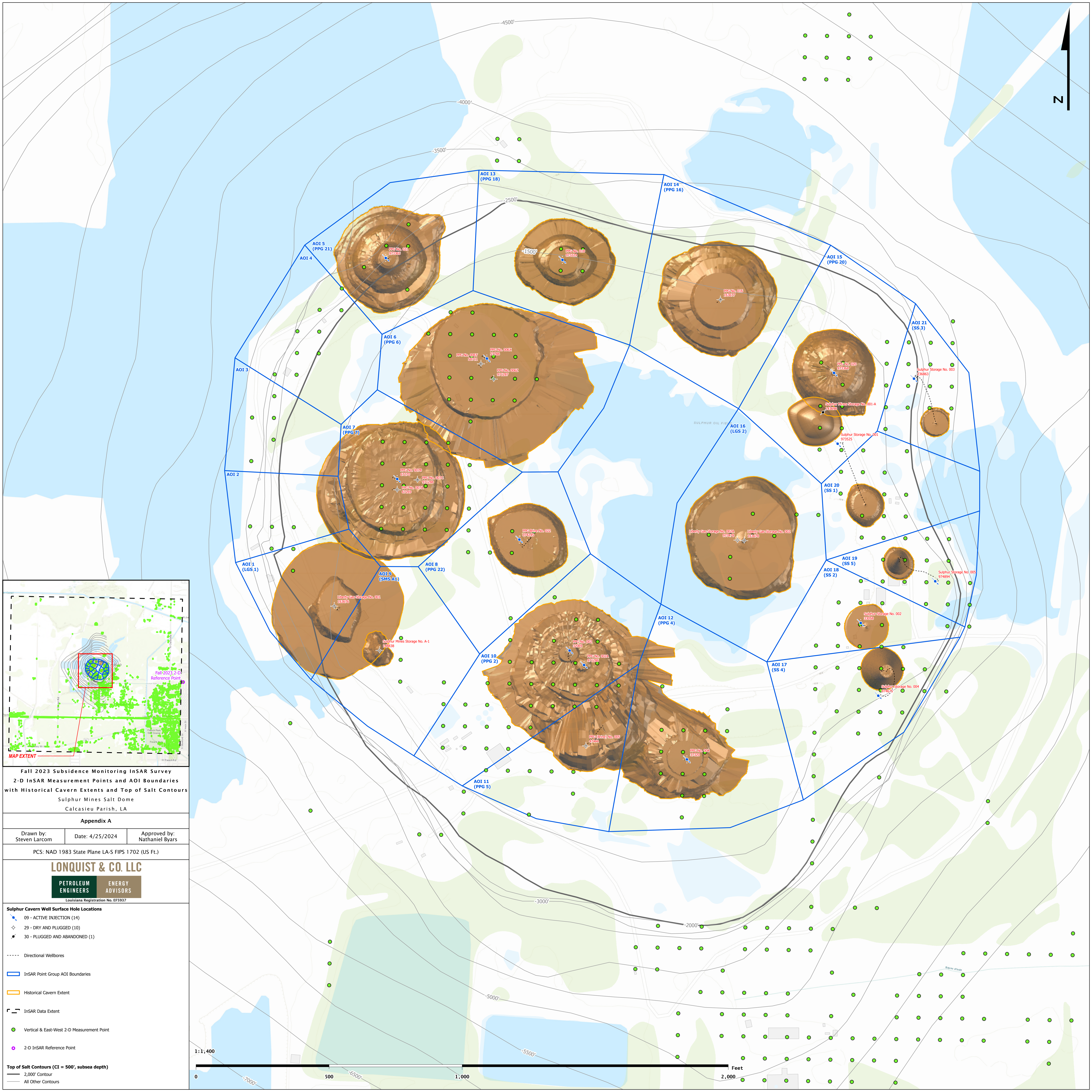

Fall 2023 Subsidence Monitoring InSAR Survey

2-D InSAR Measurement Points and AOI Boundaries

with Historical Cavern Extents and Top of Salt Contours

Sulphur Mines Salt Dome

Calcasieu Parish, LA

Appendix A

Drawn by: Steven Larcom	Date: 4/25/2024	Approved by: Nathaniel Byars

PCS: NAD 1983 State Plane LA-S FIPS 1702 (US Ft.)

LONQUIST & CO. LLC

PETROLEUM ENGINEERS | ENERGY ADVISORS

Louisiana Registration No. EF5937

Sulphur Cavern Well Surface Hole Locations

- 09 - ACTIVE INJECTION (14)
- 29 - DRY AND PLUGGED (10)
- 30 - PLUGGED AND ABANDONED (1)

Directional Wellbores

InSAR Point Group AOI Boundaries

Historical Cavern Extent

InSAR Data Extent

Vertical & East-West 2-D Measurement Point

2-D InSAR Reference Point

Top of Salt Contours (CI = 500', subsea depth)

- 2,000' Contour
- All Other Contours

Appendix B – Vertical & East-West Displacement Time Series – AOI Point Groups

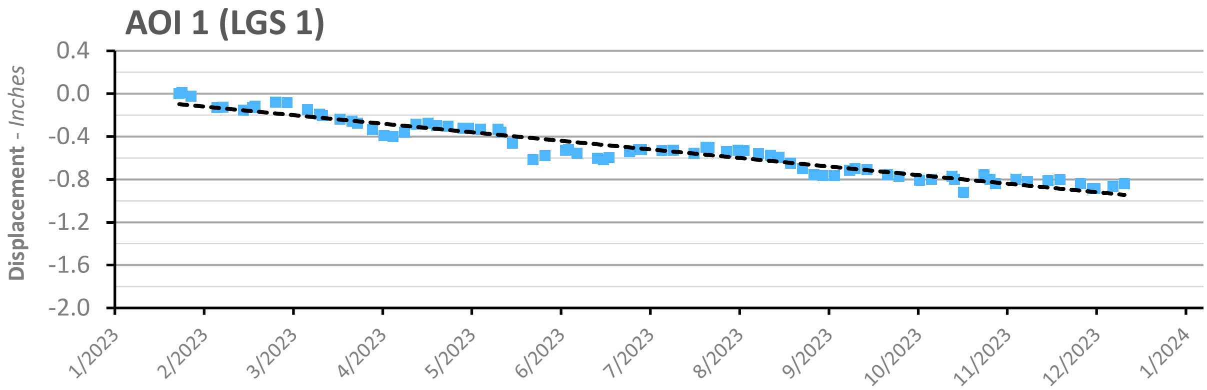
AOI 1 (LGS 1)
Displacement - Inches
0.4
0.0
-0.4
-0.8
-1.2
-1.6
-2.0
1/2023
2/2023
3/2023
4/2023
5/2023
6/2023
7/2023
8/2023
9/2023
10/2023
11/2023
12/2023
1/2024

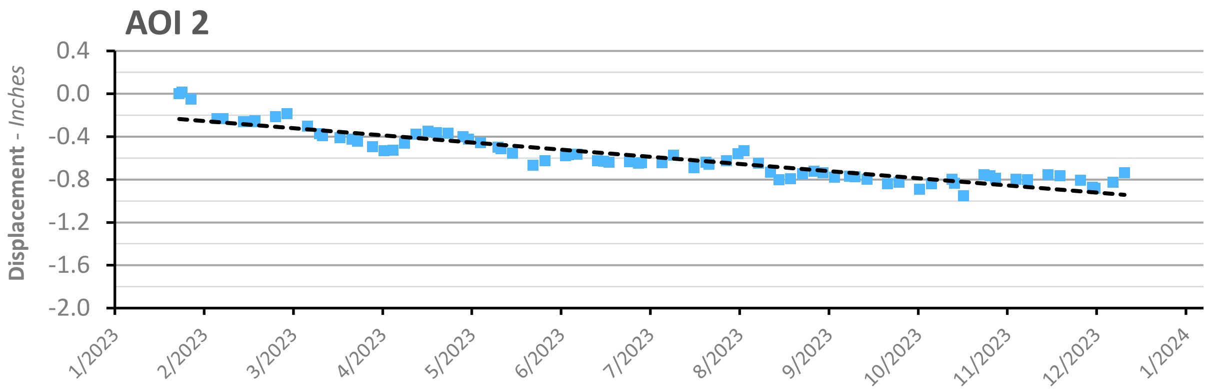
AOI 2
Displacement - Inches
0.4
0.0
-0.4
-0.8
-1.2
-1.6
-2.0
1/2023
2/2023
3/2023
4/2023
5/2023
6/2023
7/2023
8/2023
9/2023
10/2023
11/2023
12/2023
1/2024

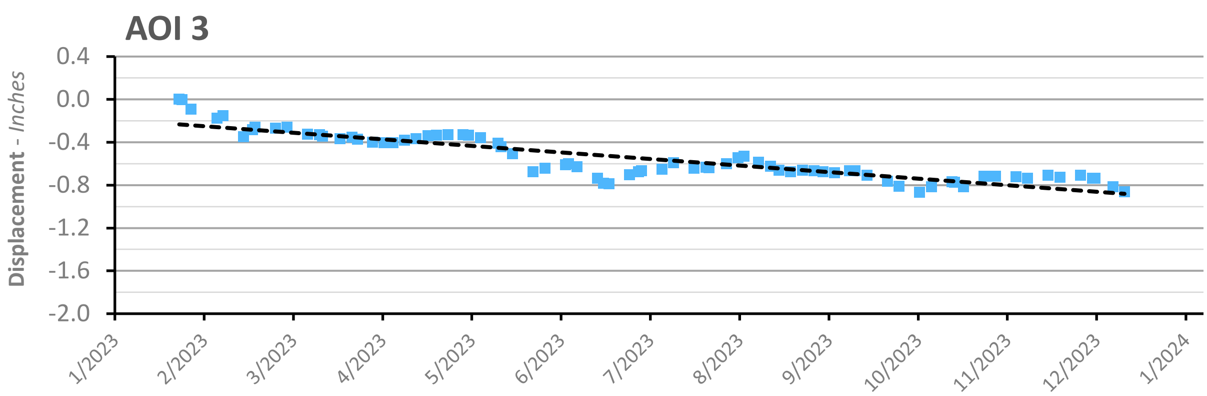
AOI 3
Displacement - Inches
0.4
0.0
-0.4
-0.8
-1.2
-1.6
-2.0
1/2023
2/2023
3/2023
4/2023
5/2023
6/2023
7/2023
8/2023
9/2023
10/2023
11/2023
12/2023
1/2024

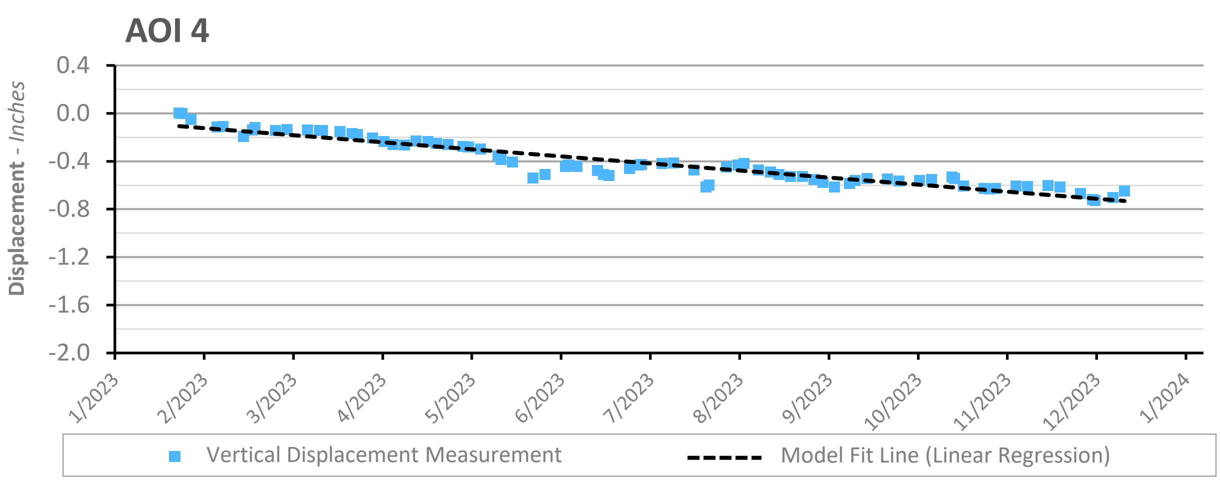
AOI 4
Displacement - Inches
0.4
0.0
-0.4
-0.8
-1.2
-1.6
-2.0
1/2023
2/2023
3/2023
4/2023
5/2023
6/2023
7/2023
8/2023
9/2023
10/2023
11/2023
12/2023
1/2024
Vertical Displacement Measurement
Model Fit Line (Linear Regression)

Averaged Vertical Displacement Time Series - AOI Point Groups

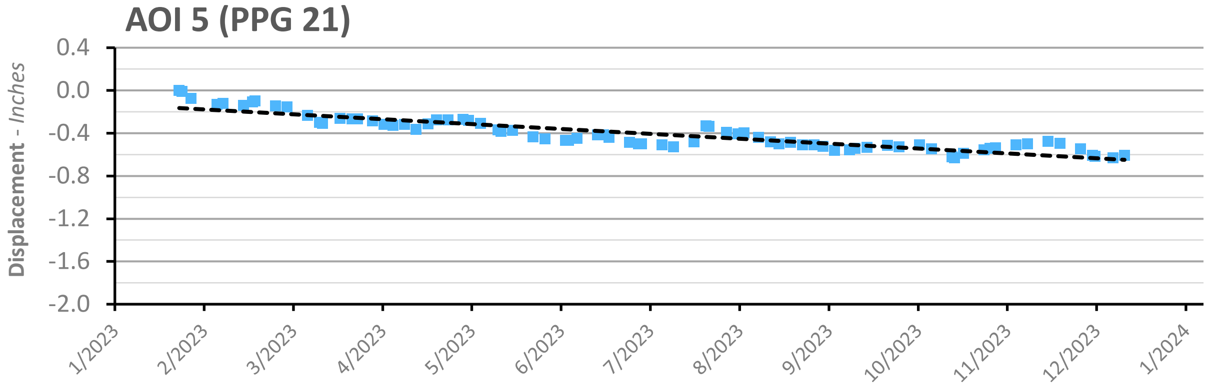

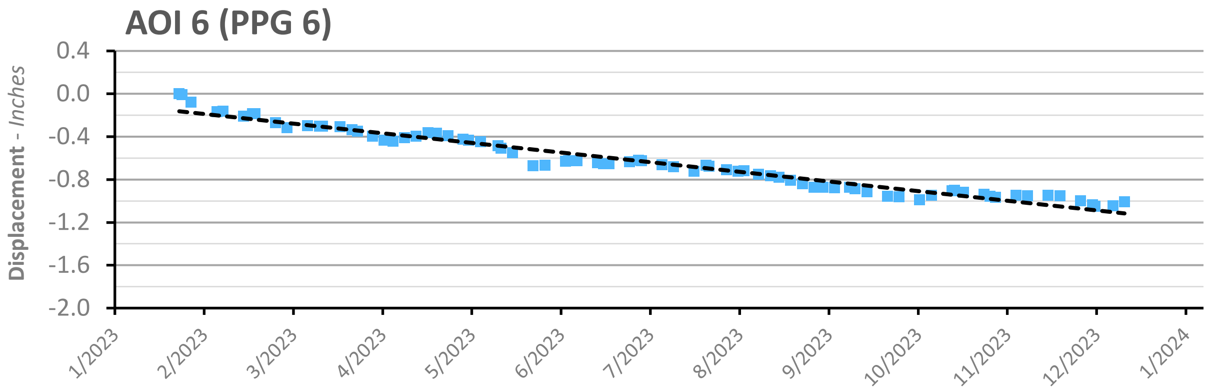

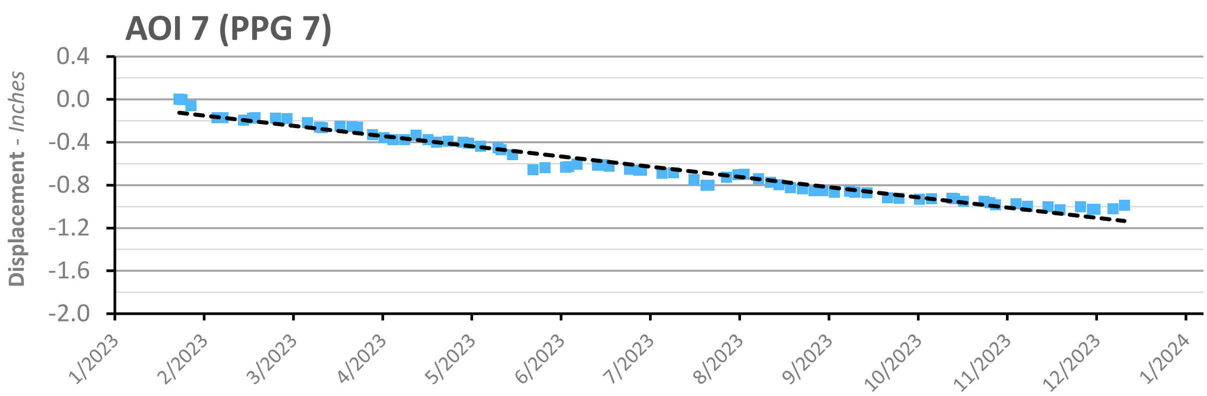

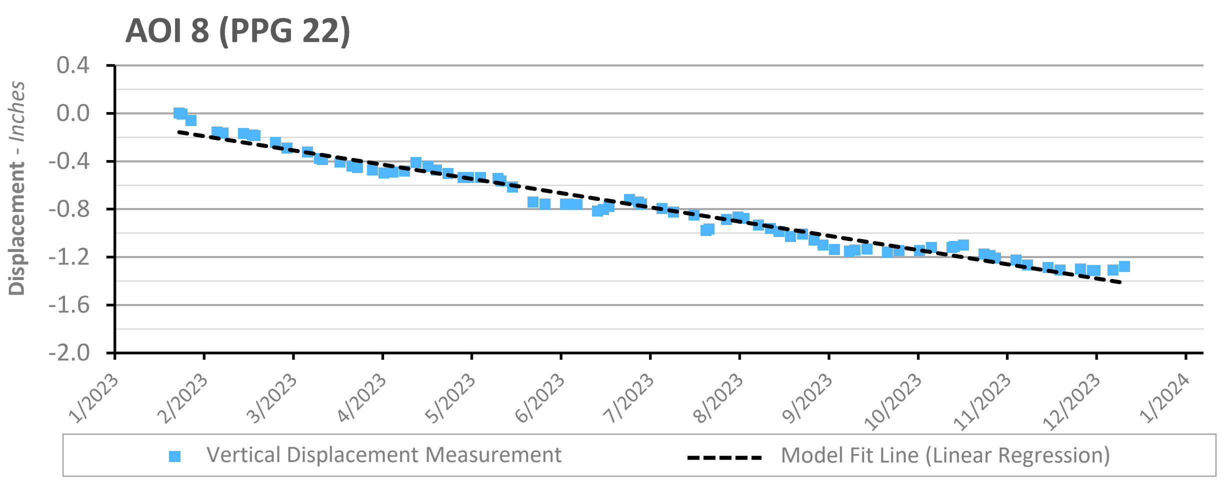

Averaged Vertical Displacement Time Series - AOI Point Groups

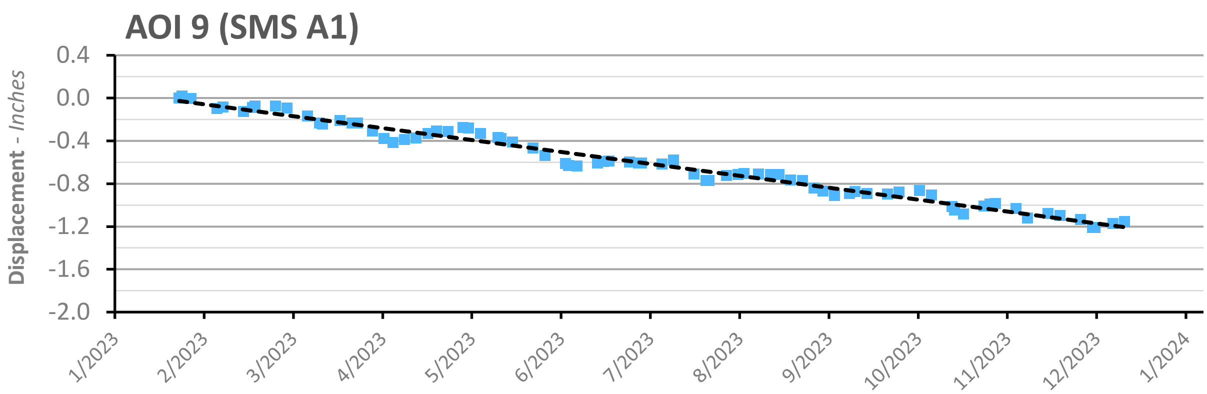

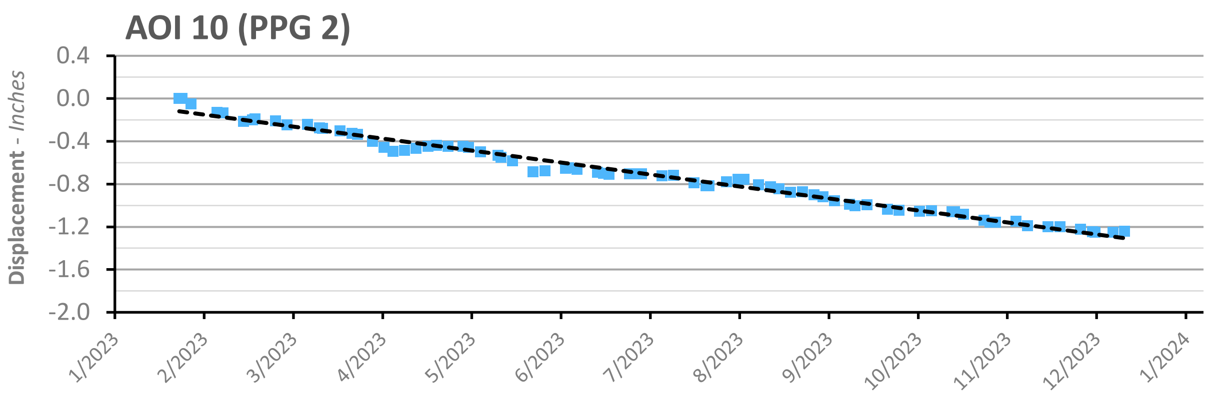

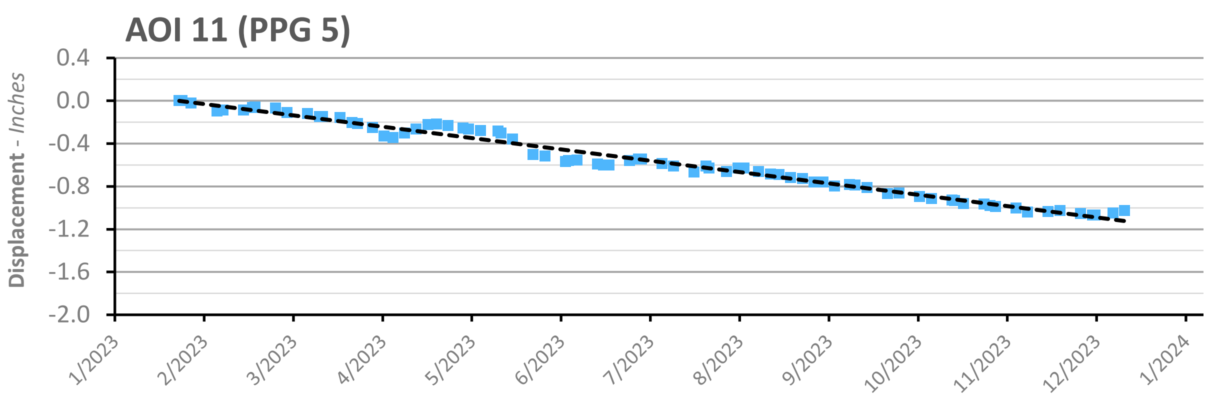

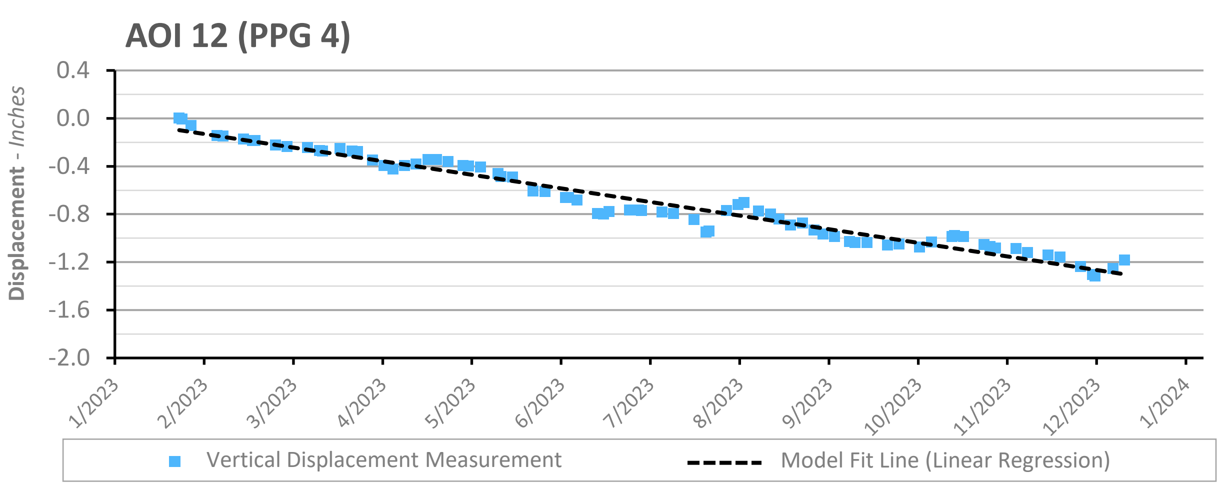

Averaged Vertical Displacement Time Series - AOI Point Groups

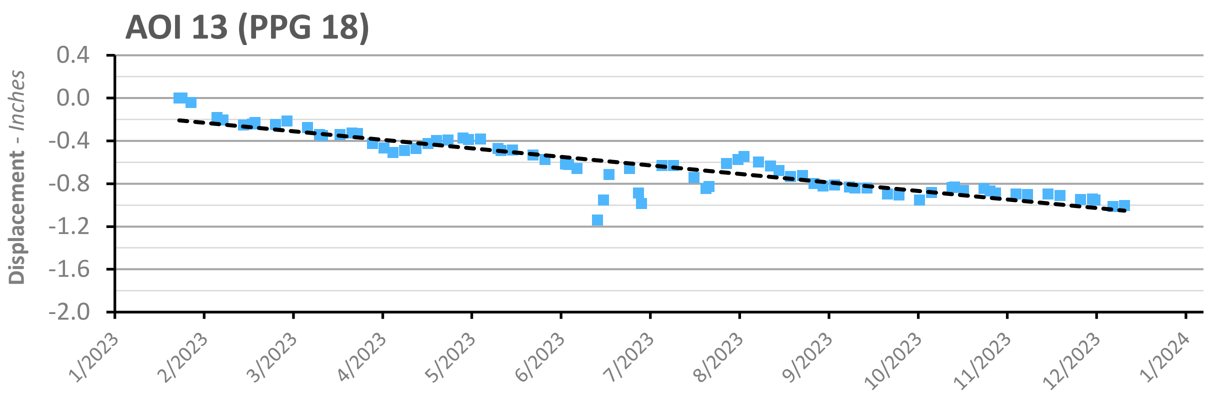

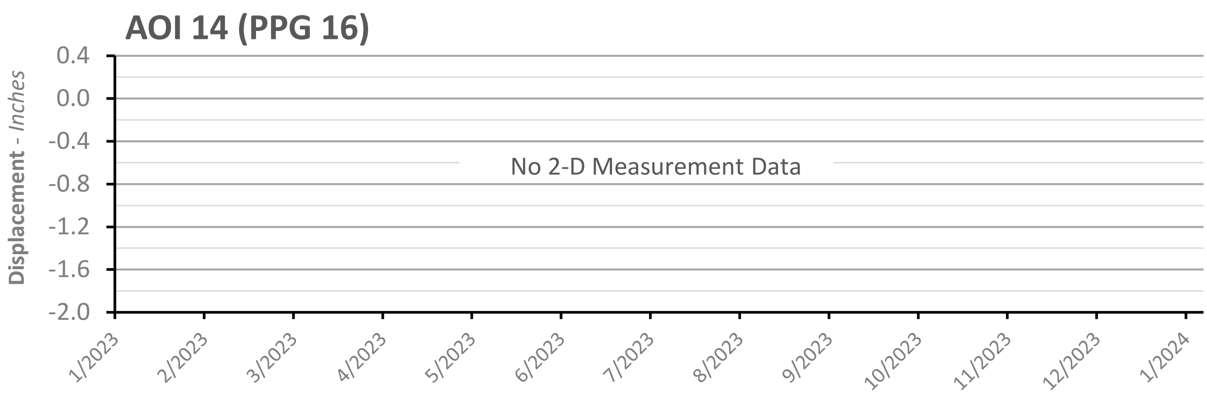

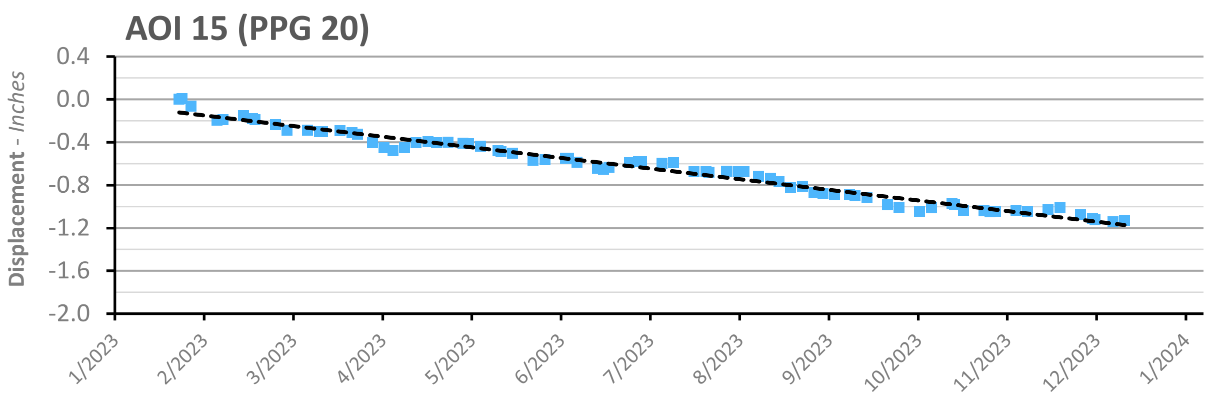

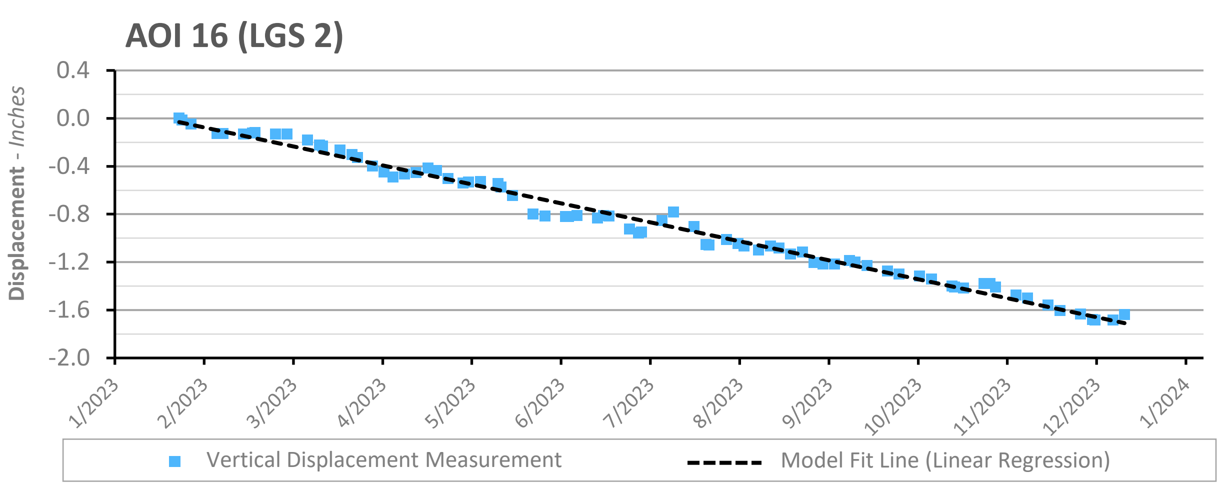

Averaged Vertical Displacement Time Series - AOI Point Groups

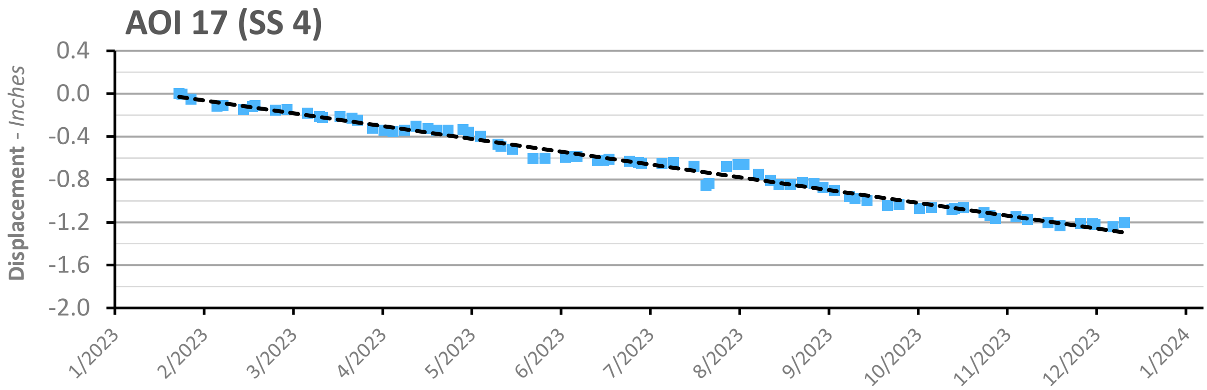

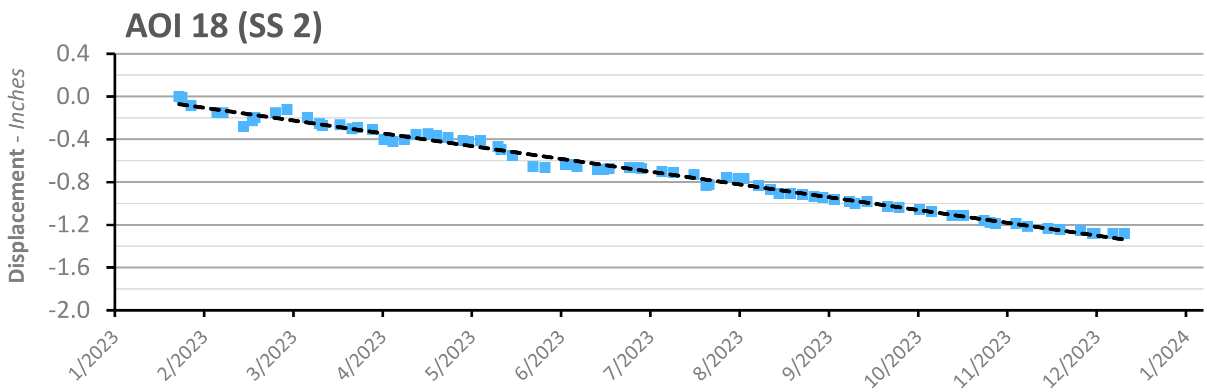

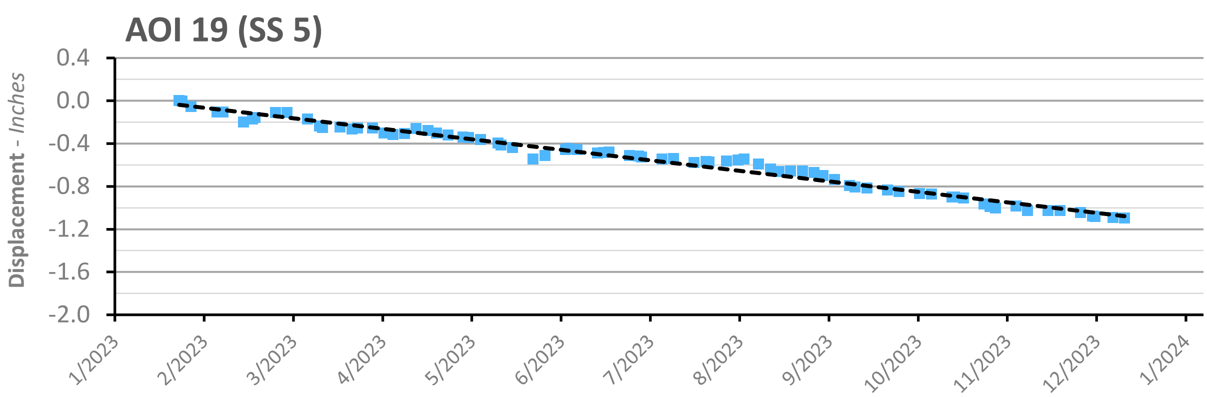

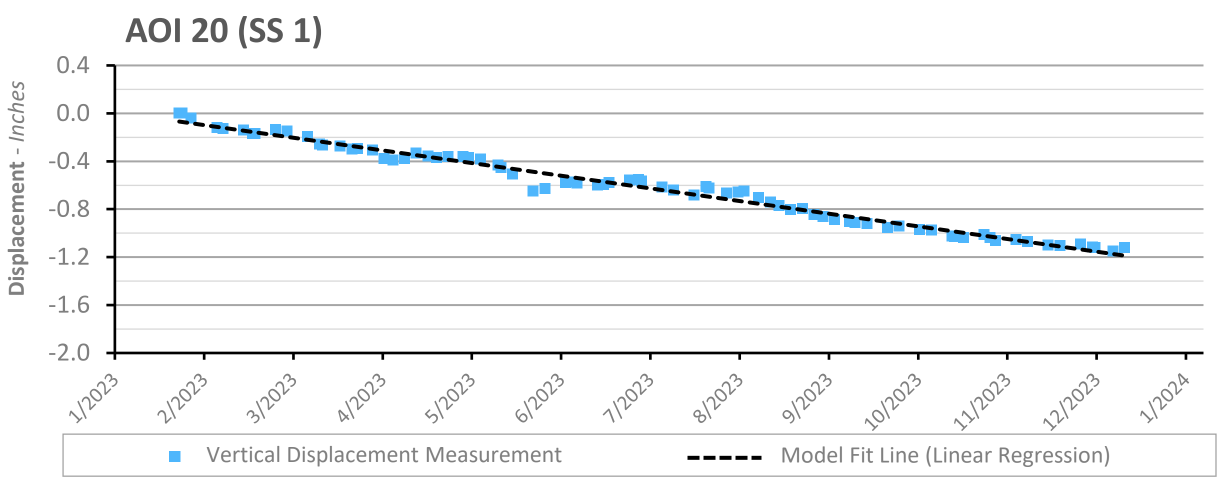

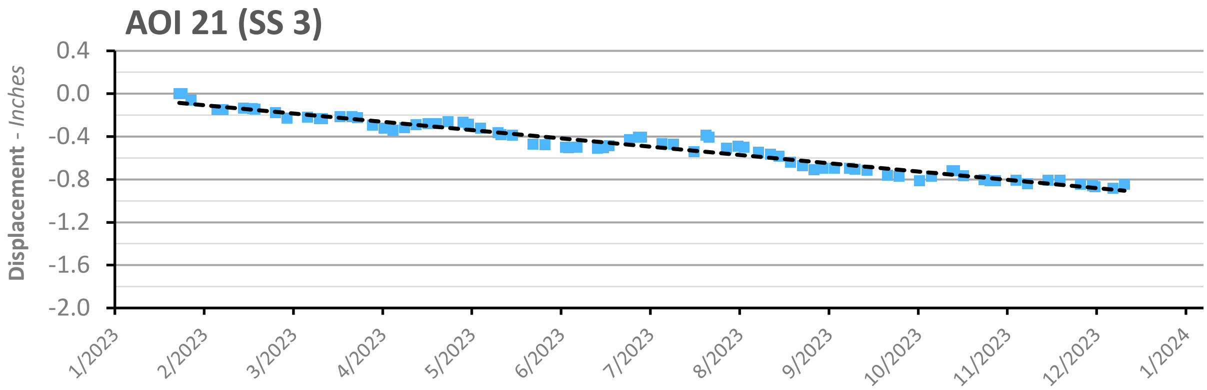

Vertical Displacement Measurement

Model Fit Line (Linear Regression)

Averaged East-West Displacement Time Series - AOI Point Groups

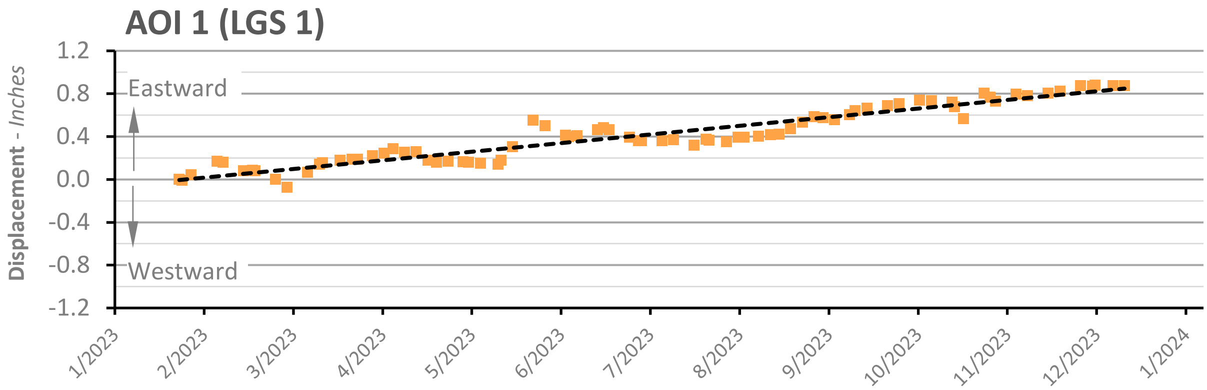

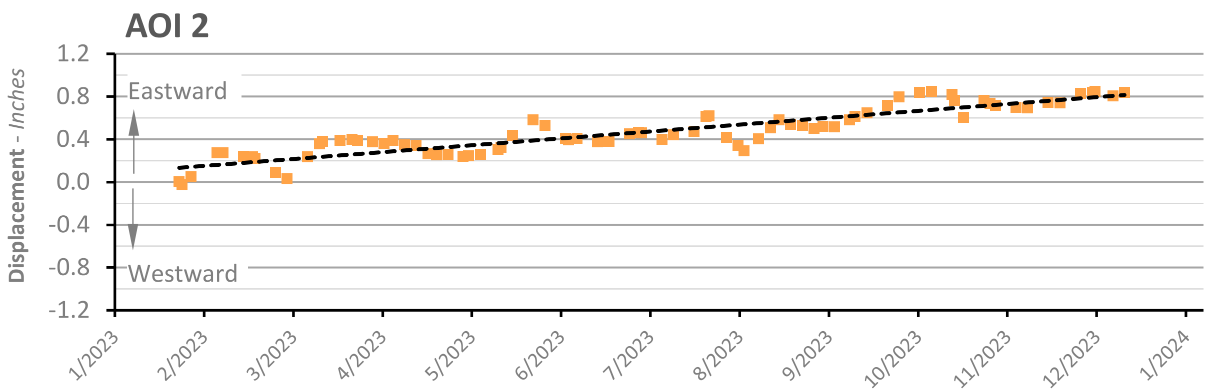

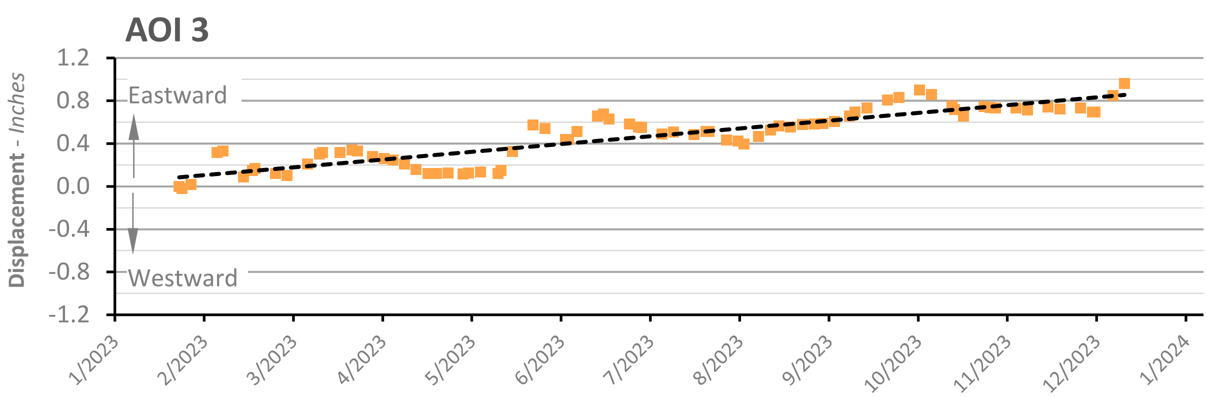

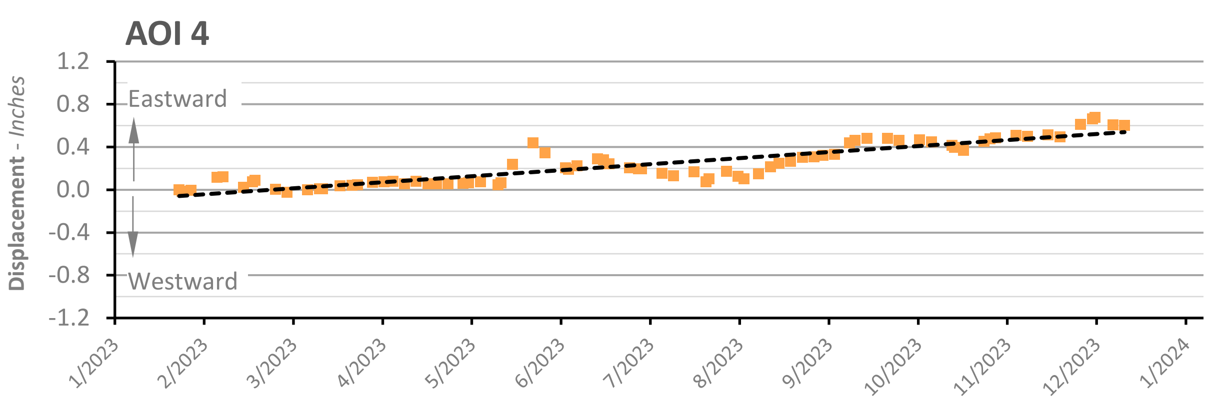

East-West Displacement Measurement   Model Fit Line (Linear Regression)

Averaged East-West Displacement Time Series - AOI Point Groups

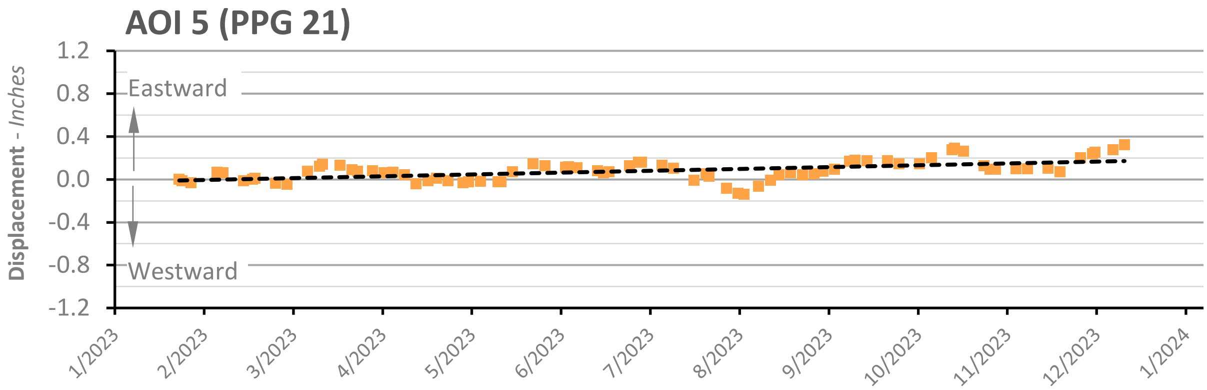

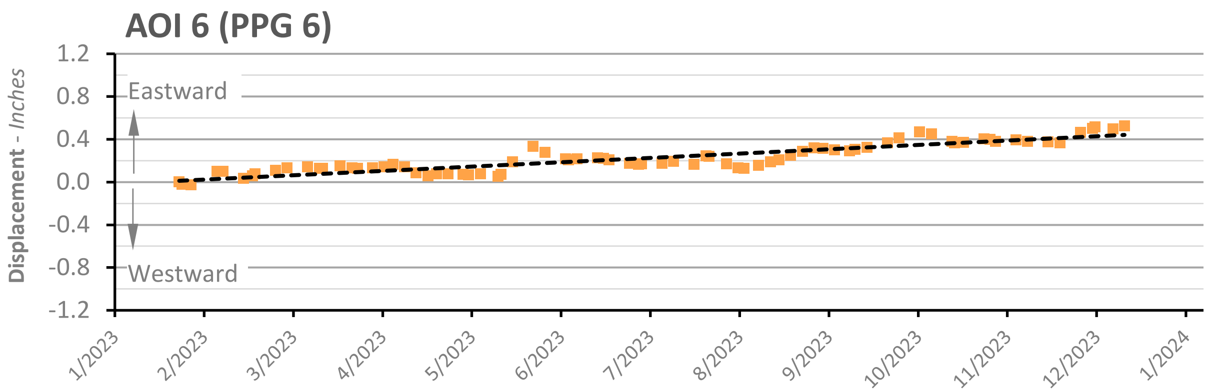

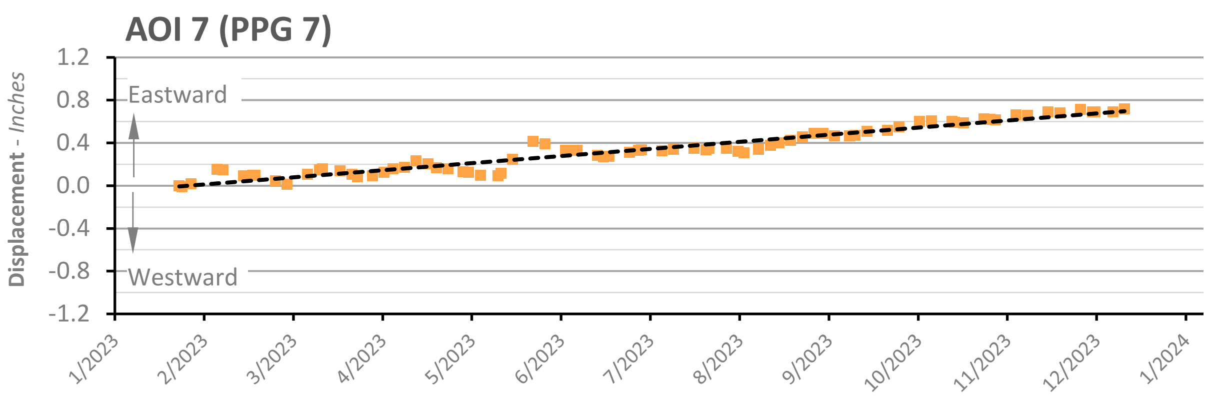

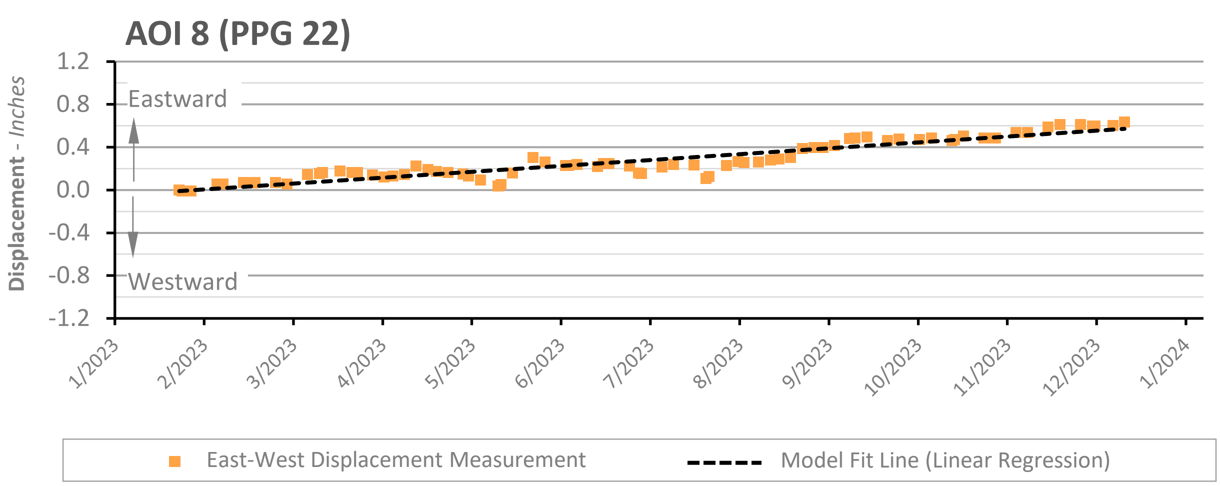

Averaged East-West Displacement Time Series - AOI Point Groups

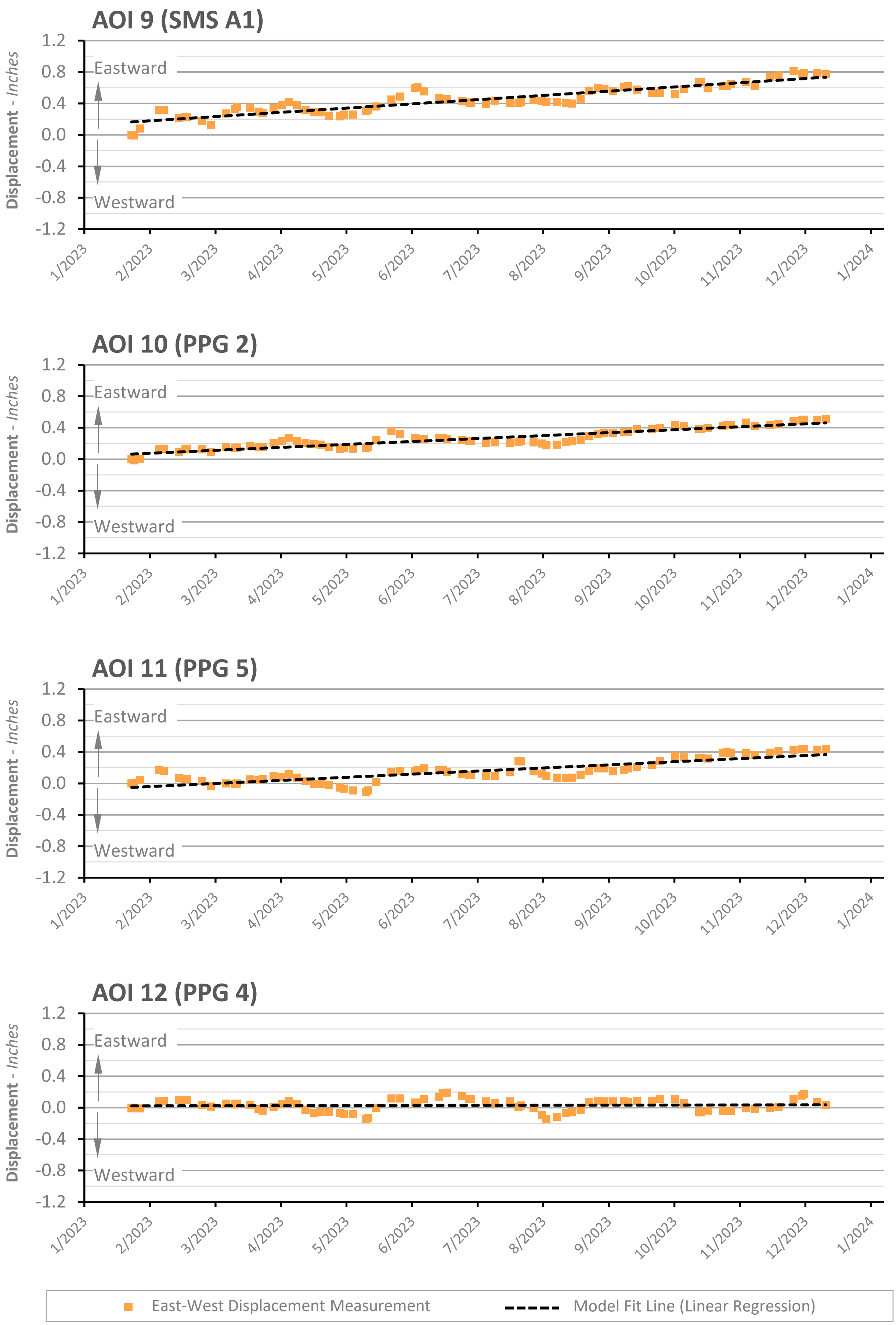

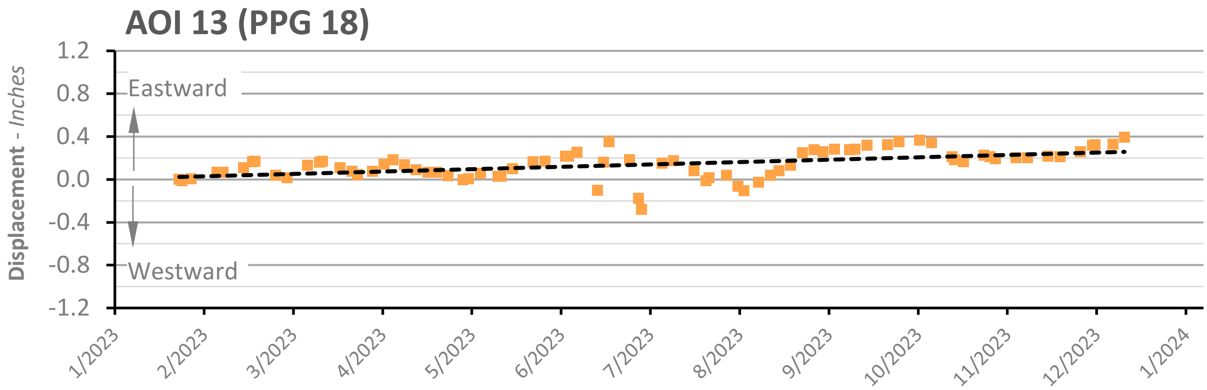
AOI 13 (PPG 18)
Displacement - Inches
Eastward
Westward
1.2
0.8
0.4
0.0
-0.4
-0.8
-1.2
1/2023
2/2023
3/2023
4/2023
5/2023
6/2023
7/2023
8/2023
9/2023
10/2023
11/2023
12/2023
1/2024

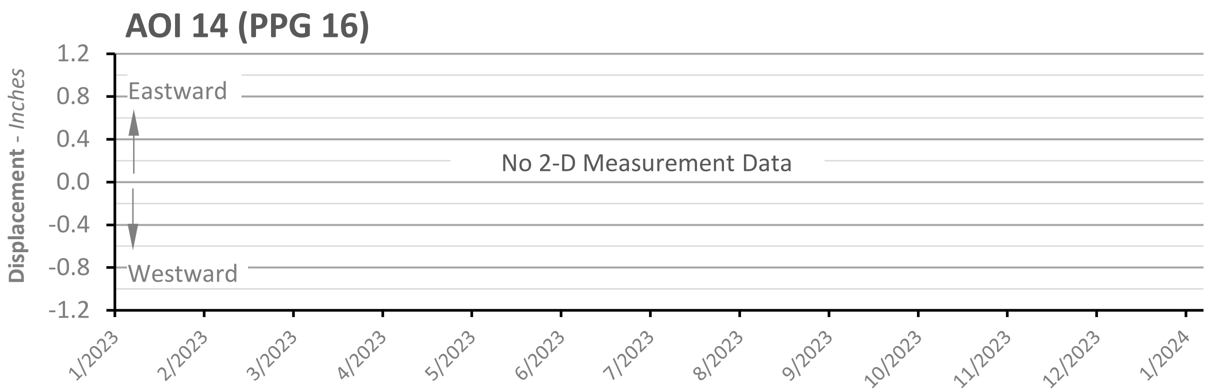
AOI 14 (PPG 16)
Displacement - Inches
Eastward
Westward
No 2-D Measurement Data
1.2
0.8
0.4
0.0
-0.4
-0.8
-1.2
1/2023
2/2023
3/2023
4/2023
5/2023
6/2023
7/2023
8/2023
9/2023
10/2023
11/2023
12/2023
1/2024

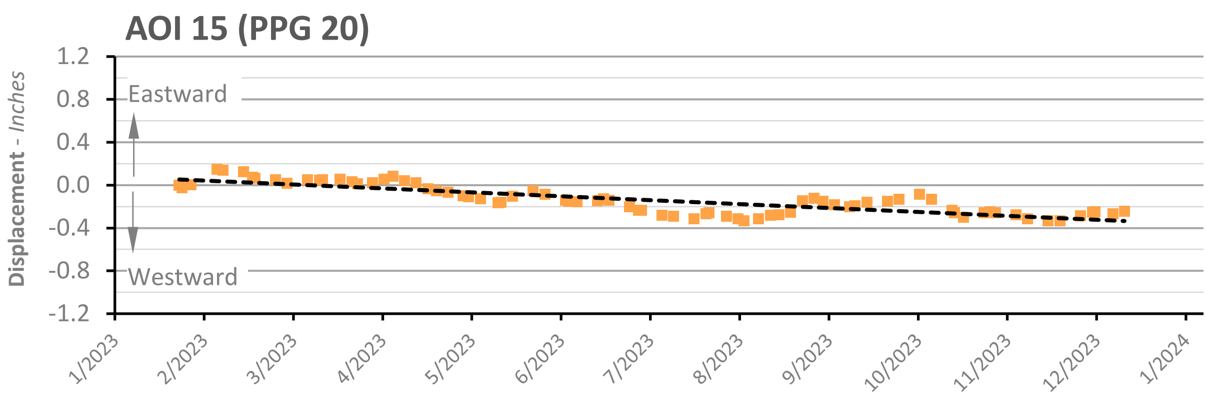
AOI 15 (PPG 20)
Displacement - Inches
Eastward
Westward
1.2
0.8
0.4
0.0
-0.4
-0.8
-1.2
1/2023
2/2023
3/2023
4/2023
5/2023
6/2023
7/2023
8/2023
9/2023
10/2023
11/2023
12/2023
1/2024

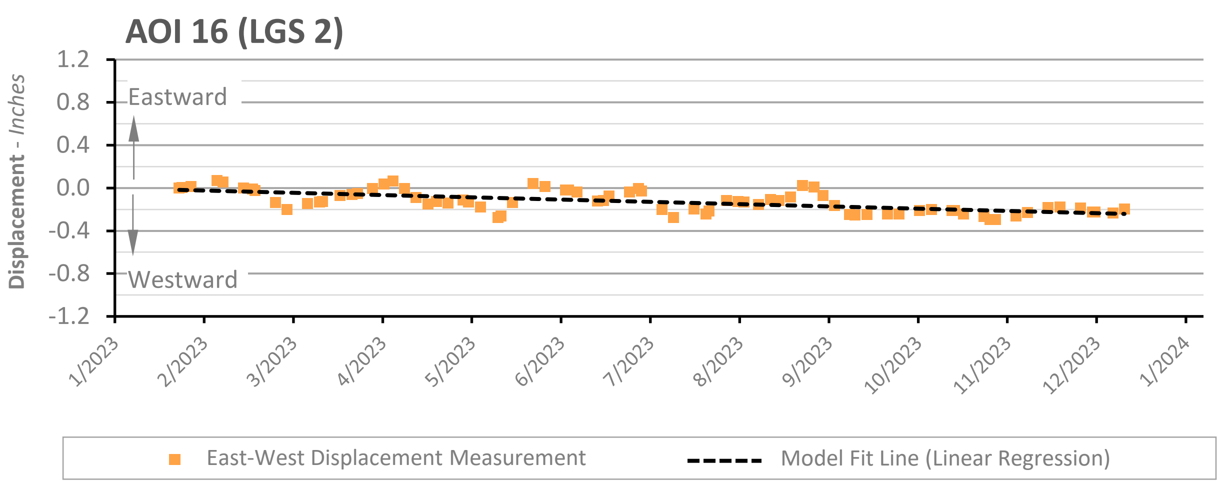
AOI 16 (LGS 2)
Displacement - Inches
Eastward
Westward
1.2
0.8
0.4
0.0
-0.4
-0.8
-1.2
1/2023
2/2023
3/2023
4/2023
5/2023
6/2023
7/2023
8/2023
9/2023
10/2023
11/2023
12/2023
1/2024
East-West Displacement Measurement
Model Fit Line (Linear Regression)

Averaged East-West Displacement Time Series - AOI Point Groups

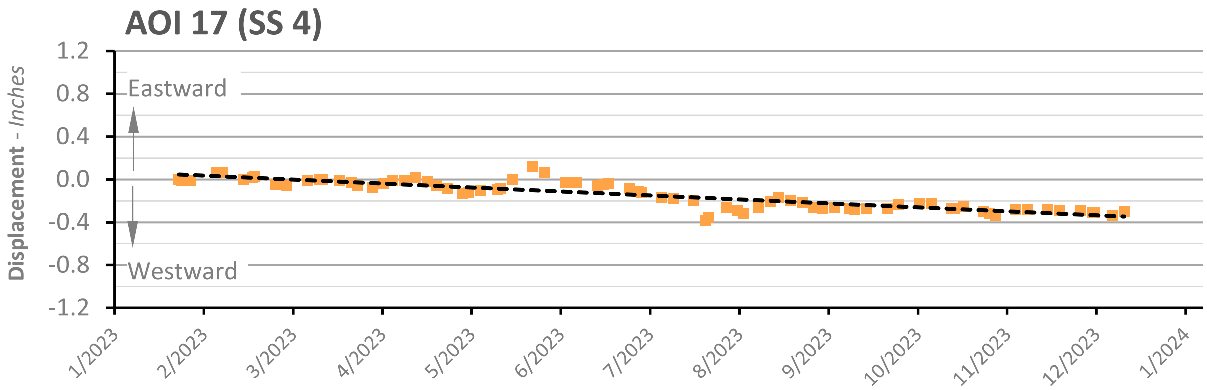

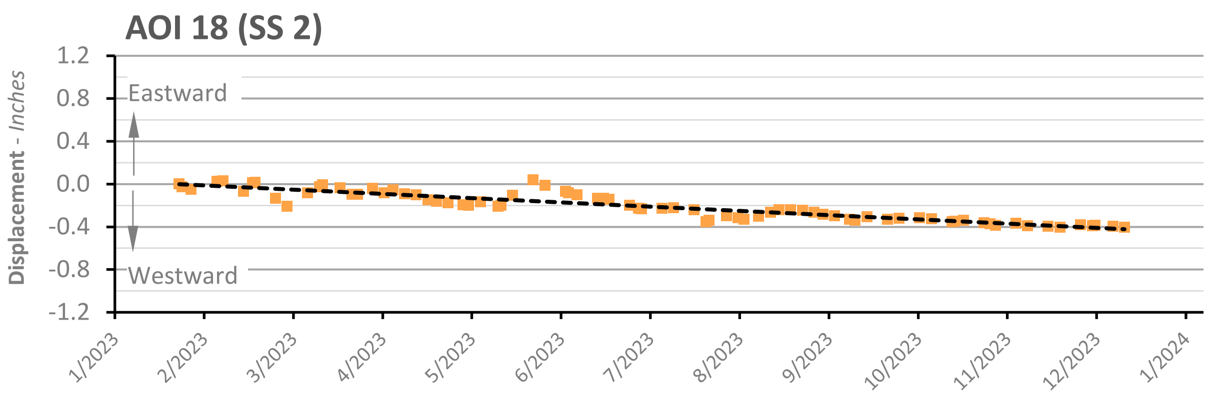

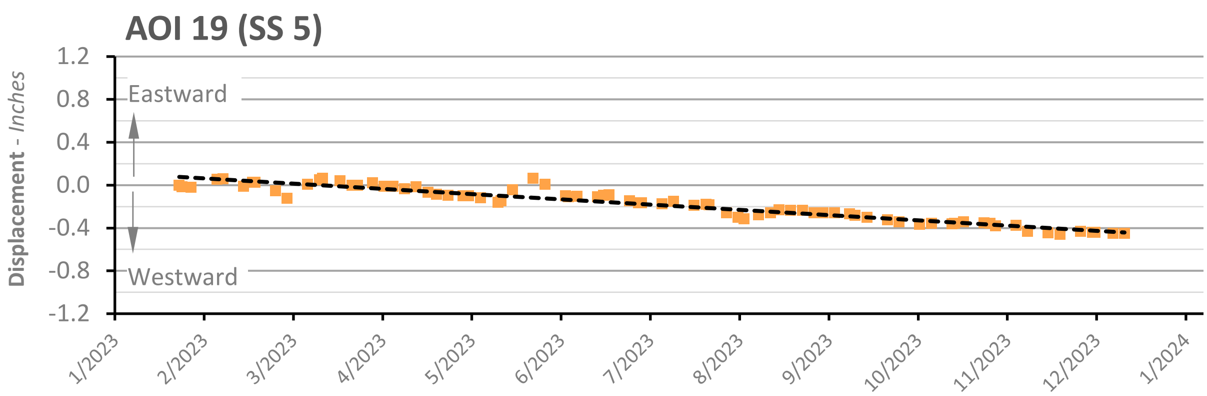

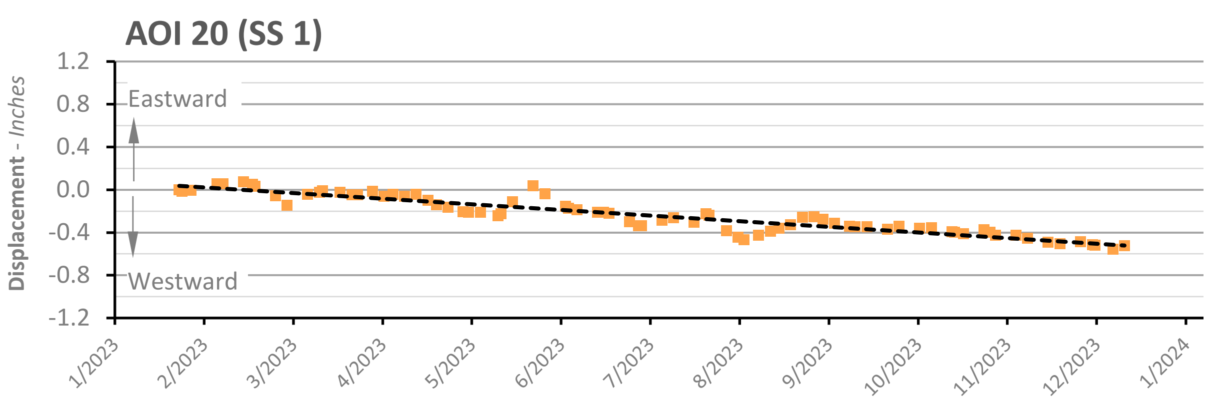

East-West Displacement Measurement — Model Fit Line (Linear Regression)

Averaged East-West Displacement Time Series - AOI Point Groups

Appendix C – Map of Vertical Displacement Velocity Contours (Inches/year)

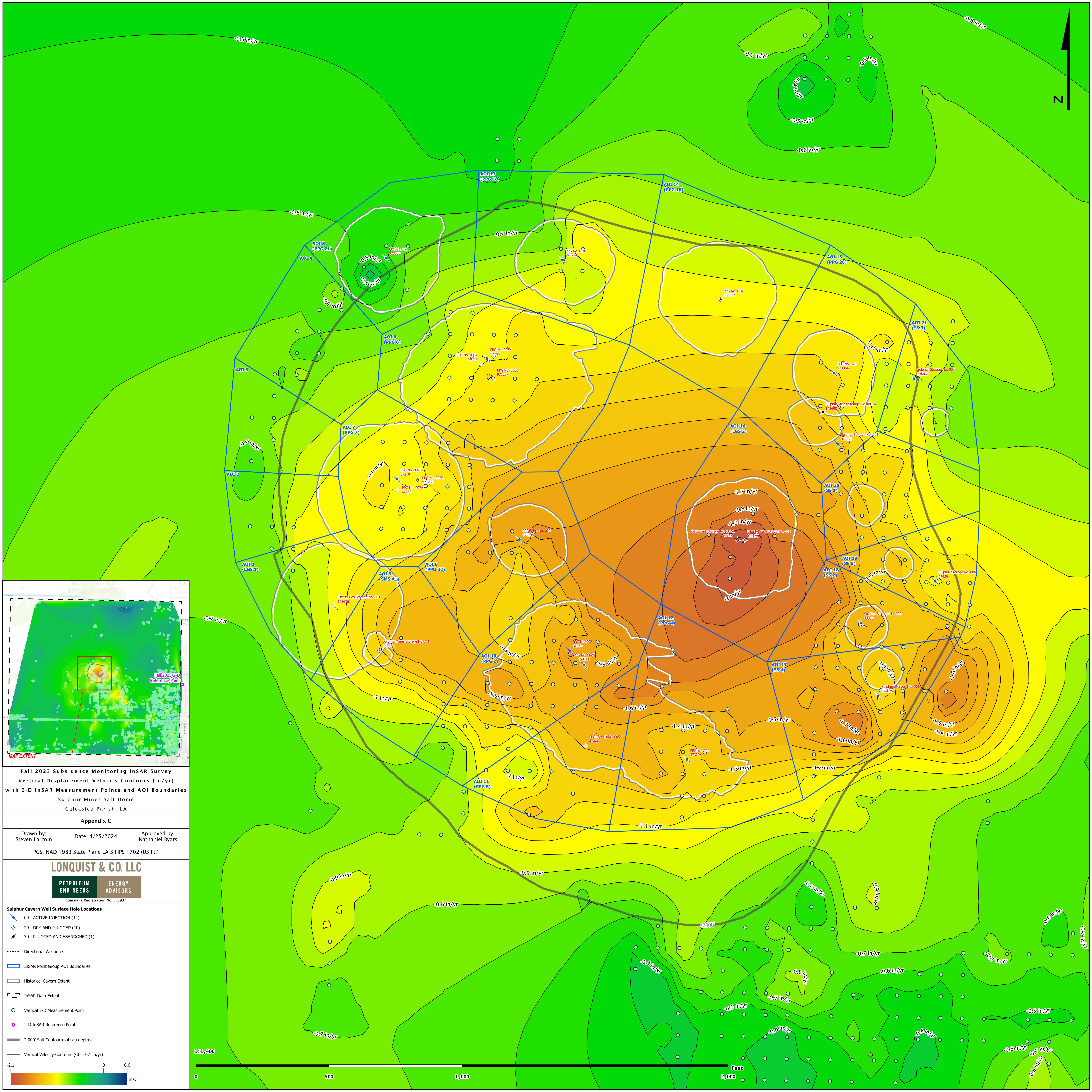
Fall 2023 Subsidence Monitoring InSAR Survey
Vertical Displacement Velocity Contours (in/yr)
with 2-D InSAR Measurement Points and AOI Boundaries
Sulphur Mines Salt Dome
Calcasieu Parish, LA
Appendix C
Drawn by: Steven Larcom
Date: 4/25/2024
Approved by: Nathaniel Byars
PCS: NAD 1983 State Plane LA-S FIPS 1702 (US Ft.)
LONQUIST & CO. LLC
PETROLEUM ENGINEERS
ENERGY ADVISORS
Louisiana Registration No. EF5937
Sulphur Cavern Well Surface Hole Locations
09 - ACTIVE INJECTION (14)
29 - DRY AND PLUGGED (10)
30 - PLUGGED AND ABANDONED (1)
Directional Wellbores
InSAR Point Group AOI Boundaries
Historical Cavern Extent
InSAR Data Extent
Vertical 2-D Measurement Point
2-D InSAR Reference Point
2,000' Salt Contour (subsea depth)
Vertical Velocity Contours (CI = 0.1 in/yr)
-2.1
0
0.6
in/yr
MAP EXTENT
Fall 2023 2-D Reference Point
1:1,400
Feet
0
500
1,000
2,000
N
AOI 1 (LGS 1)
AOI 2
AOI 3
AOI 4
AOI 5 (PPG 21)
AOI 6 (PPG 6)
AOI 7 (PPG 7)
AOI 8 (PPG 22)
AOI 9 (SMS A1)
AOI 10 (PPG 2)
AOI 11 (PPG 5)
AOI 12 (PPG 4)
AOI 13 (PPG 18)
AOI 14 (PPG 16)
AOI 15 (PPG 20)
AOI 16 (LGS 2)
AOI 17 (SS 4)
AOI 18 (SS 2)
AOI 19 (SS 5)
AOI 20 (SS 1)
AOI 21 (SS-3)
-0.5 in/yr
-0.6 in/yr
-0.7 in/yr
-0.8 in/yr
-0.9 in/yr
-1 in/yr
-1.1 in/yr
-1.2 in/yr
-1.3 in/yr
-1.4 in/yr
-1.5 in/yr
-1.6 in/yr
-1.7 in/yr
-1.8 in/yr
-1.9 in/yr
-2 in/yr
-0.4 in/yr
-2000'

Appendix D – Map of East-West Displacement Velocity Contours (Inches/year)

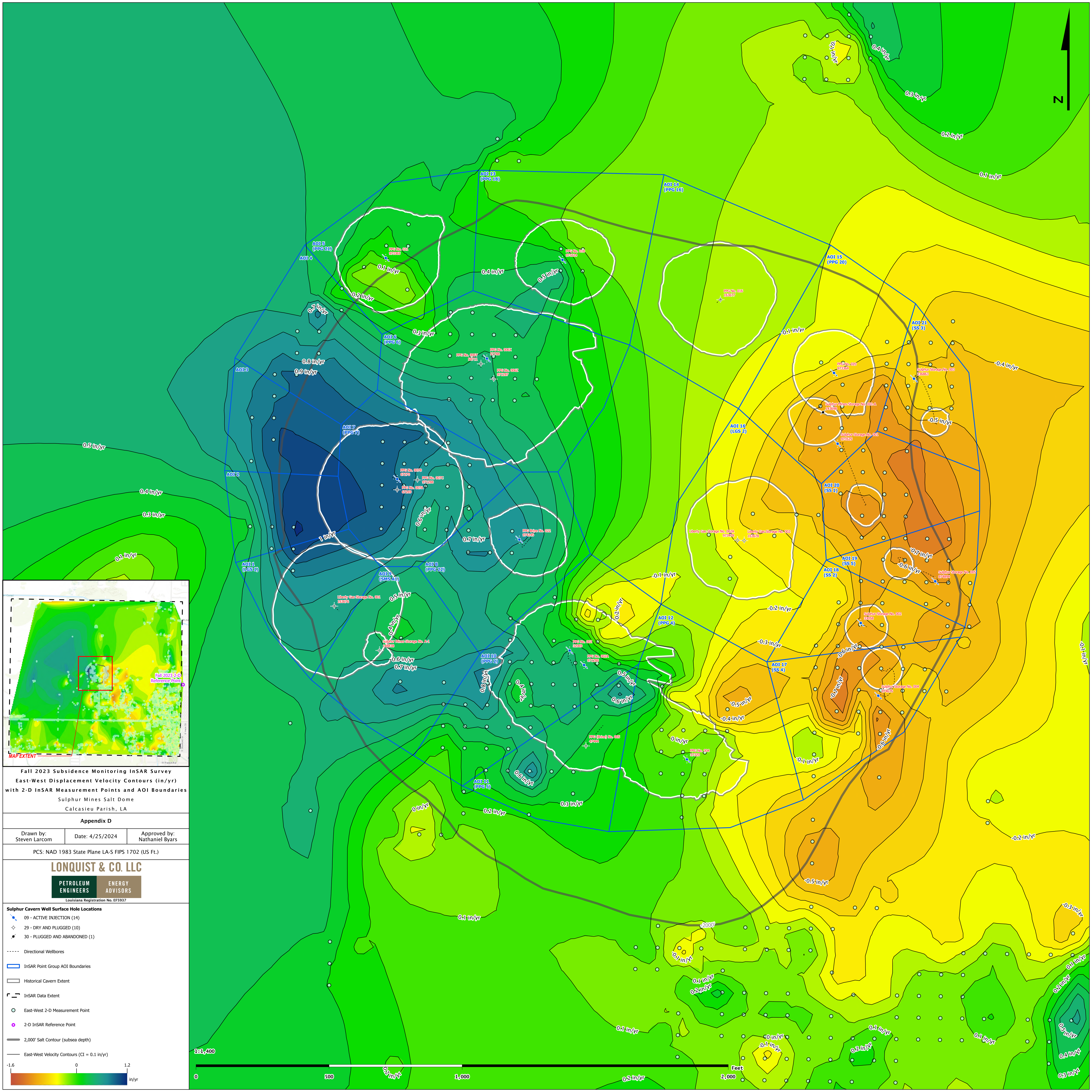

Fall 2023 Subsidence Monitoring InSAR Survey
East-West Displacement Velocity Contours (in/yr)
with 2-D InSAR Measurement Points and AOI Boundaries
Sulphur Mines Salt Dome
Calcasieu Parish, LA

Appendix D

Drawn by: Steven Larcom	Date: 4/25/2024	Approved by: Nathaniel Byars

PCS: NAD 1983 State Plane LA-S FIPS 1702 (US Ft.)

LONQUIST & CO. LLC
PETROLEUM ENGINEERS
ENERGY ADVISORS
Louisiana Registration No. EF5937

Sulphur Cavern Well Surface Hole Locations

- 09 - ACTIVE INJECTION (14)
- 29 - DRY AND PLUGGED (10)
- 30 - PLUGGED AND ABANDONED (1)
- Directional Wellbores
- InSAR Point Group AOI Boundaries
- Historical Cavern Extent
- InSAR Data Extent
- East-West 2-D Measurement Point
- 2-D InSAR Reference Point
- 2,000' Salt Contour (subsea depth)
- East-West Velocity Contours (CI = 0.1 in/yr)

-1.6 0 1.2 in/yr

Appendix E – TRE-Altamira InSAR Analysis of Ground Displacement

InSAR Analysis of Ground Displacement over Sulphur Mines, Louisiana

TRE ALTAMIRA
A CLS Group Company

December 2023
Technical Report

Report Specifications

Client:	**Lonquist & Co. LLC**
Attention:	Nathaniel Byars, P.E.
Address:	12912 Hill Country Blvd. Suite F-200, Austin Texas 78738

Reference:	
Title:	InSAR Analysis of Ground Displacement over Sulphur Mines, Louisiana – December 2024
TRE ALTAMIRA Delivery Reference:	JO23-2104-CA
Client Reference (Proposal Reference)	TRE Ref: TREA_LON_2022_019R2

Prepared by:	**TRE ALTAMIRA Inc.**
Address:	#410 - 475 West Georgia Street Vancouver, BC, V6B 4M9, Canada
Author:	Hannah Raffler
Verified and Approved by:	Giacomo Falorni
Date:	30 April 2024
Document Number and Version:	1.2

Executive Summary

TRE Altamira Inc. is monitoring ground displacement at the Sulphur Mines Salt Dome in Louisiana, USA, for Lonquist & Co. LLC. This monitoring employs Interferometric SAR (InSAR) technology, utilizing both low-resolution Sentinel (SNT) and high-resolution TerraSAR-X (TSX)/PAZ satellite imagery.

The monitoring plan delivers frequent ground displacement updates aligned with satellite image acquisitions. This includes two high-resolution TerraSAR-X/PAZ updates every 11 days (alternating 4 and 7 days) from a descending orbit, lower resolution Sentinel updates every 12 days from an ascending orbit, and 2-D (vertical and E-W) updates also every 12 days.

This Technical Report presents findings up to the end of 2023, focusing on areas of interest specified by Lonquist.

Key Findings (see Section 4 and for additional information):

- Subsidence observed across the entire dome, with the highest rates (-1.90 in/yr) on the east side (AOI 16).
- Westward displacement concentrated on the east side (AOI 21), with the highest rate at -0.63 in/yr.
- Eastward displacement concentrated on the west side, reaching +0.97 in/yr.
- AOIs 16, 17, and 18 exhibit the highest subsidence rates.
- AOIs 1, 3, and 7 show the most significant lateral (eastward) displacement.

Additional Notes:

SNT and TSX/PAZ satellites continue to maintain their image acquisition frequencies (12 and 11 days respectively) and ongoing monitoring continues with that frequency.

TREA recommends periodically resetting the Sulphur Mines baseline (approximately every 12-24 months) to optimize measurement quality. This interval is influenced by data quality, coverage, and local conditions.

Table of Contents

Acronyms and Abbreviations

AOI	Area of Interest
ATS	Average Time Series
CR	Corner Reflector
DEM	Digital Elevation Model
DInSAR	Differential Interferometric SAR
DS	Distributed Scatterer(s)
GIS	Geographic Information System
InSAR	Interferometric Synthetic Aperture Radar
LOS	Line of Sight
MP	Measurement Point
NR	Natural Reflector
PS	Permanent Scatterer(s)
SAR	Synthetic Aperture Radar
SNT	Sentinel Satellite
SqueeSAR®	The most recent InSAR algorithm patented by TRE
TS	Time Series
TSX	TerraSAR-X satellite

1. Introduction

TRE Altamira Inc. (TREA) is contracted by Lonquist & Co. LLC (Lonquist) to monitor ground displacement at the Sulphur Mines Salt Dome in Louisiana, USA (Figure 1). This monitoring utilizes Interferometric SAR (InSAR) technology and our proprietary SqueeSAR® algorithm to provide precise measurements of ground movement over the assets and caverns on the salt dome, with the area of interest (AOI) covering 13.70 mi². We process data from both low-resolution Sentinel (SNT) imagery (65 x 16 ft resolution) and high-resolution TerraSAR-X (TSX)/PAZ satellites (3 x 3 ft resolution) for the analysis.

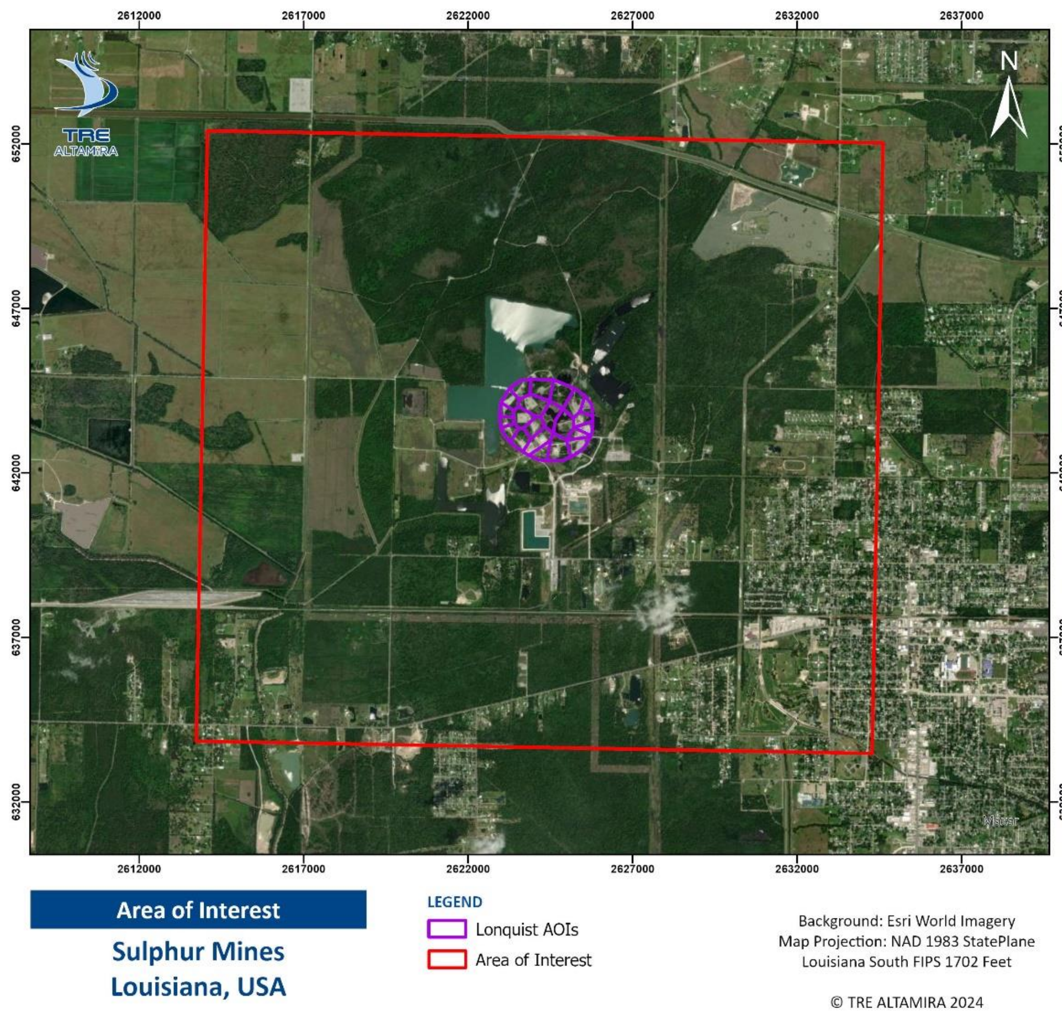

Figure 1. Area of interest (red) and focus areas of interest provided by Lonquist (purple).

To optimize monitoring, we initiated the project with a baseline analysis using 16 images (January 2023 – April 2023). Due to evolving ground conditions, we recommended a baseline reset in September 2023, utilizing 41 images for improved data quality and robustness. This reset has improved measurement quality across the AOI. The data coverage has remained consistent over the main area of interest for both baselines and has decreased over peripheral areas, where more ground surface variations occur. The re-baselined data forms the basis for the current monitoring.

The current monitoring plan delivers:

- High-resolution TSX/PAZ updates every 4 and 7 days.
- Sentinel updates every 12 days.
- 2-D (vertical and E-W) updates every 12 days.

Note that SNT updates, and hence the 2-D results, depend on the satellite acquisition plan, which is controlled by the European Space Agency.

This Technical Report presents the findings up to the end of 2023 (Update 2024-01-02 TSX/PAZ and Update 2023-12-17 SNT/2-D) with a special focus on Lonquist's designated areas of interest.

2. Radar Imagery

The current analysis utilizes radar data acquired from both low- and high-resolution satellites:

– Sentinel (SNT): Low-resolution (65 x 16 ft pixel resolution) images acquired between October 2016 and December 2023 from an ascending (south to north) orbit.

– TerraSAR-X (TSX): High-resolution (3 x 3 ft) images acquired between January 2023 and December 2023 from a descending (north to south) orbit.

Key Points:

– Satellite orbits are referred to as ascending or descending according to the flight direction of the satellite: Ascending orbits fly south to north, imaging to the east. Descending orbits fly north to south, imaging to the west.

– Line of Sight (LOS): The satellite's LOS is angled relative to vertical and north-south directions (see Figure 3). InSAR measurements project the actual displacement onto this LOS, indicated as θ (theta) in Table 2.

This report focuses on data collected through the end of 2023 (see Figure 2 and Table 2 for details).

Table 1: Satellite characteristics

Satellite	Band	Wavelength	Pixel Resolution	Revisit frequency
SNT	C-band	2.32 in	65 x 16 ft	12 days
TSX/PAZ (*Spotlight*)	X-band	1.22 in	3 x 3 ft	11 days

Table 2: Satellite acquisition parameters and image acquisition information.

Satellite	Orbit	LOS Angle (Θ)	# of Images	Date Range
SNT	Ascending	42.45°	193	04 Oct 2016 – 15 Dec 2023
TSX/PAZ	Descending	37.06°	62	24 Jan 2023 – 31 Dec 2023

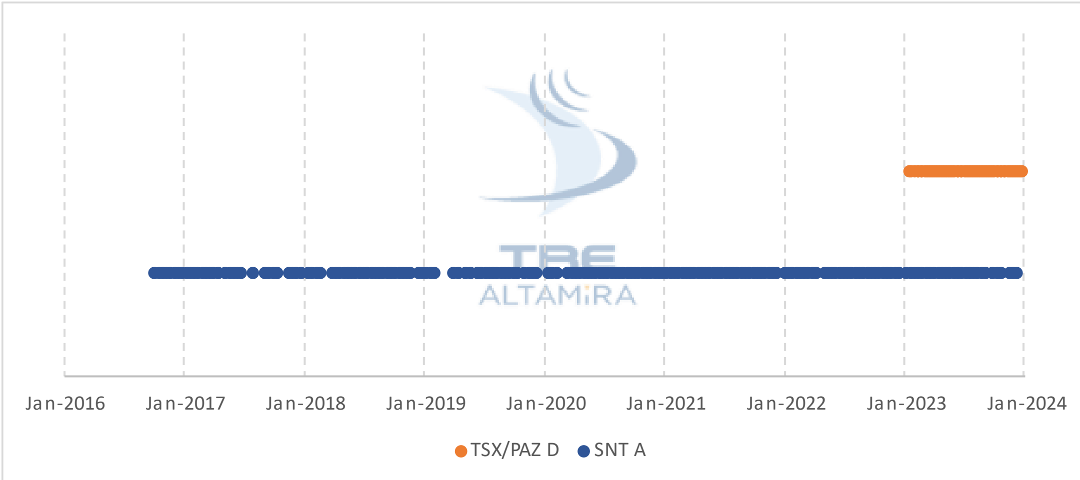

Figure 2: Temporal distribution of the radar images processed over the site.

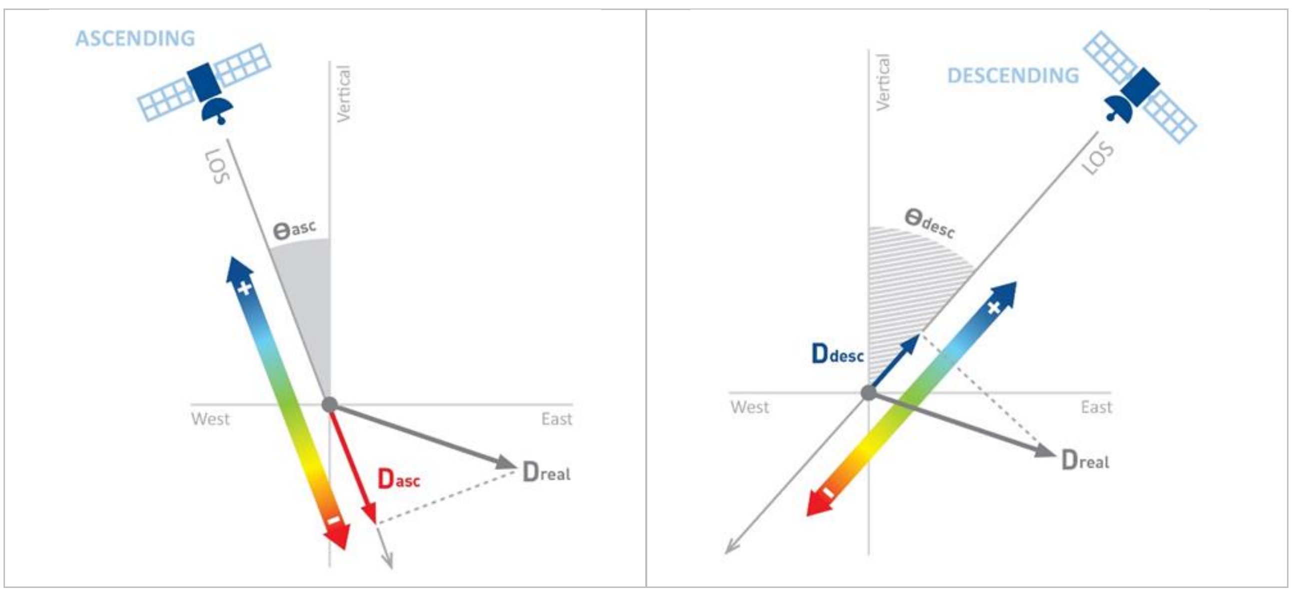

Figure 3: Ascending vs. Descending InSAR Geometries: InSAR projects real displacement (Dreal) onto the satellite's Line of Sight (LOS). LOS angle and orbit direction impact the measured value. Positive values (green-blue) denote movement towards the satellite, negative values (green-red) indicate movement away.

3. Results

The SqueeSAR® processing of radar imagery provided detailed point clouds of ground displacement measurements for both ascending and descending orbits. Here's what you'll find within each point cloud:

- Individual Measurement Points (MP): Each MP contains:
    - Cumulative Displacement: Total movement relative to the initial reference image.
    - Average Displacement Rate: Average annual movement rate over the analysis period (October 2016 - December 2023 for SNT, January 2023 - December 2023 for TSX/PAZ).
    - Acceleration: Change in displacement rate over the analysis period.
- Line-of-Sight (LOS) readings: Ascending and descending measurements are 1-D, obtained by projecting real displacement onto the satellite's LOS (see Figure 3).
- 2-D Analysis: We combine spatially overlapping LOS data onto an 82 x 82 ft grid to calculate:
    - Vertical Displacement: Up/down movement.
    - East-West Displacement: Horizontal E-W movement.

Additional Details:

This section: provides an overview of LOS and 2-D results.

Focus areas of interest: Section 4 offers in-depth observations.

Appendix 1: Lists all deliverables.

Appendix 2: Information on the SqueeSAR® technique.

3.1. Line of Sight (LOS) Results

Ascending and descending LOS results are shown in Figure 4 and Figure 5, respectively. The analysis provides good coverage over most of the dome while, as expected, the density of points is lower over areas with heavy vegetation as well as areas of water.

Interpreting Figure 4 and Figure 5:

- Measurement points are colour-coded according to the displacement rate between October 2016 – December 2023 (SNT ascending) and January 2023 – December 2023 (TSX/PAZ descending).
- Yellow to red indicates movement away from the satellite (negative values), pale to dark blue indicates movement towards the satellite (positive values) (Figure 3).

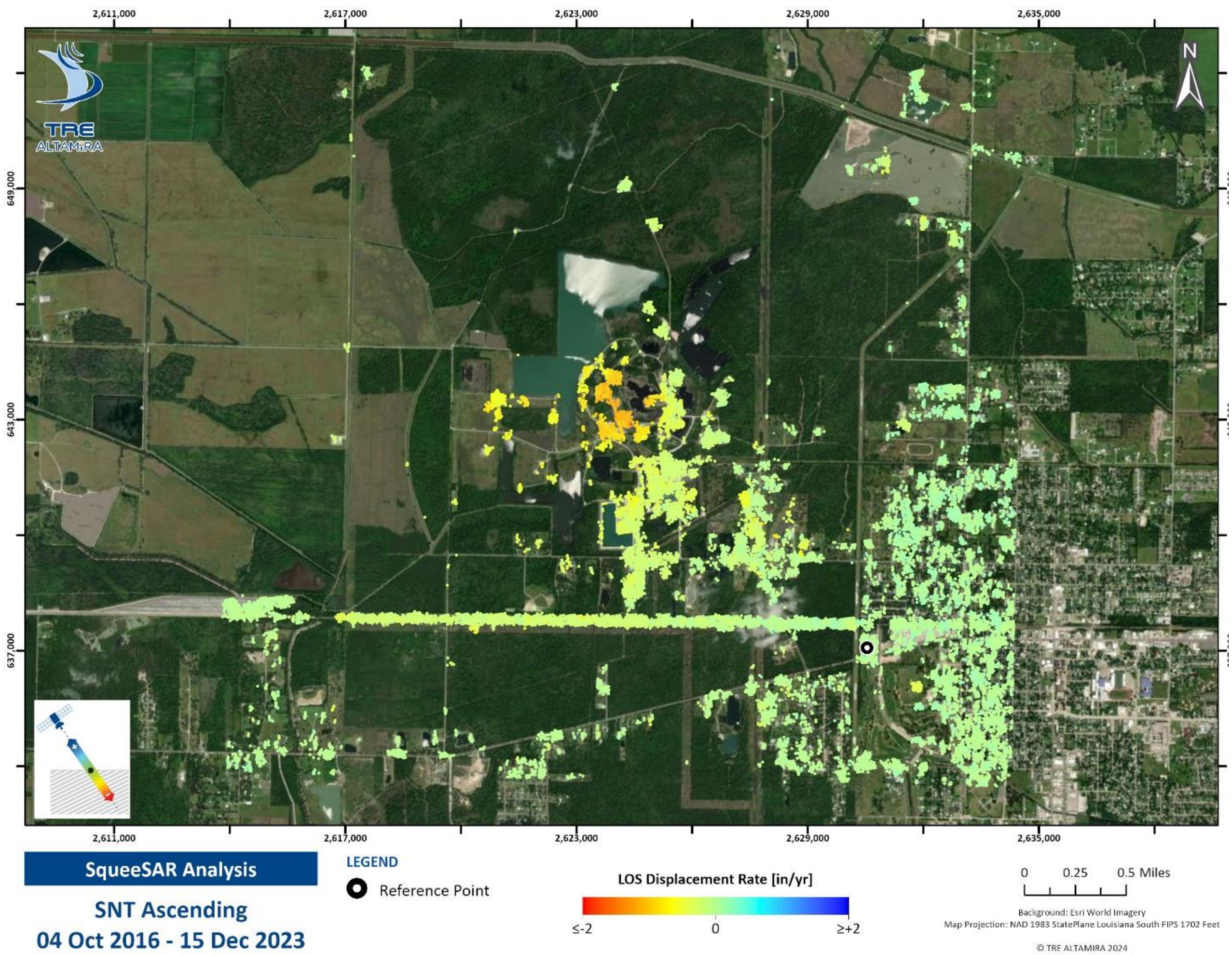

Figure 4. Sentinel ascending LOS SqueeSAR annual displacement rate (October 2016 - December 2023).

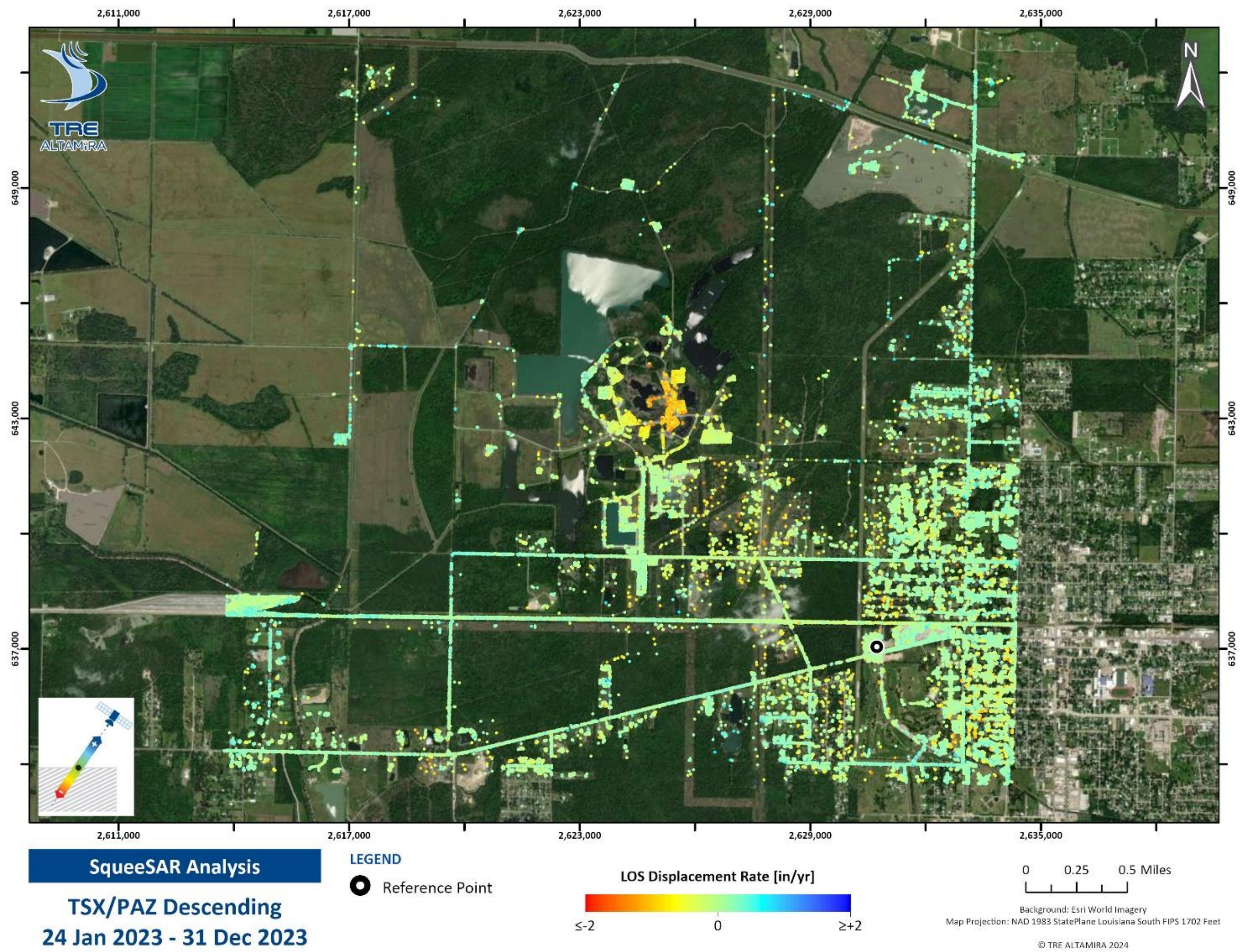

Figure 5. TerraSAR-X descending LOS SqueeSAR annual displacement rate (January 2023 – December 2023).

SqueeSAR measurements are differential compared to a local reference point (REF) and provided with two precision indices:

- Displacement rate standard deviation (V_STDEV): Indication of the error bar associated to the annual rate measurements with respect to the REF.
- Time series error bar (STD_DEF): Indication of the error bar associated to the displacement time series of each measurement point.

A summary of the LOS SqueeSAR results, REF location and precision indices obtained with the analysis are reported in Table 3.

Table 3: Summary of the SqueeSAR analyses characteristics.

Analysis characteristics	LOS Ascending (SNT)	LOS Descending (TSX)
Period covered	04 Oct 2016 – 15 Dec 2023	24 Jan 2023 – 31 Dec 2023
N. of images processed	193	62
Reference point location (NAD 1983 StatePlane Louisiana South FIPS 1702 (US Feet))	Long = 2,630,538.2109 Lat = 637,076.6076	Long = 2,630,728.7159 Lat = 637,055.8882
Number of measurement points (PS/DS)	25,747 PS: 8,507 DS: 17,240	54,269 PS: 53,016 DS: 1,253
Average Point Density	1,880 pts/mi^2	3,963 pts/mi^2
Average displacement rate standard deviation (V_STDEV)	< ± 0.04 in/yr	± 0.05 in/yr
Average time series error bar (STD_DEF)	± 0.20 in	± 0.07 in

3.2. 2-D (Vertical and East-West) Results

Ascending and descending Line-of-Sight (LOS) results are combined to generate 2-D (vertical and east-west) ground displacement measurements over the shared data period (24 January 2023 – 13 December 2023). How it works:

- Spatial Grid: To integrate data from different orbits, we overlay an 82 x 82 ft grid onto the area of interest. LOS readings from both orbits within a grid cell are averaged.
- 2-D Data Points: 2-D measurements are available only where both ascending and descending readings fall within the same grid cell.

Interpreting Figure 6 & Figure 7:

- Vertical (Figure 6): Yellow to red indicates subsidence (downward), pale to dark blue indicates uplift (upward).
- East-West (Figure 7): Yellow to red/brown indicates westward motion, pale to dark blue indicates eastward motion.
- Note: with current satellite configurations, InSAR is not able to measure north-south movement.

Data Details:

- Reference Point (REF): 2-D measurements are calculated relative to a reference point.
- Precision: The standard deviation of the displacement rate indicates measurement precision.
- Table 4: Summarizes 2-D results, REF location, and precision indices.

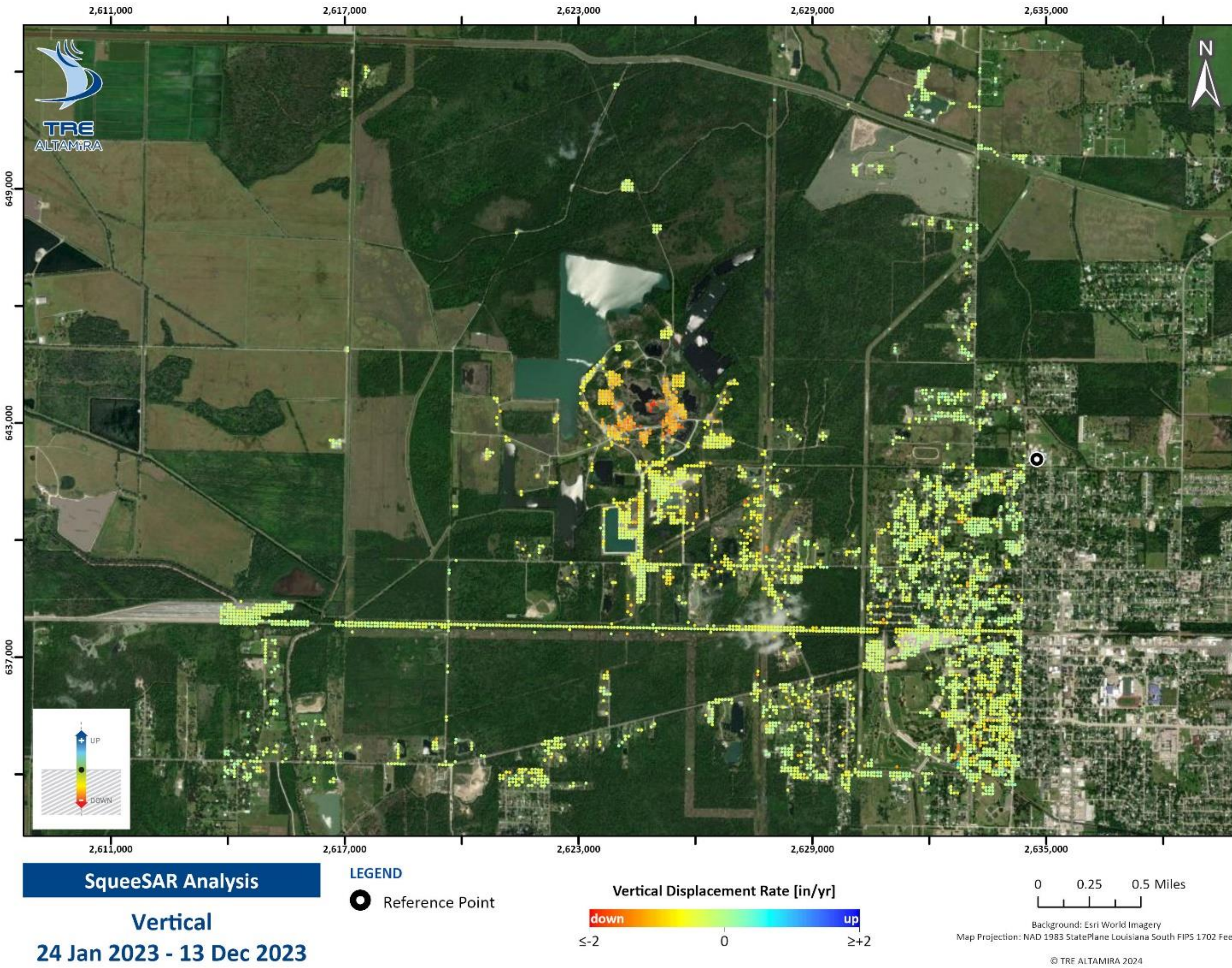

Figure 6: Vertical annual displacement rate (January 2023 – December 2023).

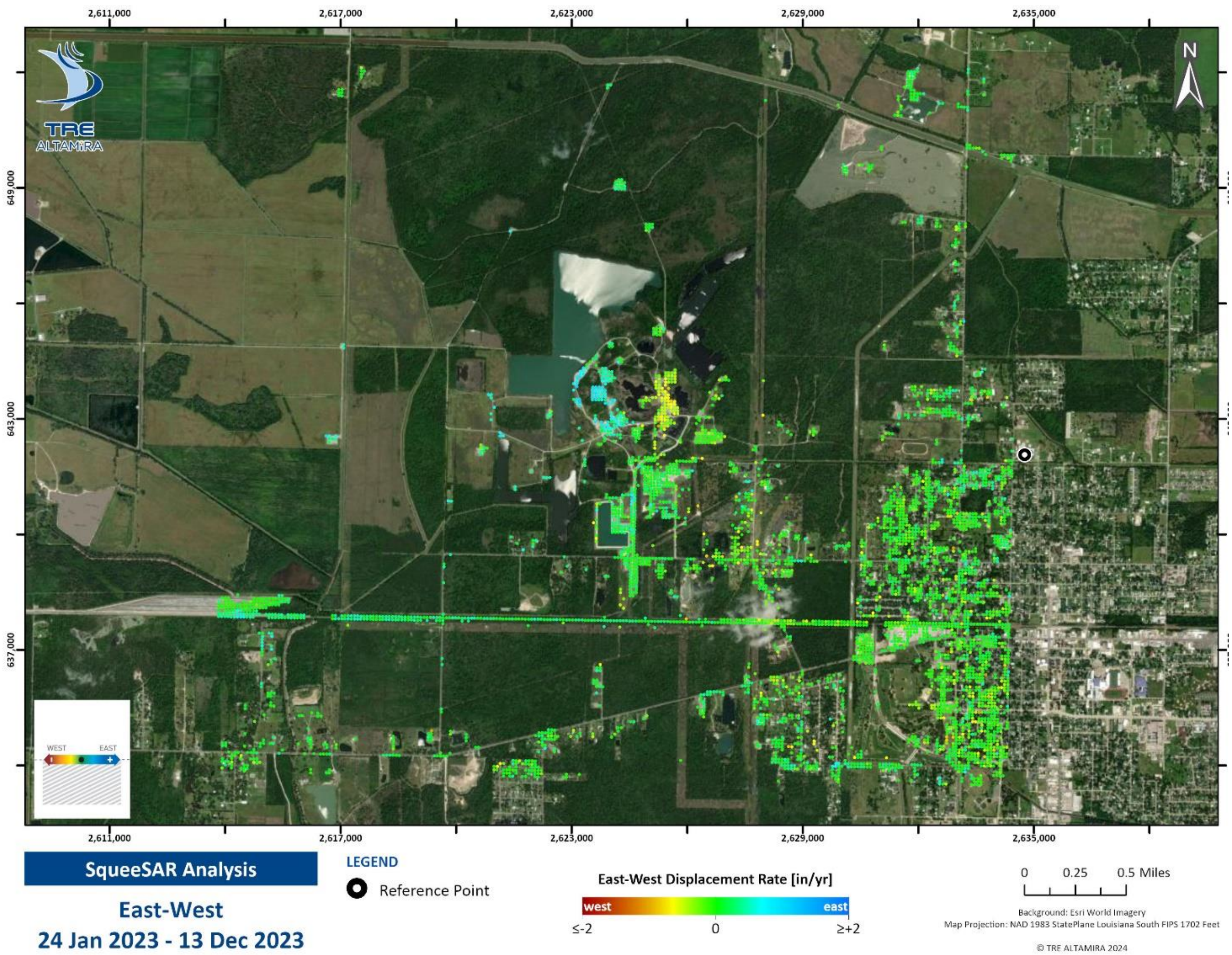

Figure 7: East-West annual displacement rate (January 2023 – December 2023).

Table 4: Summary of the 2-D SqueeSAR analysis.

Analysis characteristics	Vertical	East-West
Period covered	24 January 2023 – 13 December 2023	
N. of images	79	
Reference point location (NAD 1983 StatePlane Louisiana South FIPS 1702 (US Feet))	Long = 2,634,759.1404 Lat = 642,069.6617	
Number of cells	3,895	
Cell size	82 x 82 ft	
Average displacement rate standard deviation (V_STDEV)	±0.02 in/yr	±0.02 in/yr

4. Observations

Ground displacement observations are based on the 2-D results (vertical and east-west) over the areas of interest (Figure 8) provided by Lonquist (InSAR_AOIs_2-12-2024), by means of maps of the displacement rate, and average time series (ATS).

- ATS: calculates the average displacement of all measurement points within a polygon/area.
- The displacement rate, cumulative displacement and displacement rate error bar values are displayed in the legend at the top of each figure in imperial units.

In areas where the 2-D results are sparser or do not have good coverage, it is recommended to refer to the LOS results for greater detail.

Figure 8: Focus areas of interest provided by Lonquist.

4.1. Average Time Series over Focus Areas of Interest

ATS over the areas of interest calculate the average displacement of all measurement points that fall within the polygon (number of points will vary). Figure 9 indicates the AOIs used for the ATS, along with the vertical and east-west displacement rates, respectively.

Key Findings:

- Highest vertical displacement rate at Area 16, reaching -1.90 in/yr of subsidence (Figure 10).
- Highest E-W horizontal movement at Area 1, reaching +0.97 in/yr eastward (Figure 10).

A summary of displacement rates within all ATS polygons is shown in Table 5 and the individual average time series are shown in Appendix 3. No 2-D displacement rate information is available for Area 14 as there are no overlapping LOS points in this polygon – for additional information, refer to the LOS data.

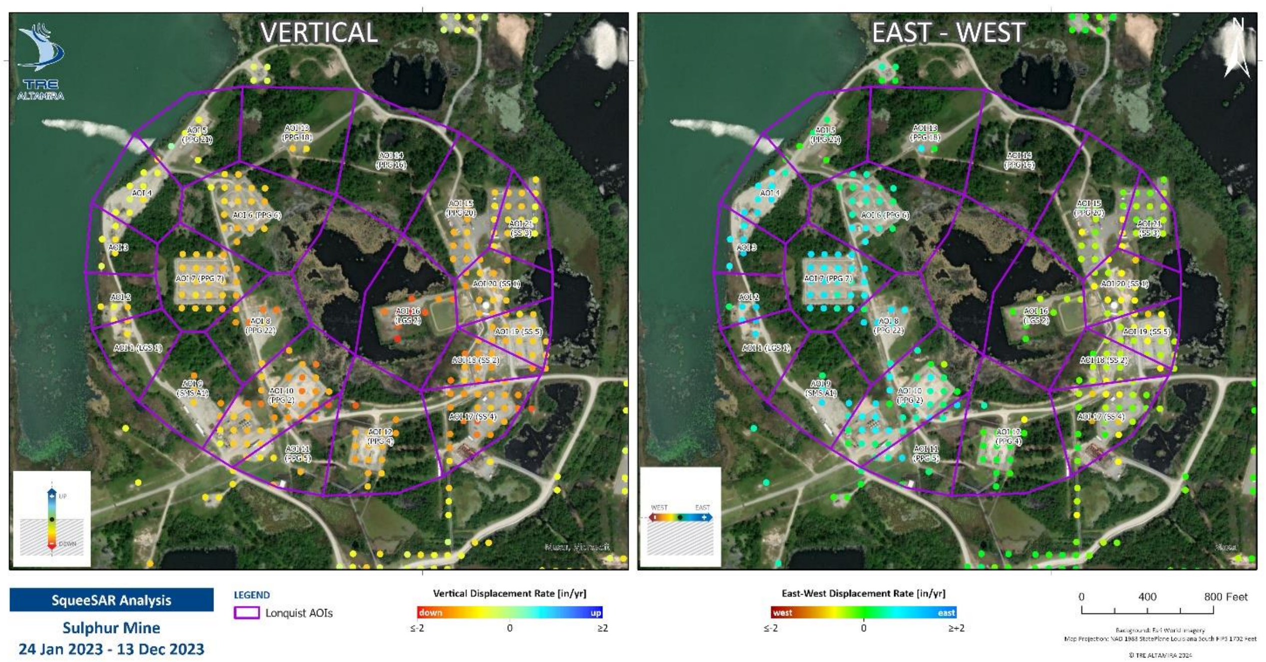

Figure 9: Vertical and East-West displacement rates over the focus AOIs used for ATS polygons located over the dome.

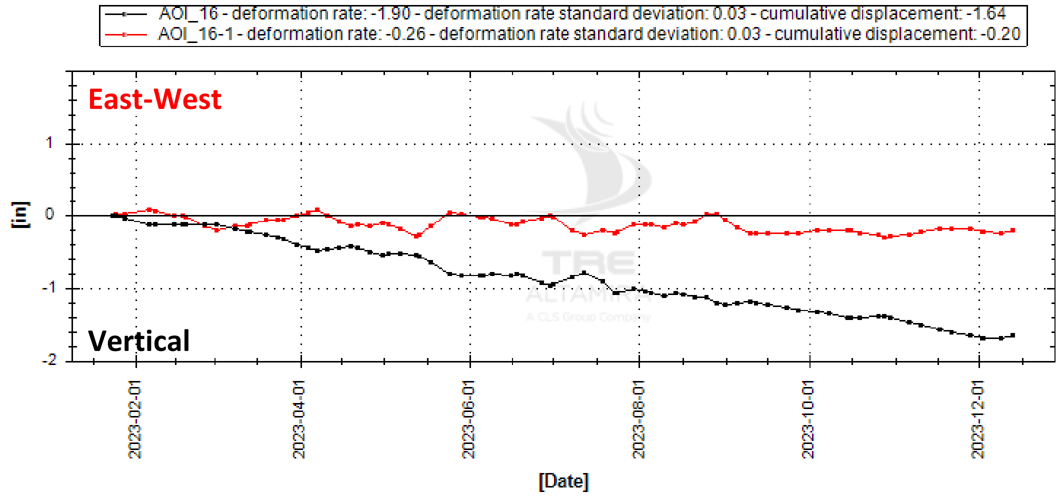

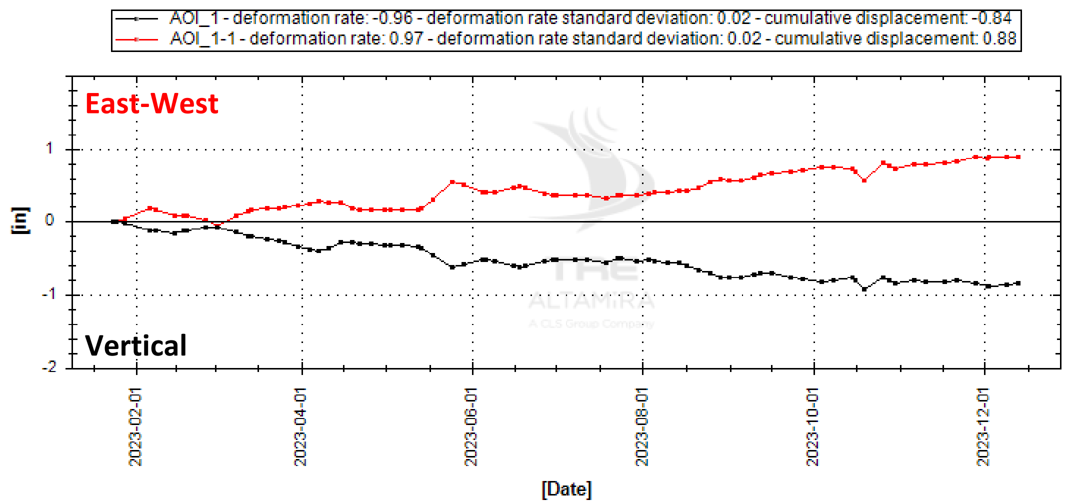

Figure 10: Average time series of Area 16 and Area 1 showing the highest vertical and east-west displacement rates, respectively.

Table 5. Summary of the Vertical and East-West displacement rates and associated standard deviation values observed within each of the focus area ATS polygons.

Monument	VERT Displacement Rate ± Standard Deviation (in/yr)	EW Displacement Rate ± Standard Deviation (in/yr)
AOI 1 (LGS 1)	-0.96 ± 0.02	+0.97 ± 0.02
AOI 2	-0.80 ± 0.03	+0.77 ± 0.03
AOI 3	-0.73 ± 0.02	+0.87 ± 0.03
AOI 4	-0.71 ± 0.03	+0.67 ± 0.03
AOI 5 (PPG 21)	-0.55 ± 0.02	+0.21 ± 0.03
AOI 6 (PPG 6)	-1.08 ± 0.02	+0.49 ± 0.02
AOI 7 (PPG 7)	-1.14 ± 0.02	+0.80 ± 0.02
AOI 8 (PPG 22)	-1.42 ± 0.03	+0.66 ± 0.04
AOI 9 (SMS A1)	-1.33 ± 0.03	+0.64 ± 0.03
AOI 10 (PPG 2)	-1.33 ± 0.02	+0.44 ± 0.02
AOI 11 (PPG 5)	-1.29 ± 0.02	+0.50 ± 0.03
AOI 12 (PPG 4)	-1.36 ± 0.02	+0.02 ± 0.02
AOI 13 (PPG 18)	-0.95 ± 0.04	+0.27 ± 0.05
AOI 14 (PPG 16)	-	-
AOI 15 (PPG 20)	-1.19 ± 0.02	-0.44 ± 0.02
AOI 16 (LGS 2)	-1.90 ± 0.03	-0.26 ± 0.03
AOI 17 (SS 4)	-1.43 ± 0.02	-0.45 ± 0.03
AOI 18 (SS 2)	-1.43 ± 0.02	-0.48 ± 0.02
AOI 19 (SS 5)	-1.18 ± 0.02	-0.59 ± 0.02
AOI 20 (SS 1)	-1.26 ± 0.02	-0.63 ± 0.02
AOI 21 (SS 3)	-0.93 ± 0.01	-0.42 ± 0.02

5. Summary

The InSAR monitoring of the Sulphur Mines Salt Dome integrates low-resolution Sentinel (SNT) imagery (acquired since October 2016) with high-resolution TerraSAR-X/PAZ (TSX/PAZ) imagery (acquired since January 2023) to provide continuous ground displacement updates, including 2-D (vertical and east-west) data.

This annual technical report (covering 24 January 2023 – 13 December 2023) draws upon the monitoring of the past year to provide observations over the key areas of interest designated by Lonquist.

Key Findings:

– Subsidence: A subsidence bowl is present, with maximum rates at Area 16 (central-eastern side of the dome).

– Eastward Displacement: Highest displacement rates are observed at Area 1 (western side).

Monitoring:

– Ongoing monitoring is continuing with 4/7-day frequency (TSX/PAZ) and 12-day (SNT and 2-D) frequency.

Recommendation:

To maintain optimal data quality, TREA recommends periodically resetting the Sulphur Mines baseline approximately every 12-24 months. This interval depends on data coverage and local conditions (e.g., flooding).

Appendix 1: Delivered Files

All results are delivered via TREmaps® web platform (https://signin.main.tremaps.com/login/#/) our proprietary online GIS platform to view and interrogate the SqueeSAR data. For login instructions and main functionalities, please use the Help page (https://en.ums.tre-altamira.com)

Table 6 lists the deliverables including the present report and the InSAR data files, delivered via the TREmaps platform.

The SqueeSAR data is provided in shapefile (.shp) format, imperial units and NAD 1983 State Plane Louisiana South FIPS 1702 ft coordinate system. The shapefile of each elaboration contains details about the measurement points, such as displacement rate, acceleration rate, cumulative displacement, and quality indexes. The information associated within the database files (dbf) are described in Table 7.

Description		File name
SqueeSAR Data	**ASC**	SULPHUR_MINE_SNT_T136_A_20231215_IMP_3452_Xflxkp01cA008S.shp SULPHUR_MINE_SNT_T136_A_20231215_Xflxkp01cA3S.shp
	DESC	SULPHUR_MINE_TSX_T67_D_20231231_IMP_3452_Xflxkp06xA008S.shp SULPHUR_MINE_TSX_T67_D_20231231_Xflxkp06xA1S.shp
	2-D	SULPHUR_MINE_SNT_VERT_20231213_IMP_3452_Xflxkp01cA023V.shp SULPHUR_MINE_SNT_VERT_20231213_Xflxkp01cA1V.shp SULPHUR_MINE_SNT_EW_20231213_IMP_3452_Xflxkp01cA025E.shp SULPHUR_MINE_SNT_EW_20231213_Xflxkp01cA2E.shp
Technical Report		TREA_Lonquist_SulphurMines_InSAR_Monitoring_Report_Dec2023.pdf

Table 6: List of deliverables.

Field	Description
CODE	Measurement Point (MP) identification code.
HEIGHT	Topographic Elevation referred to input DEM [ft].
H_STDEV	Height standard deviation of the measurement point [ft].
VEL	MP displacement rate [in/yr]. – **LOS:** Positive values correspond to motion toward the satellite; negative values correspond to motion away from the satellite. – **Vertical (VEL_V):** Positive values indicate uplift; negative values indicate downward movement. – **E-W Horizontal (VEL_E):** Positive values indicate eastward movement; negative values westward movement.
V_STDEV	Displacement rate standard deviation [in/yr].
ACC*	Acceleration rate [in/yr^2].
A_STDEV*	Standard deviation of the acceleration value [in/yr^2].
COHERENCE*	Quality measure between 0 and 1.
STD_DEF*	Displacement time series error bar [in]
EFF_AREA*	This parameter represents the effective extension of the area [ft^2] covered by Distributed Scatterers (DS). For permanent scatterers (PS), its value is set to 0.
Dyyyymmdd	Series of columns that contain the displacement values of successive acquisitions relative to the first acquisition available [in].

Table 7: Description of the fields contained in the LOS and 2-D database. *Field is only present in LOS data sets.

Appendix 2: Technique Description

6. SqueeSAR®

SqueeSAR® is the advanced multi-image InSAR algorithm patented by TREA that provides high precision measurements of ground displacement in the form of a point cloud. By analyzing a stack of SAR images acquired over a site, the SqueeSAR algorithm identifies and measures the movement of radar reflectors on the ground surface that remain visible and coherent throughout the period of the analysis.

Radar reflectors belong to two different families (Figure 11):

– Permanent Scatterers (PS): point-wise radar targets characterized by highly stable radar signal returns (e.g. buildings, rocky outcrops, infrastructures, etc.)
– Distributed Scatterers (DS): patches of ground exhibiting a lower but homogenous radar signal return (e.g. rangeland, debris fields, arid areas, etc.). DS are represented as individual points, but the information does not refer to a single target, but rather to the patch of ground associated with each DS (the size [km2] but not the exact shape of the patch is provided).

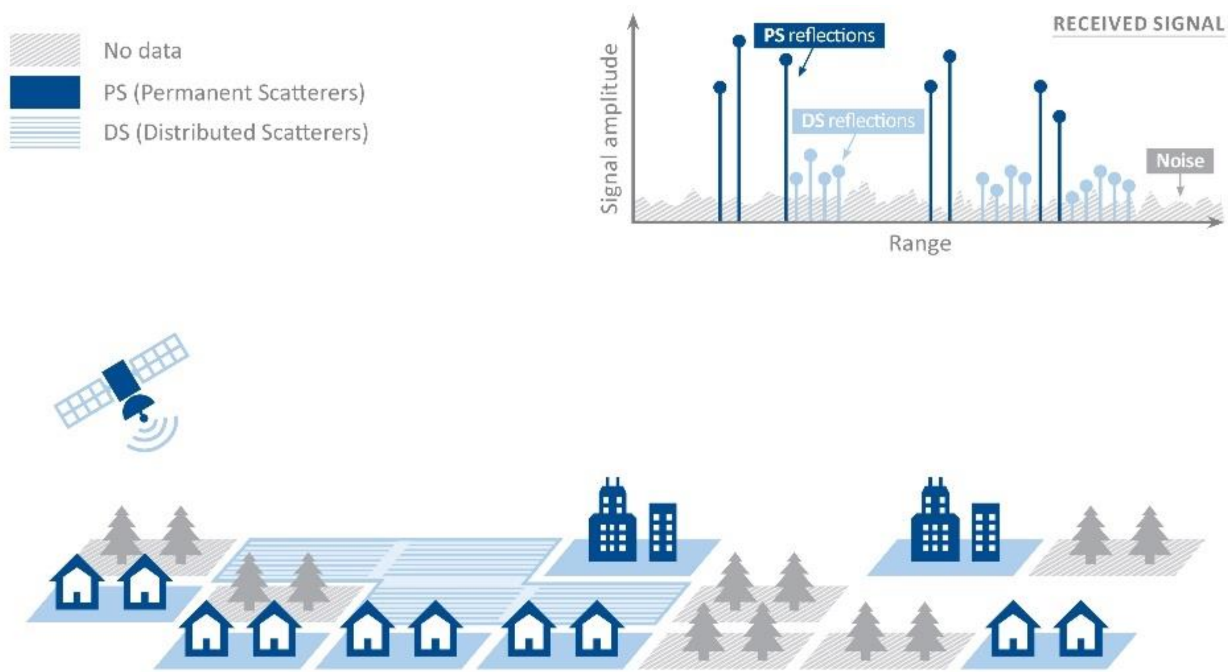

Figure 11: Schematic of PS and DS radar targets.

6.1. 1-D (LOS) Measurements

SAR satellites image the ground from ascending and descending orbits, according to the flight direction, from south to north (imaging to the east) and from north to south (imaging to the west) respectively (Figure 12). InSAR measures the projection of the real vector of displacement onto the satellite line-of-sight (LOS) and provides 1-D measurements along the LOS, which is inclined with respect to the vertical and north-south direction (θ and δ angle, respectively).

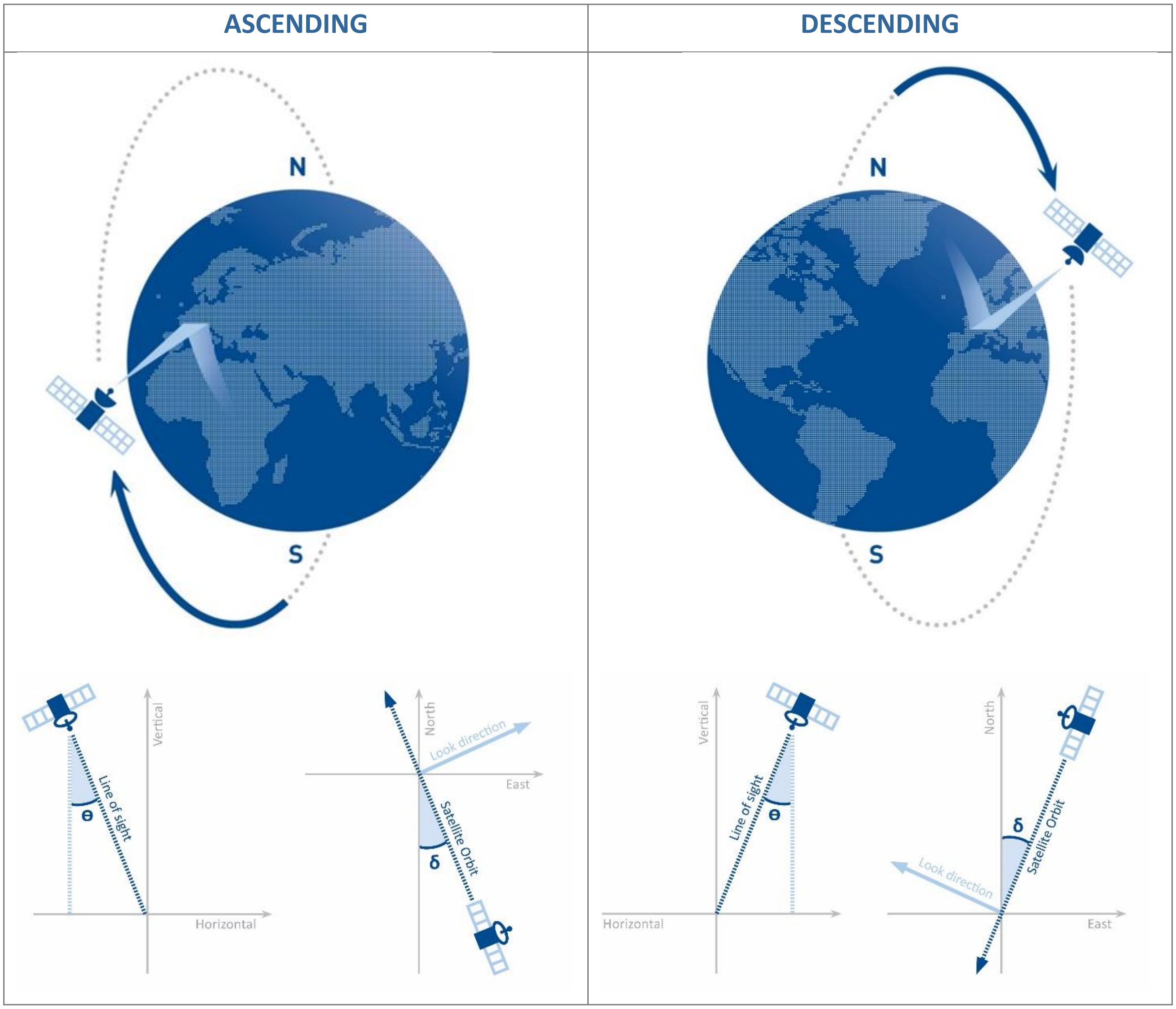

Figure 12: SAR satellites image the ground from ascending and descending orbits, according to the flight direction, from south to north (imaging to the east) and from north to south (imaging to the west), respectively. The satellite Line Of Sight (LOS) is inclined with respect to the vertical and north-south direction (θ and δ angle, respectively).

As SqueeSAR measurements are 1-D (i.e. away or toward the satellite), the sign and value of the displacement depends on the orientation of the real displacement with respect to the LOS (Figure 13). Negative values (from green to red) indicate movement away from the satellite, while positive values (from green to blue) indicate movement towards the satellite. A same displacement produces different readings when viewed from different LOS angles (Figure 13).

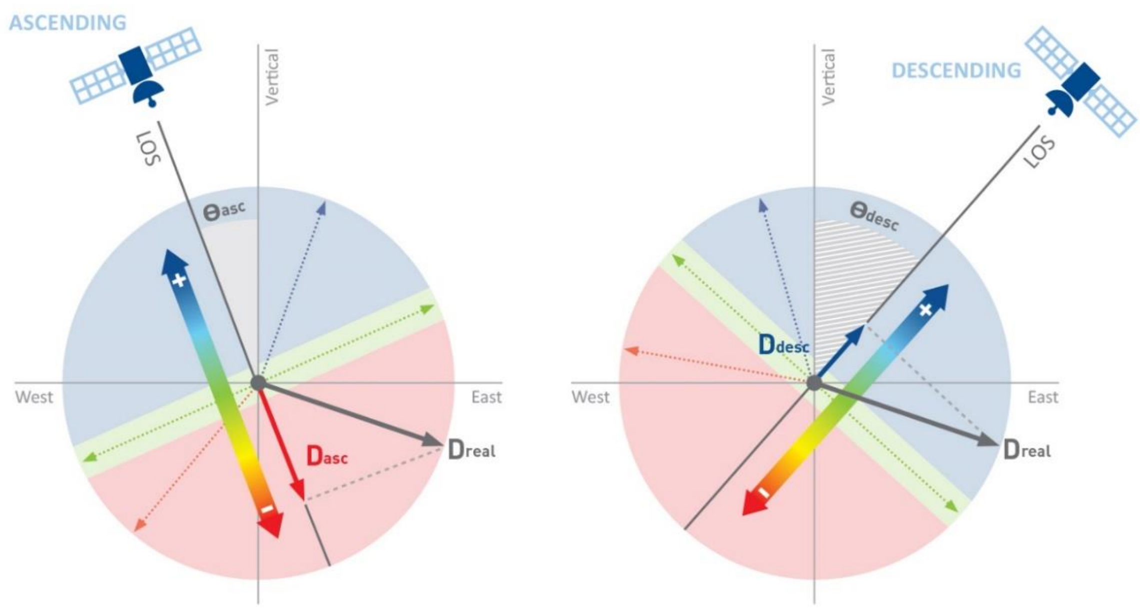

Figure 13: SqueeSAR measures the projection of real movement (Dreal) onto the LOS. The same real movement (Dreal) produces a different value from a different LOS (different inclination or different orbits). Real displacement vectors (Dreal) within the blue areas will produce positive LOS measurements while those within the red areas will produce negative LOS values. Real displacement vectors within the green band (i.e. perpendicular to the satellite LOS) will produce small (i.e. close to zero) LOS measurements.

SqueeSAR measurements are differential in space and time: spatially they are related to a local reference point (REF) and temporally to the date of the first available satellite image. The REF is assumed to be motionless and selected for its radar properties to optimize the quality of the measurements. It corresponds to a radar target with a high coherence signal in all the images of the archive and that is not affected by displacement rate variations (non-linear movement or cyclical deformations) in the analysis period. The selection of the REF is imagery dependent. If the imagery changes (number of images and/or time span), the MP selected as the REF can change. The absolute movement of the REF point can be defined only with calibration to a GNSS network.

For each measurement point (MP), SqueeSAR provides the following main information:

- Position and elevation estimated with respect to the input DEM [ft].
- Displacement time series (TS) representing the evolution of the displacement for each acquisition date [mm or in] and measured along the LOS direction.
- Annual average displacement rate [in/yr], calculated from a linear regression of the displacement time series over the analysis period and referred to the REF.

SqueeSAR is best suited for displacement rates < 3.3ft /yr.

6.1.1. Measurement Point Density and Coverage

The density and distribution of MPs identified by the analysis depends on the resolution of the imagery, the surface characteristics, changes over time and topography of the area. In detail, MP density and coverage increases with satellite resolution and decreases over (Figure 14):

- Vegetated and low reflectivity areas (i.e., areas where the signal backscattered to the satellite is low).
- Areas affected by temporal decorrelation (i.e. radar signal is not coherent over time), which is generally associated with rapid surface changes (such as active operations areas), seasonal surface changes (such as floods or snow-coverage) or fast movement (displacement rate >3.3ft/yr)
- Areas where the satellite has visibility limitations, because of the Line of Sight (LOS) orientation with respect to the local topography.

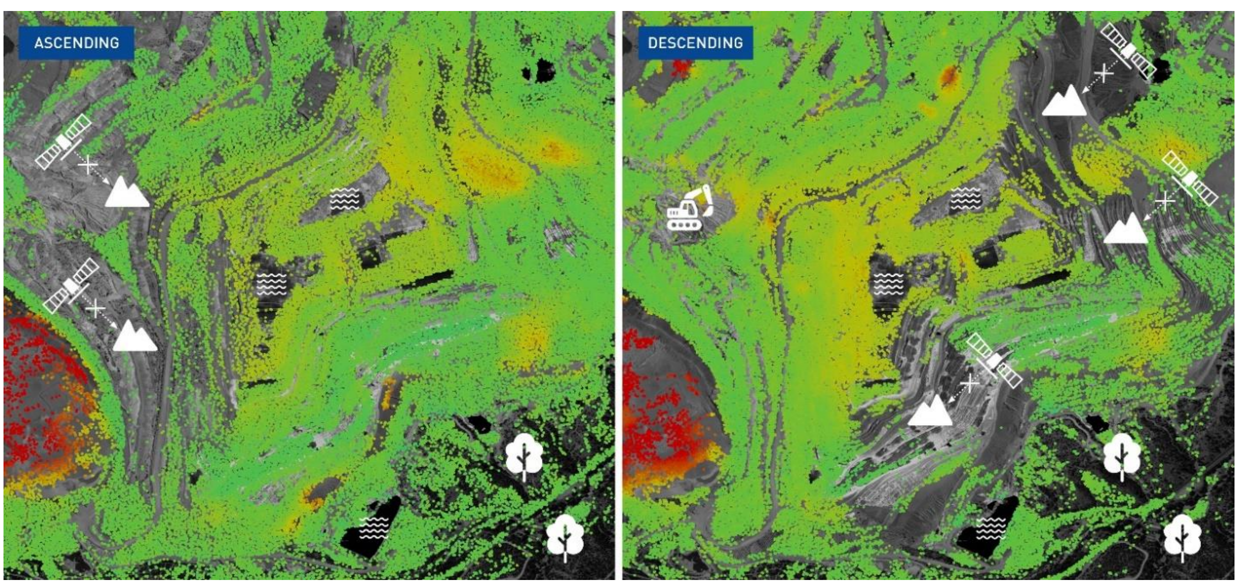

Figure 14: Example of point coverage over a mine site. The MPs coverage is low over areas with vegetation, areas of surface operations or where the visibility is limited due to the orientation of the slope with respect to the satellite line of sight. Generally, west-facing slopes have a better coverage in ascending orbit while east-facing slopes has a better visibility on descending orbit.

6.1.2. Measurement Precision

SqueeSAR can measure displacement with precision up to one-hundredth of an inch. The precision depends on a correct phase unwrapping and atmospheric contribution estimation and increases with the quality of the imagery and the coherence of the signal. In particular, the precision:

- Increases with the number of processed images, the length of the period of the analysis, the frequency of acquisitions, the coherence of the signal (i.e. the absence of vegetation or surface disturbances) and the density of points.
- Decreases with the presence of gaps in the acquisitions, strong atmospheric disturbances, and surface variations in the period of the analysis (e.g. snow, floods, changes to the ground surface).

Typical displacement precision values obtained with a dataset of at least 30 images are reported in Table 8. SqueeSAR LOS measurements are provided with two displacement precision indices:

- The displacement rate standard deviation (V_STDEV), which provides an indication of the precision of the annual deformation rate with respect to the REF. Given the standard deviation (σ), and assuming that the errors are normally distributed (Gaussian), 95% of the rate values tend to be included in a ±2σ range. The displacement rate standard deviation increases with the distance of the point from the REF.
- The time series error bar (STD_DEF), which provide an indication of the precision of single displacement measurements. It depends on the coherence of the phase signal over time: the higher the coherence, the higher the precision of the measurements. This parameter is calculated as standard deviation of the residuals with respect to an analytic model (i.e. how well the model fits the displacement time series). The model is selected individually for each MP with an advanced Model Order Selection technique that take into consideration the quality of the imagery (number of images, time span and possible gaps in the acquisitions).

LOS measurements	Displacement rate standard deviation	Error bar of single measurement
Precision	±0.04 in/yr	±0.20 in

Table 8: Typical precision values for a MP less than 0.62 mi from the REF and a data set of at least 30 SAR scenes.

While the precision of the displacement measurements is within the order of one-hundredth of an inch, the location of individual measurement points is known with metric accuracy and depends on the satellite system being used (Table 9) As for the measurement precision, the location accuracy increases with the quality of the imagery, the coherence of the signal and the density of points.

Satellite	Band	Wavelength [in]	Resolution RGxAZ [ftxft]	North-South [ft]	East-West [ft]	Elevation [ft]
ERS - ENVI	C-band	2.20	65x16	± 6	± 23	± 5
RSAT (*Standard Beam*)	C-band	2.20	65x16	± 6	± 23	± 5
SNT	**C-band**	**2.32**	**16x65**	**± 26**	**± 39**	**±26**
CSK	X-band	1.23	10x10	± 3	± 3	±1.6
TSX (*Stripmap*)	X-band	1.22	10x10	± 3	± 10	± 5
TSX (*Spotlight*)	**X-band**	**1.22**	**3x3**	**± 1.6**	**± 10**	**± 5**
ALOS-1 (*Fine Beam*)	L-band	9.29	54x54	± 5	± 10	± 3
ALOS-2 (*Fine SM3 Beam*)	L-band	9.37	32x32	± 5	± 10	± 3

Table 9: Typical precision values (1 sigma) associated to the UTM coordinates of a MP at mid-latitudes. Values are referred to a MP less than 0.62 mi from the REF and a dataset of at least 30 SAR scenes. Satellites used in this analysis are in bold.

6.1.3. Fast Movements and Phase Unwrapping

SqueeSAR is best suited to measure displacement rates below 3.3 ft/yr. In a case of rapid deformation, the measurements can be affected by phase unwrapping inaccuracies.

Figure 15 represents a schematic of a radar target affected by a phase unwrapping error. The target is represented at an initial distance R_0 (in blue), while in red there are three possible cases that are shifted by different amounts. Without prior information, the radar system is not able to estimate the correct number of wavelengths ($n\lambda$), therefore, all three cases will produce equivalent ΔRs.

In theory, on a single isolated radar target, only displacement that is below half a wavelength can be correctly detected. A greater displacement may be underestimated. In extreme cases, if the target moved exactly half a wavelength between two acquisitions the target would still be observed as perfectly stable.

These theoretical limits refer to movements affecting single isolated radar targets. The limits increase significantly in cases where the movement is spatially correlated, and the MP density is adequate. Figure 16 shows a schematic of spatially correlated subsidence. When the radar target density is adequate, the phase can be correctly unwrapped and displacement exceeding the $\lambda/2$ limit can be measured. In cases where the radar target distribution is not adequate, incorrect phase unwrapping can occur and will usually cause displacement to be underestimated.

The temporal distribution of the acquisitions also impacts the phase unwrapping procedure: a higher acquisition frequency means a higher sampling frequency and thus the ability measure more rapid movement.

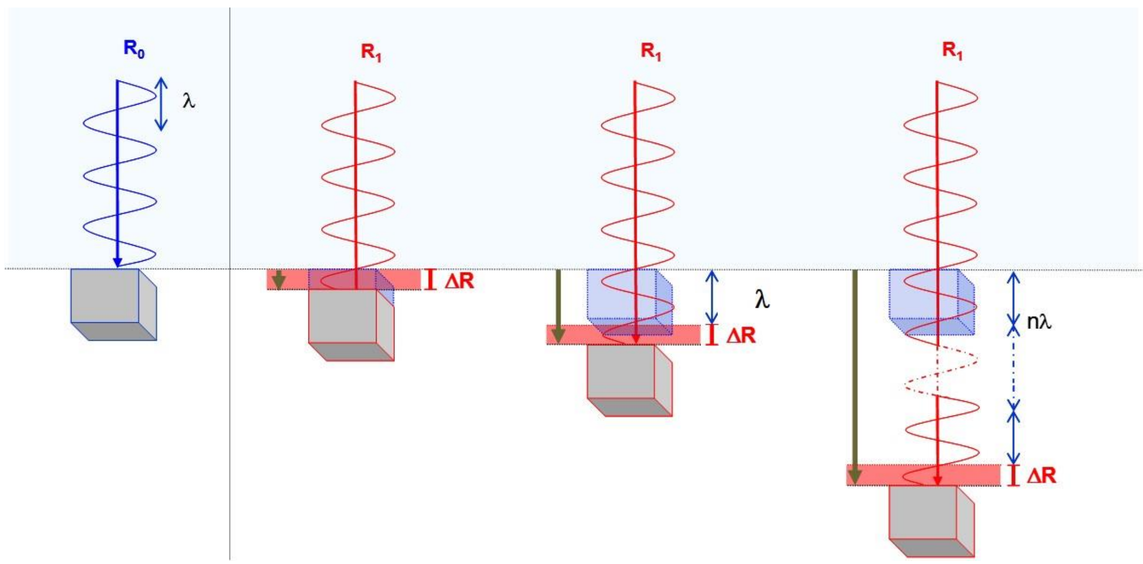

Figure 15: Schematic of a sinusoidal phase of the electromagnetic wave incident on a moving target (grey solid). Without prior information, it is not possible to estimate the correct number of wavelengths (nλ) which occur and in all three cases an equivalent ΔR shift is measured.

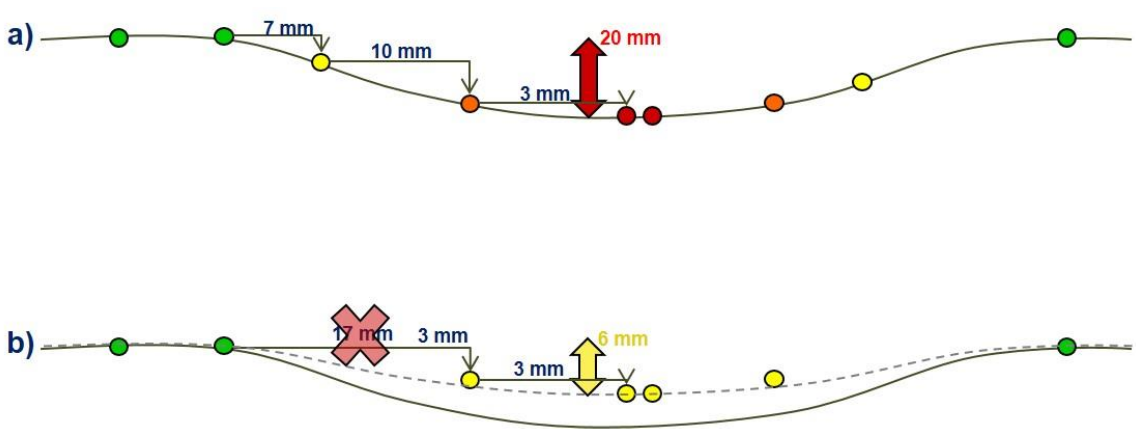

Figure 16: Schematic of spatially correlated subsidence. The MPs are colour-coded according to the displacement measured. Considering a X-band satellite (λ=1.22), a total displacement of 0.79 in (higher than the λ/2 limit of 0.61 in) can be measured when the MP are well distributed along the subsiding profile (a). When the MP distribution is not adequate, an underestimation of the real displacement occurs (b).

6.2. 2-D (Vertical and East-West) Measurements

The combination of 1-D (LOS) SqueeSAR results obtained from ascending and descending orbits over the same area and overlapping period, produces 2-D (vertical and east-west) measurements.

The estimation of the 2-D measurements requires the following steps and assumptions:

- Satellites travelling in ascending and descending orbits identify different radar targets on the ground, entailing that the 2-D procedure requires a spatial grid to capture MPs from both orbits within each cell. It is assumed that MPs that fall within the same cell are affected by the same motion. All MPs within a same cell are then averaged. This entails that the 2-D cells do not represent radar targets on the ground, but rather synthetic points located at the centre of the cells (Figure 17).
- A 2-D time series is calculated by combining all ascending and descending time series using trigonometry. Only cells that contain points from both input LOS data sets will produce a 2-D time series. This entails that the spatial coverage of the 2-D information is thus generally lower than that of the individual LOS data sets (Figure 17).
- Since the images are acquired on different dates from each orbit, the LOS displacement time series must be re-sampled in time. The final output includes all ascending and descending acquisition dates and covers the overlapping period in common for the two data sets.
- North-south movement cannot be measured with InSAR as SAR satellites are not sensitive to movement parallel to their travel direction.

As in LOS analyses, average annual displacement rates in a 2-D analysis are calculated from a linear regression of the displacement measured over the entire period of the study and all measurements are relative to a reference point that is assumed to be stable.

The convention for displacement sign and point colour is the following (Figure 18):

- In a vertical data set, negative values (from yellow to red) indicate downward displacement (subsidence), while positive values (from pale to dark blue) indicate upward displacement (uplift or heave).
- In an east-west data set, negative values (from yellow to red) indicate westward motion, while positive values (from pale to dark blue) indicate eastward motion.

Although 2-D measurements are generally easier to interpret than LOS data, but they have a lower spatial resolution, which means that in detailed analysis of localized features it may be beneficial to use the full resolution LOS results.

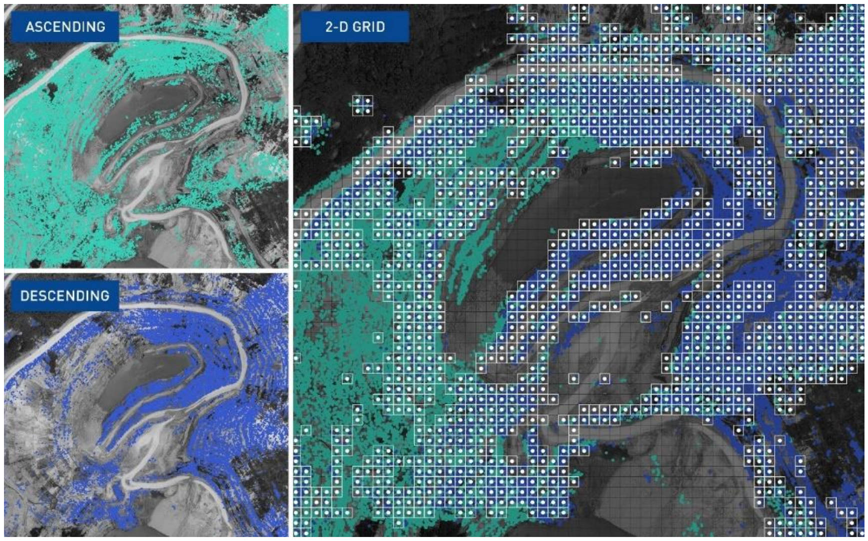

Figure 17: 2-D measurements are estimated by subsampling ascending and descending data on a common spatial grid. The measurements of all MPs contained within the same cell are averaged to produce 2-D measurement points located at the centre of the cell. The 2-D procedure only produces readings for cells containing MP from both orbits (white cells).

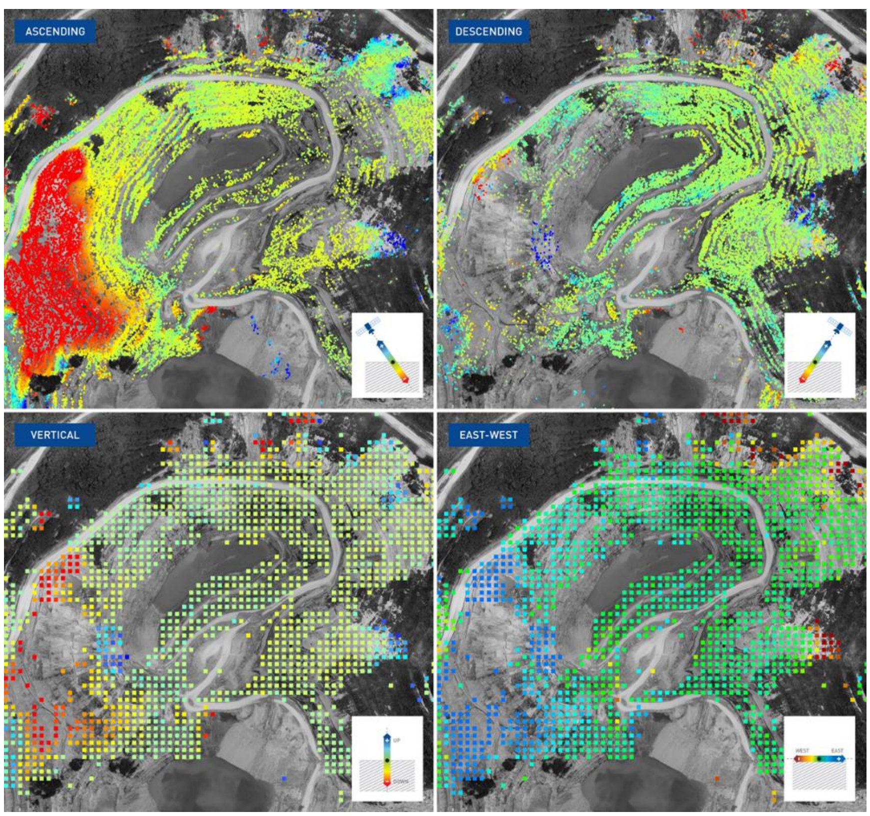

Figure 18: Ascending and descending LOS measurements correspond to the full resolution network of natural reflectors identified on the ground and provide the projection of the real movement to the specific LOS The combination of ascending and descending data produces a regular grid of vertical and east-west measurements.

6.3. SqueeSAR vs Other Surface Monitoring Techniques

When comparing SqueeSAR data with other measurements, the main characteristics to take into consideration are the following:

- SqueeSAR measurements are referred to a local REF. The REF is selected for its radar properties to optimize the quality of the measurements and corresponds to a radar target with high coherence signal and not affected by displacement rate variations in the period of the analysis. The “absolute” stability of the REF point can be verified with a GNSS network.
- SqueeSAR provides displacement measurements with precision in the order of one-hundredth of an inch but point location accuracy is in the order of feet.
- SqueeSAR provides a dense network of measurement points (from 259 to over 25,900 MP/mi^2, depending on the satellite resolution and the land cover) that is not achievable with other in-situ monitoring techniques. This dense network of natural benchmarks allows InSAR to provide very accurate relative movement (estimation of how a point is moving with respect to another point) but less accurate absolute measurements because all the measurements are referred to a local reference point.
- InSAR does not measure the full displacement vector but its projection onto the satellite line of sight. SqueeSAR measurements are 1-D (LOS) and an accurate estimation of the vertical motion component is only possible by combining LOS measurements obtained from ascending and descending orbits over the same area and overlapping period.
- InSAR is not sensitive to movement along the orbit direction (Azimuth), which is approximately north-south (i.e. SqueeSAR do not provide north-south measurements).

Table 10 reports a comparison between the main characteristics of InSAR measurements with respect to other conventional surface monitoring techniques.

Main Characteristics	SqueeSAR	Manual GNSS	Permanent GNSS	Levelling
Spatial density of points	259 - >125,900 points/mi^2	few points/mi^2	few points/mi^2	few points/mi^2
Measurement precision* [1σ]	± 0.20 in (LOS and vert)	± 0.40 in (horizontal) ± 0.80 in (vertical)	± 0.40 in (horizontal) ± 0.40 in (vertical)	±0.04-0.08 in **
Measurement accuracy	High relative accuracy but low absolute accuracy	High absolute accuracy	High absolute accuracy	High absolute accuracy
Location accuracy**	feet	inches	inches	inches
Components	1-D (LOS) and 2-D	3-D	3-D	1-D (vert)
Acquisition frequency	Weekly to monthly	Quarterly to yearly	Hourly to daily	Quarterly to yearly

Table 10: Main characteristics of InSAR and other conventional monitoring techniques. *Precision refers to the error bar of a single measurement (i.e. the consistency of repeated measurements). **Accuracy refers to how close a measurement is to the absolute value. GNSS precision values refer to a 1-hour static session.

In general, to perform a comparison of InSAR data with other measurements it is necessary:

1. To compare the measurements along a same direction.

– As InSAR provides 1-D (LOS) measurements, it is more rigorous to project 3-D measurements to the LOS direction. The projection of the LOS measurements to the vertical direction can be performed only under the assumption of negligible horizontal motion components. Alternatively, the use of SqueeSAR measurements obtained from ascending and descending orbits over the same area and overlapping period allows an accurate estimation of the vertical motion component.

2. Define a co-location rule between the InSAR measurement points and other stations/benchmarks.

– In general, it is unusual for SqueeSAR measurement points to fall exactly at benchmark locations. It is therefore recommended to perform the comparison using all of the most coherent (highest quality) points located within a certain radius from the benchmark, rather than just an individual SqueeSAR point.

3. Use the same reference point or verify the absolute stability of the local InSAR reference point (REF).
4. Use the same reference period and consider the accuracy and frequency of the measurement techniques being compared.

6.3.1.1. Integration and Calibration of InSAR Data with a GNSS Network – Best Practices

InSAR and GNSS (Global Navigation Satellite System) are complementary techniques for monitoring surface movements and are generally integrated to take advantage of the strengths of both technologies, in terms of spatial density, precision and accuracy (Table 10). The integration of InSAR and GNSS measurements provides a high spatial density of information with optimal precision and accuracy of the measurements when a common reference system is used.

To achieve this, the SqueeSAR data is generally calibrated to an absolute GNSS network based on the following steps:

1) Projection of the GNSS measurements to the satellite LOS. The GNSS 3-D measurements are projected to the satellite 1-D LOS to create a GNSS LOS time series. This step allows a direct comparison of the two independent measurements (InSAR and GPS). The projection of the 3-D GNSS measurements onto the LOS direction can be calculated as follows:

$$D_{LOS} = D_{VERT}*V_{LOS} + D_{EW}*E_{LOS} + D_{NS}*N_{LOS}$$

with V_{LOS}, E_{LOS} e N_{LOS} are the LOS versors along the 3 directions and D_{VERT}, D_{EW} e D_{NS} are the 3 components of the GNSS measurements. The LOS versors are provided in the metadata associated to the SqueeSAR data (Figure 19) and represent the cosines of the angles between the LOS and the 3 coordinate axes.

2) Co-localization of the measurement points. Generally, GNSS benchmarks and InSAR points are not exactly co-located. Additionally, the accuracy of the InSAR point location is known to within a few metres (Table 9). The location of a GNSS benchmark is known with cm precision. For these reasons, InSAR measurement points (MP) within a certain radius of each GNSS are generally selected and used to calculate an average time series (ATS) for the overlapping period with the GNSS time series (one InSAR ATS for each GNSS). This step allows the comparison of data collected at a same location over a corresponding period.

3) Refence point stability check. GNSS measurements are absolute as they are connected to a global network, while InSAR data are referred to a local reference point (REF). GNSS measurements can be

used to verify the “absolute” stability of the REF. If there is no GNSS station close to the REF, it is suggested to just verify the stability of the InSAR points in an area around a stable GPS station.

4) Absolute calibration. If the REF check highlights discrepancies between InSAR and GNSS measurements, the InSAR measurements are calibrated to the absolute GNSS network as follows:

– Plane removal (when only a linear regional trend is present): a difference in average velocity is calculated for each ATS and corresponding GNSS. The average velocity differences calculated for each ATS and GNSS pair is then used to estimate and remove a first order surface (plane) from all InSAR measurement points. The plane is statistically estimated at regional scale by minimizing the residuals of the differences between the ATS and corresponding GNSS.

– Time series calibration (when a not-linear regional trend is present): evaluation of an average time series of residuals by comparing the ATS to the corresponding GNSS time series at each location. All the time series of residuals obtained are then averaged to define a unique common time series of residuals (cRTS) at regional scale. This cRTS represents the movement of the local InSAR reference points with respect to the absolute GNSS reference frame. The cRTS is then removed from every InSAR MP time series.

$$D_{LOS} = D_{VERT} * V_{LOS} + D_{EW} * E_{LOS} + D_{NS} * N_{LOS}$$

Satellite info

Satellite	Wavelength	Satellite geometry	Sensor mode	Satellite track
SNT	5.55 cm	ASCENDING	IW	111

Acquisition geometry

Line of sight angle	**θ:**	35.75°	**δ:**	15.47°		
Line of sight versors	**V:**	0.812	**N:**	-0.156	**E:**	-0.563

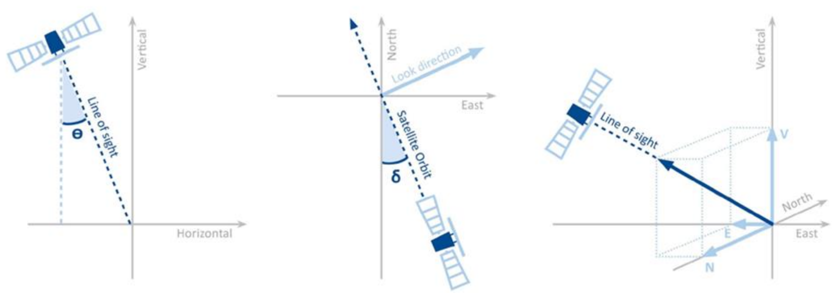

Figure 19: Example of metadata associated to the SqueeSAR measurements. LOS angles and versos can be used to transform a 3-D measurement (D_{VERT}, D_{EW} and D_{NS}) onto a LOS measurement (D_{LO}).

Appendix 3: Average Time Series over Lonquist Areas of Interest

ATS (vertical and east-west) plots for the Lonquist areas of interest (Figure 20).

- Vertical (black): Negative displacement rates indicate subsidence and positive displacement rates indicate uplift.
- East-West (red): Negative displacement rates indicate westward movement and positive displacement rate indicate eastward movement.

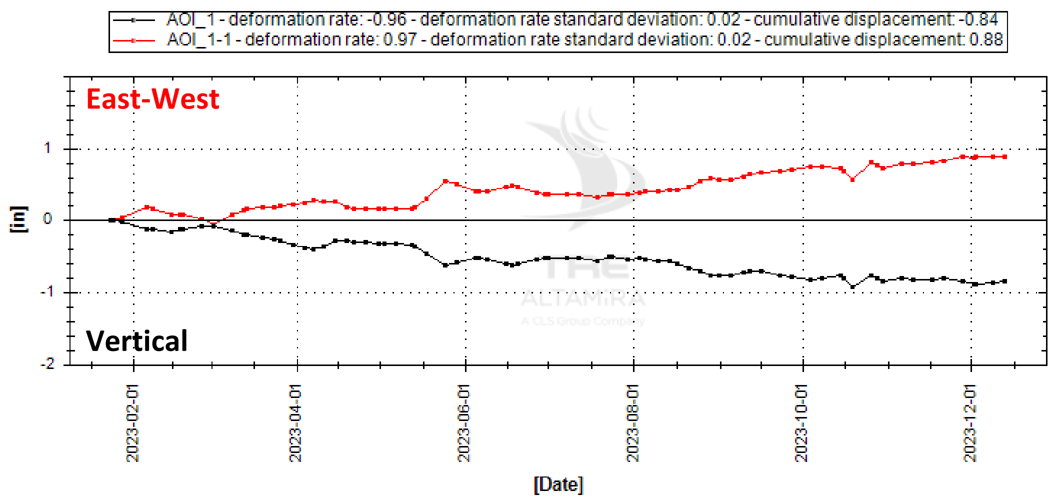

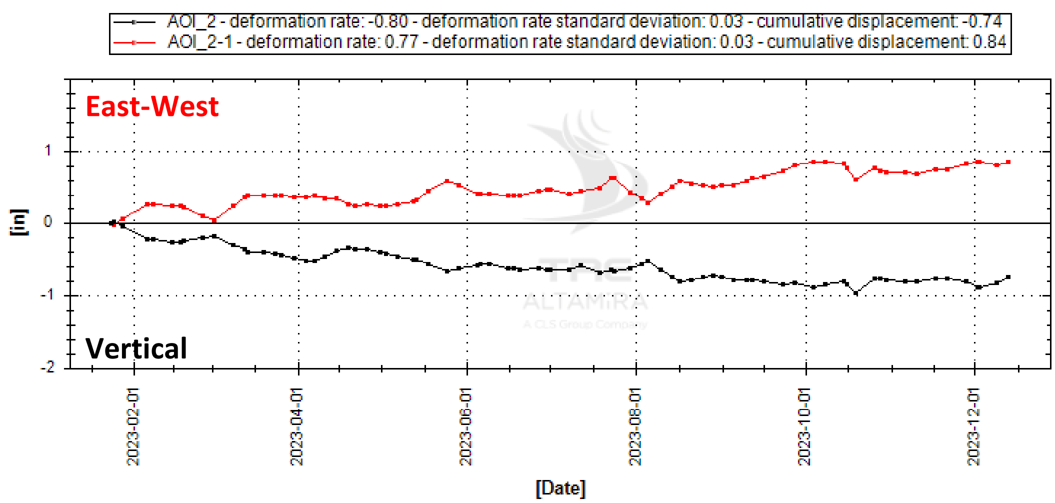

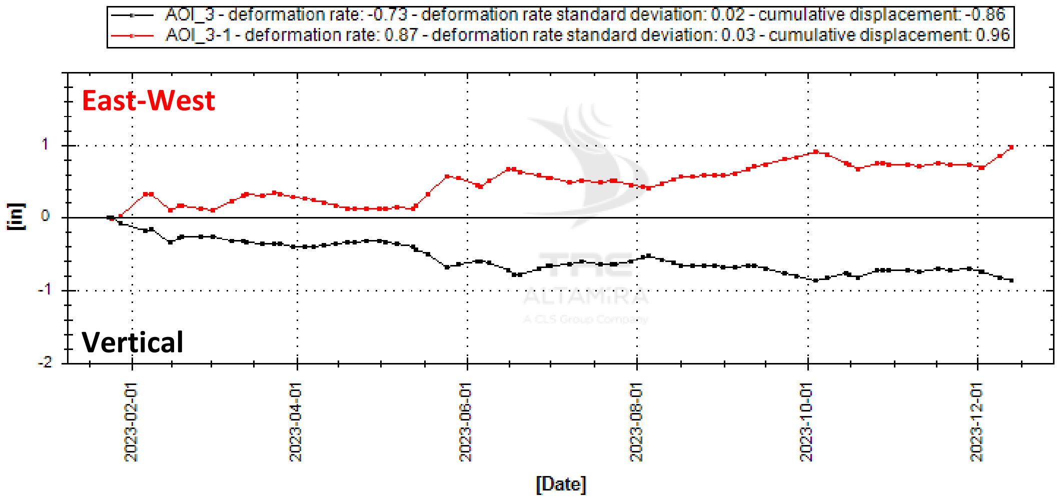
AOI_3 - deformation rate: -0.73 - deformation rate standard deviation: 0.02 - cumulative displacement: -0.86
AOI_3-1 - deformation rate: 0.87 - deformation rate standard deviation: 0.03 - cumulative displacement: 0.96
East-West
Vertical
[in]
[Date]

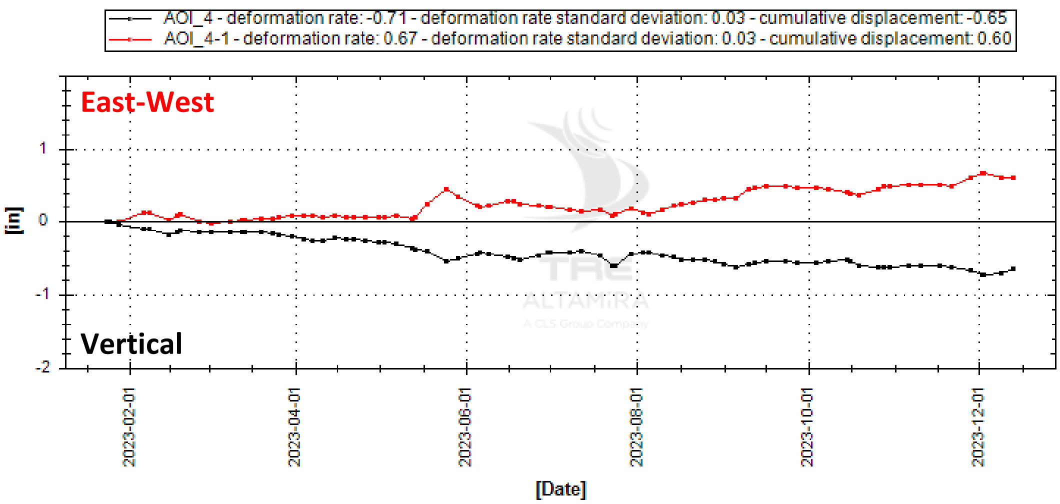
AOI_4 - deformation rate: -0.71 - deformation rate standard deviation: 0.03 - cumulative displacement: -0.65
AOI_4-1 - deformation rate: 0.67 - deformation rate standard deviation: 0.03 - cumulative displacement: 0.60
East-West
Vertical
[in]
[Date]

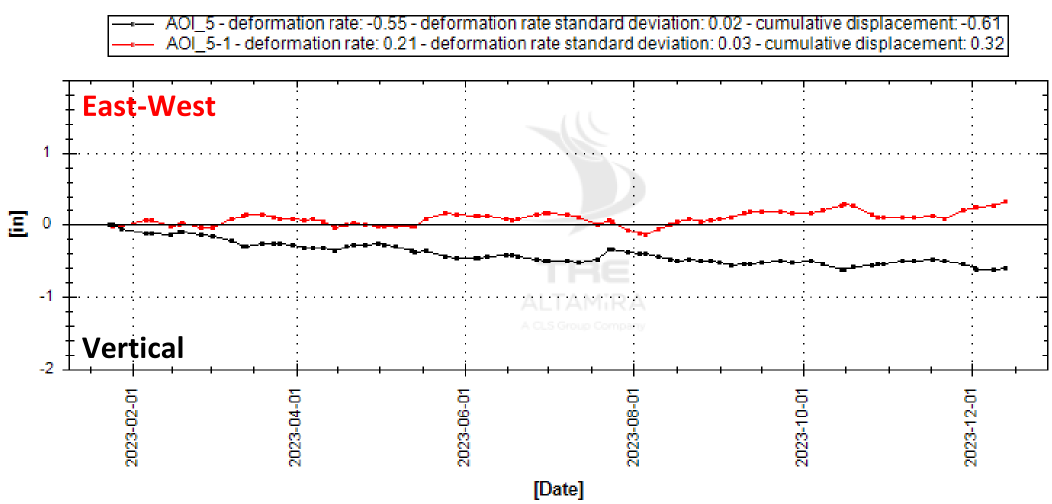
AOI_5 - deformation rate: -0.55 - deformation rate standard deviation: 0.02 - cumulative displacement: -0.61
AOI_5-1 - deformation rate: 0.21 - deformation rate standard deviation: 0.03 - cumulative displacement: 0.32
East-West
Vertical
[in]
[Date]

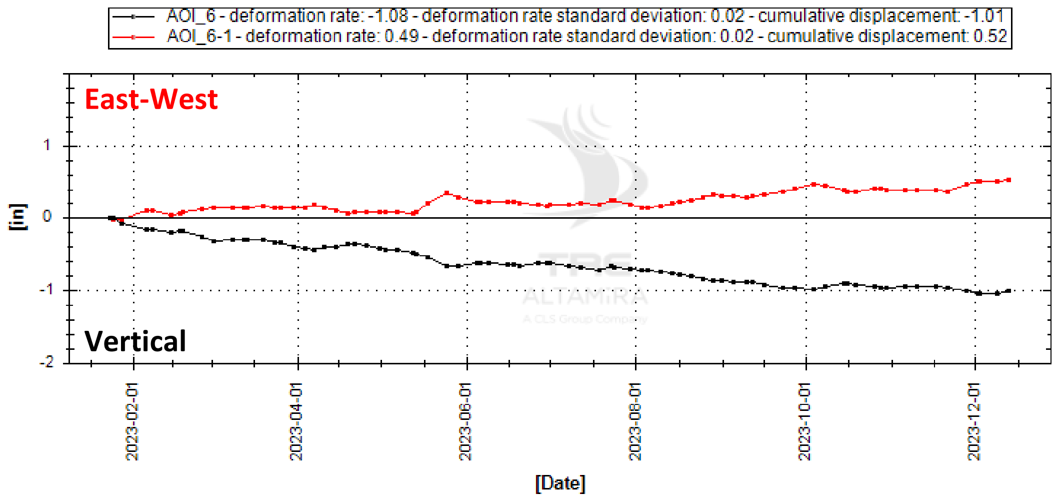
AOI_6 - deformation rate: -1.08 - deformation rate standard deviation: 0.02 - cumulative displacement: -1.01
AOI_6-1 - deformation rate: 0.49 - deformation rate standard deviation: 0.02 - cumulative displacement: 0.52
East-West
Vertical
[in]
1
0
-1
-2
2023-02-01
2023-04-01
2023-06-01
2023-08-01
2023-10-01
2023-12-01
[Date]

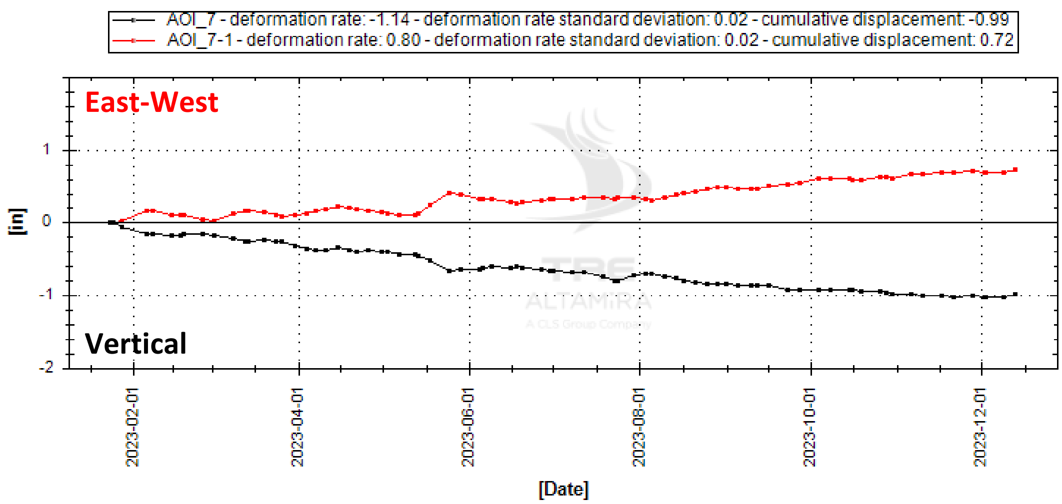
AOI_7 - deformation rate: -1.14 - deformation rate standard deviation: 0.02 - cumulative displacement: -0.99
AOI_7-1 - deformation rate: 0.80 - deformation rate standard deviation: 0.02 - cumulative displacement: 0.72
East-West
Vertical
[in]
1
0
-1
-2
2023-02-01
2023-04-01
2023-06-01
2023-08-01
2023-10-01
2023-12-01
[Date]

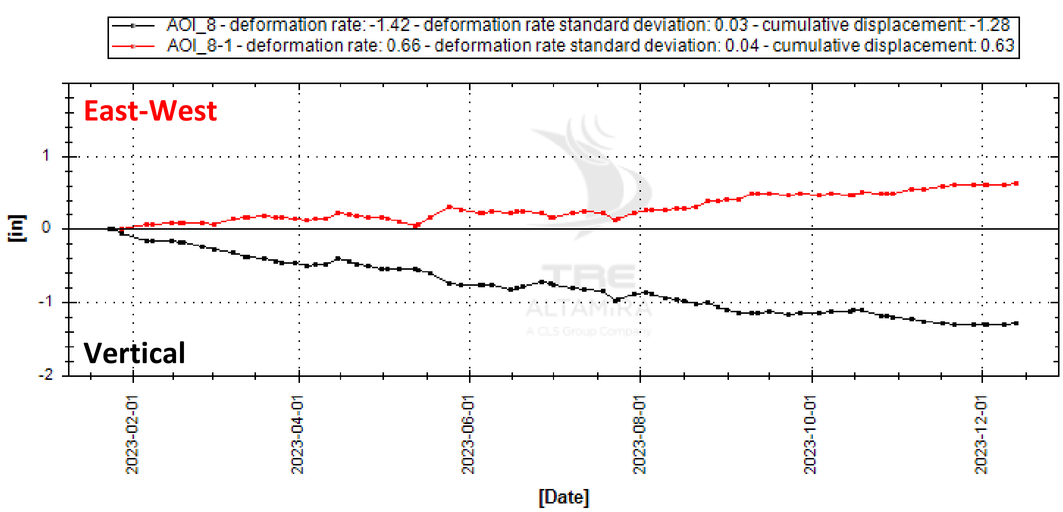
AOI_8 - deformation rate: -1.42 - deformation rate standard deviation: 0.03 - cumulative displacement: -1.28
AOI_8-1 - deformation rate: 0.66 - deformation rate standard deviation: 0.04 - cumulative displacement: 0.63
East-West
Vertical
[in]
1
0
-1
-2
2023-02-01
2023-04-01
2023-06-01
2023-08-01
2023-10-01
2023-12-01
[Date]

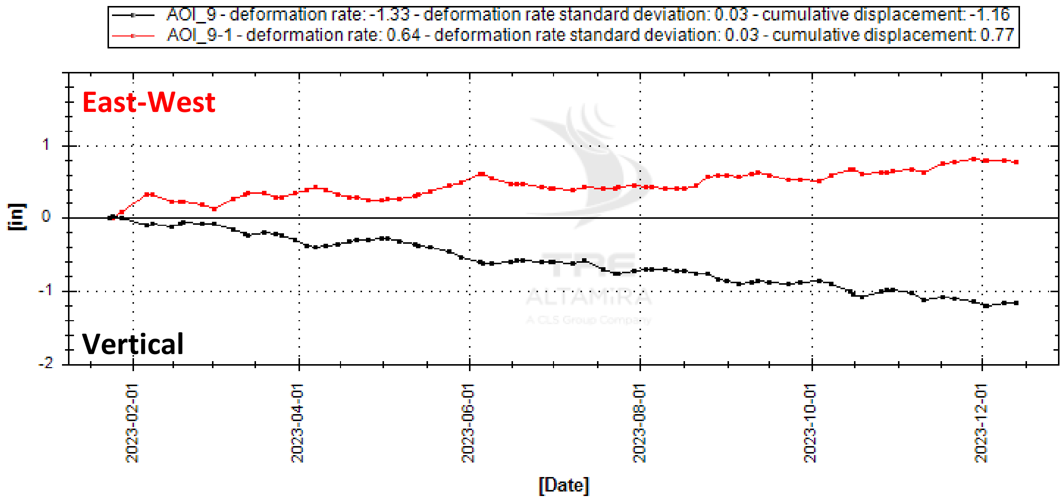
AOI_9 - deformation rate: -1.33 - deformation rate standard deviation: 0.03 - cumulative displacement: -1.16
AOI_9-1 - deformation rate: 0.64 - deformation rate standard deviation: 0.03 - cumulative displacement: 0.77
East-West
Vertical
[in]
[Date]

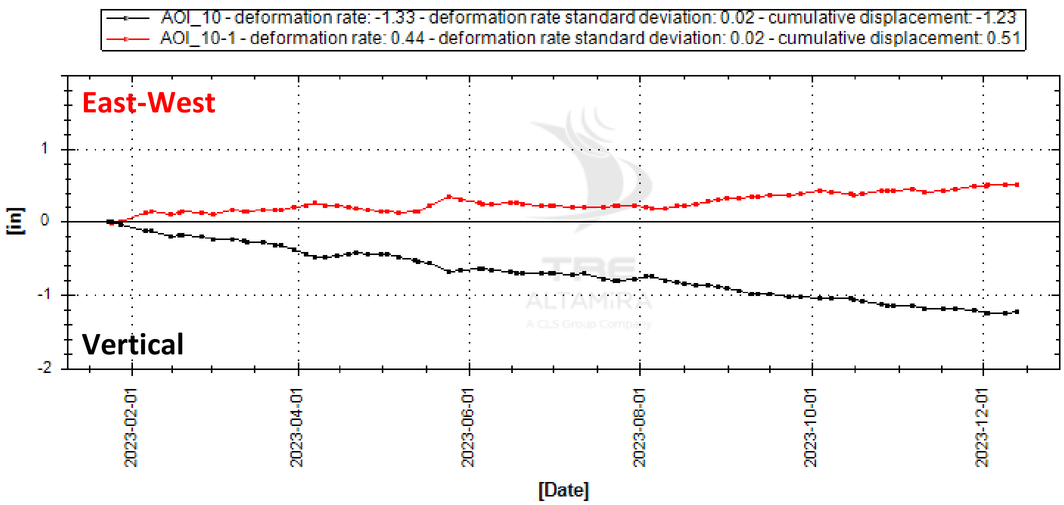
AOI_10 - deformation rate: -1.33 - deformation rate standard deviation: 0.02 - cumulative displacement: -1.23
AOI_10-1 - deformation rate: 0.44 - deformation rate standard deviation: 0.02 - cumulative displacement: 0.51
East-West
Vertical
[in]
[Date]

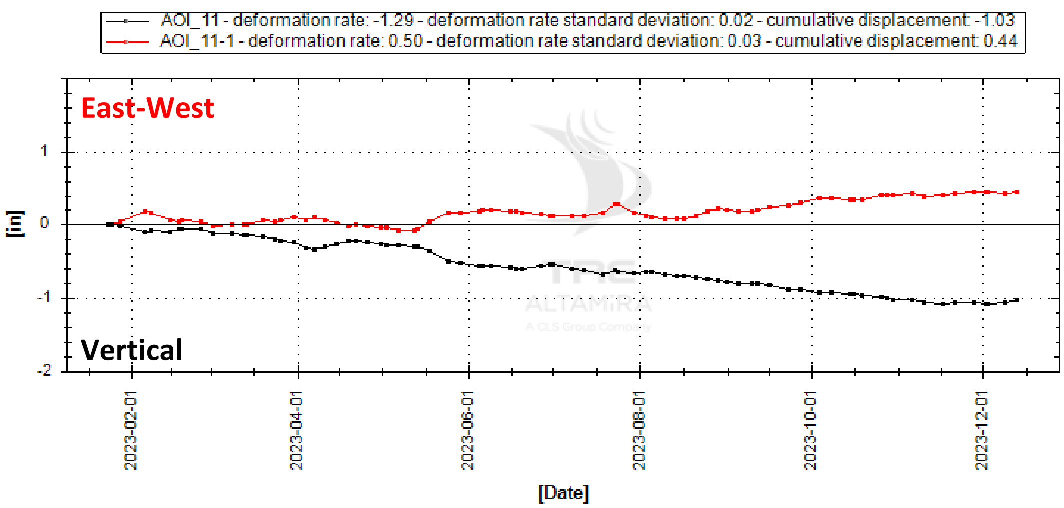
AOI_11 - deformation rate: -1.29 - deformation rate standard deviation: 0.02 - cumulative displacement: -1.03
AOI_11-1 - deformation rate: 0.50 - deformation rate standard deviation: 0.03 - cumulative displacement: 0.44
East-West
Vertical
[in]
[Date]

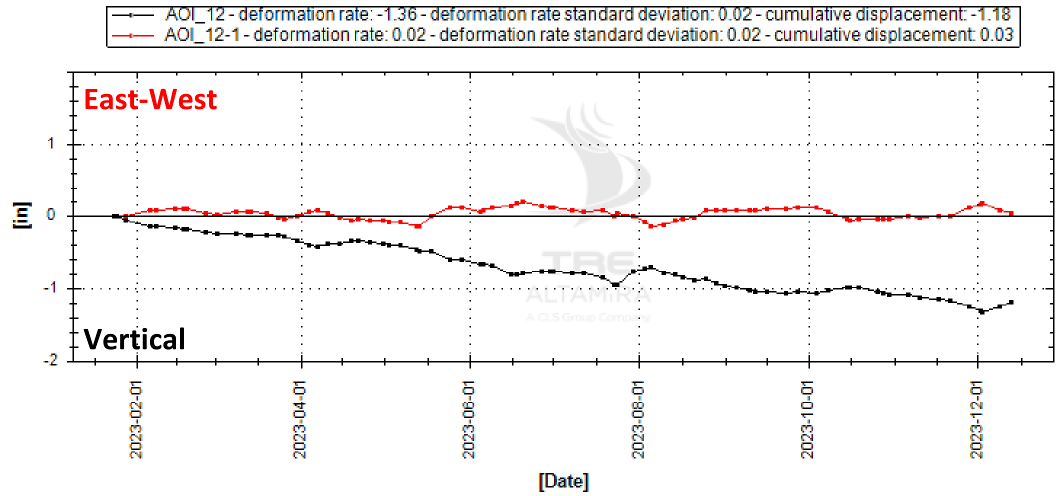
AOI_12 - deformation rate: -1.36 - deformation rate standard deviation: 0.02 - cumulative displacement: -1.18
AOI_12-1 - deformation rate: 0.02 - deformation rate standard deviation: 0.02 - cumulative displacement: 0.03
East-West
Vertical
[in]
1
0
-1
-2
2023-02-01
2023-04-01
2023-06-01
2023-08-01
2023-10-01
2023-12-01
[Date]

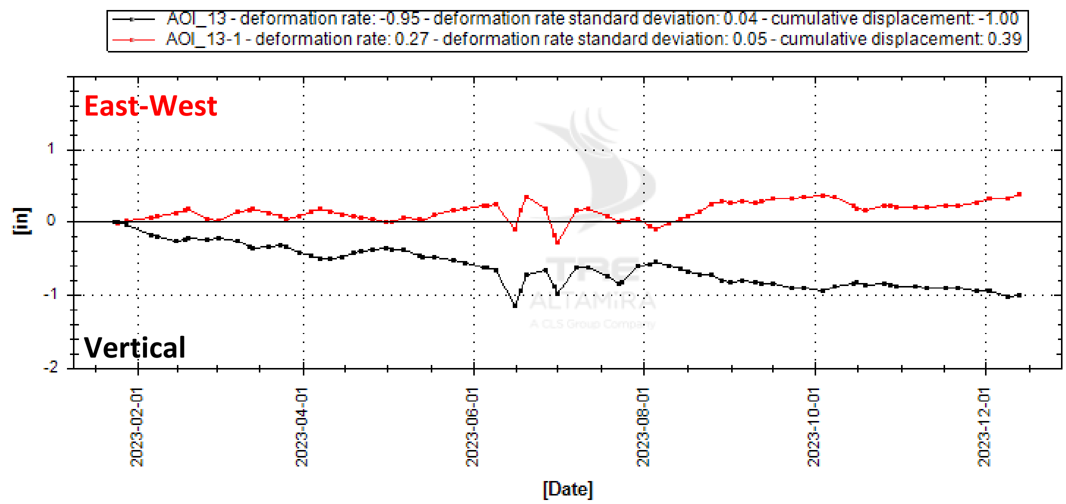
AOI_13 - deformation rate: -0.95 - deformation rate standard deviation: 0.04 - cumulative displacement: -1.00
AOI_13-1 - deformation rate: 0.27 - deformation rate standard deviation: 0.05 - cumulative displacement: 0.39
East-West
Vertical
[in]
1
0
-1
-2
2023-02-01
2023-04-01
2023-06-01
2023-08-01
2023-10-01
2023-12-01
[Date]

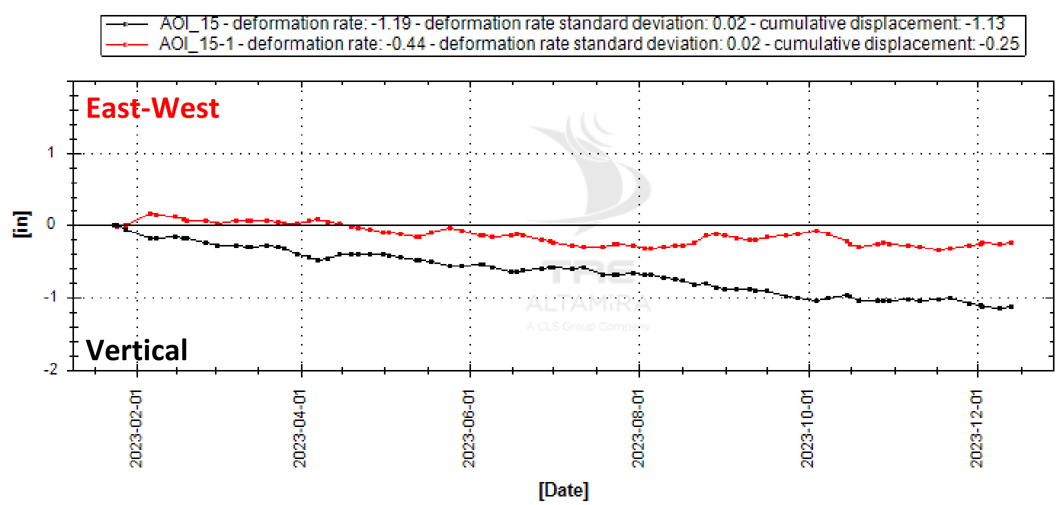
AOI_15 - deformation rate: -1.19 - deformation rate standard deviation: 0.02 - cumulative displacement: -1.13
AOI_15-1 - deformation rate: -0.44 - deformation rate standard deviation: 0.02 - cumulative displacement: -0.25
East-West
Vertical
[in]
1
0
-1
-2
2023-02-01
2023-04-01
2023-06-01
2023-08-01
2023-10-01
2023-12-01
[Date]

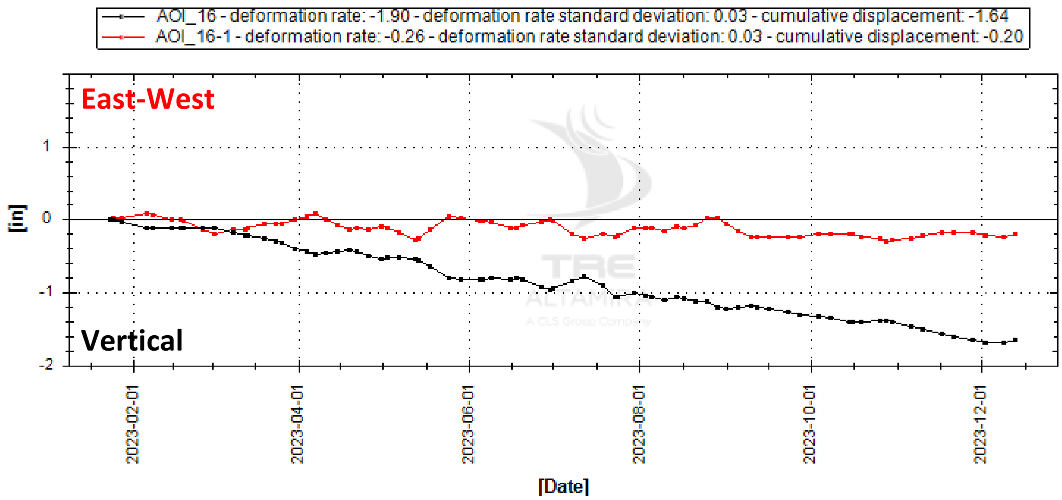
AOI_16 - deformation rate: -1.90 - deformation rate standard deviation: 0.03 - cumulative displacement: -1.64
AOI_16-1 - deformation rate: -0.26 - deformation rate standard deviation: 0.03 - cumulative displacement: -0.20
East-West
Vertical
[in]
[Date]
2023-02-01
2023-04-01
2023-06-01
2023-08-01
2023-10-01
2023-12-01

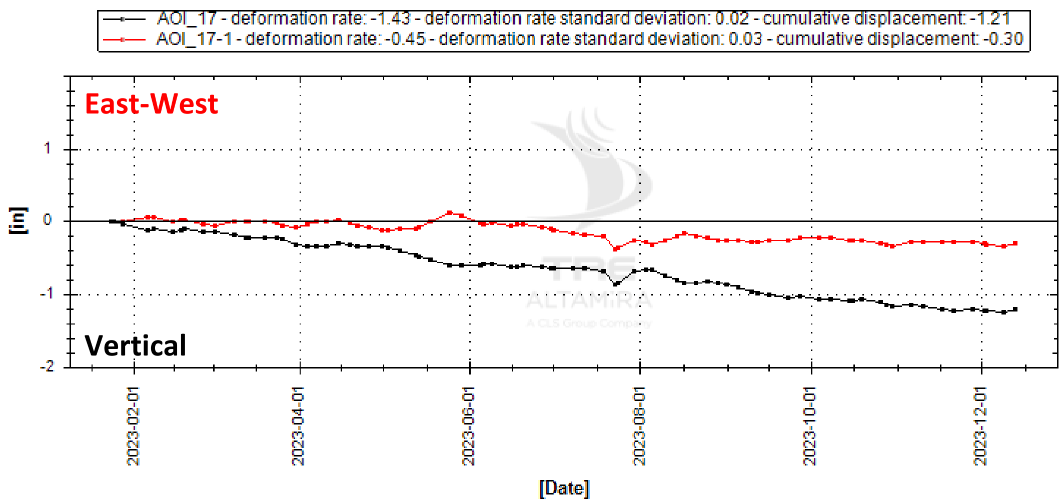
AOI_17 - deformation rate: -1.43 - deformation rate standard deviation: 0.02 - cumulative displacement: -1.21
AOI_17-1 - deformation rate: -0.45 - deformation rate standard deviation: 0.03 - cumulative displacement: -0.30
East-West
Vertical
[in]
[Date]
2023-02-01
2023-04-01
2023-06-01
2023-08-01
2023-10-01
2023-12-01

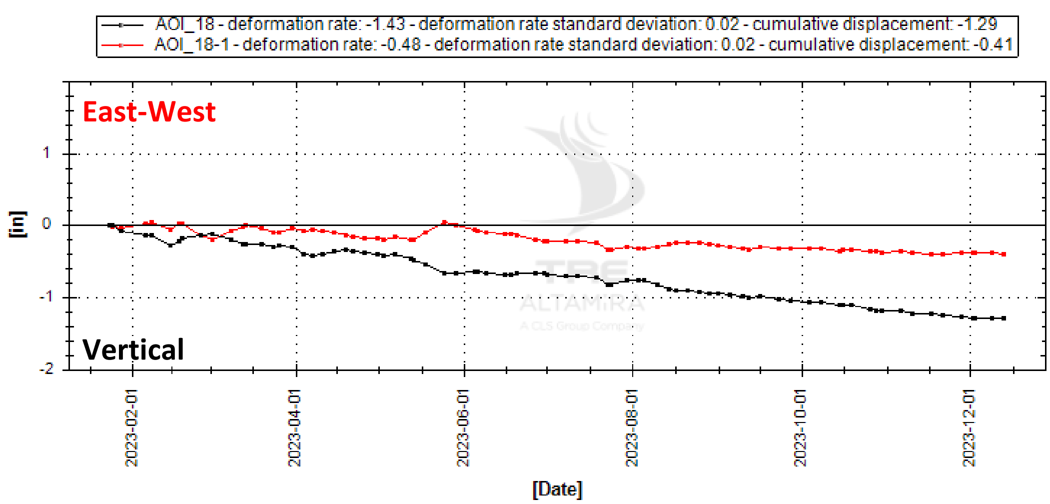
AOI_18 - deformation rate: -1.43 - deformation rate standard deviation: 0.02 - cumulative displacement: -1.29
AOI_18-1 - deformation rate: -0.48 - deformation rate standard deviation: 0.02 - cumulative displacement: -0.41
East-West
Vertical
[in]
[Date]
2023-02-01
2023-04-01
2023-06-01
2023-08-01
2023-10-01
2023-12-01

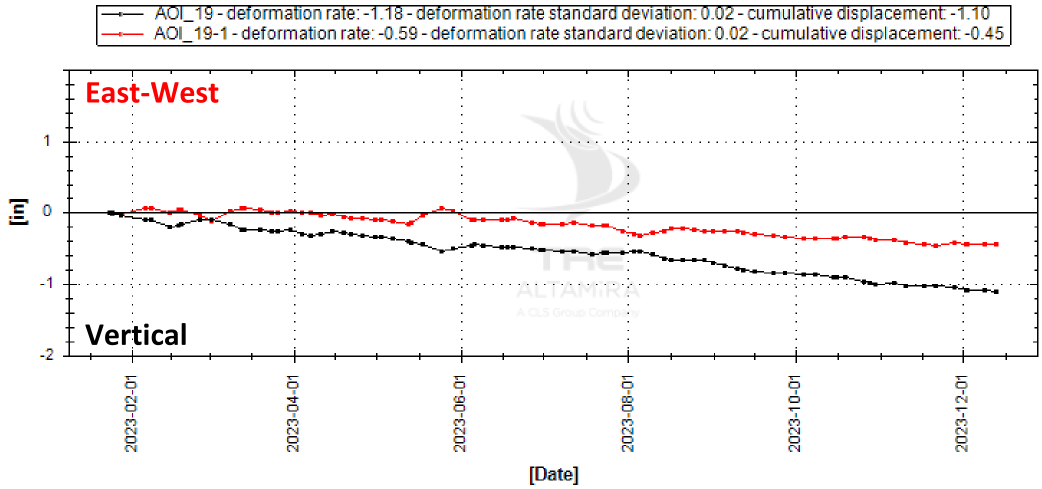

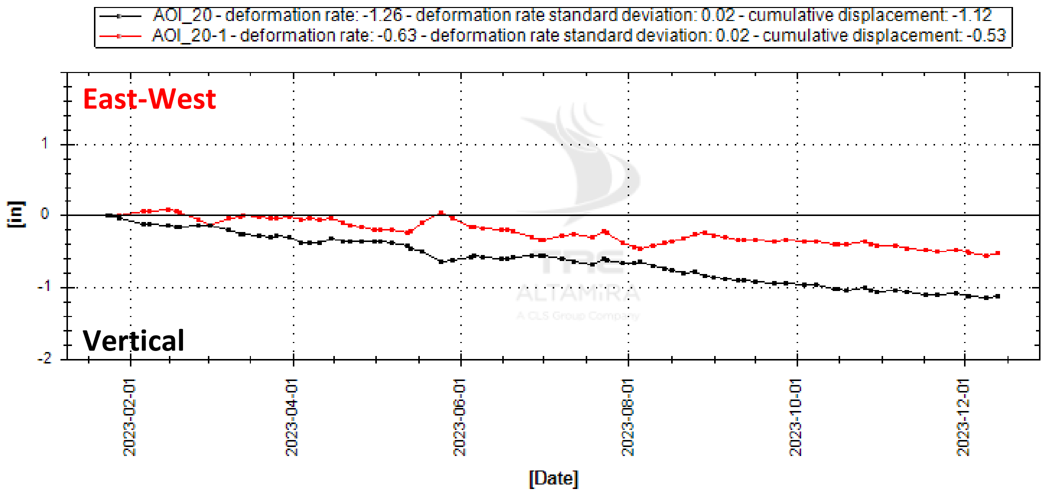

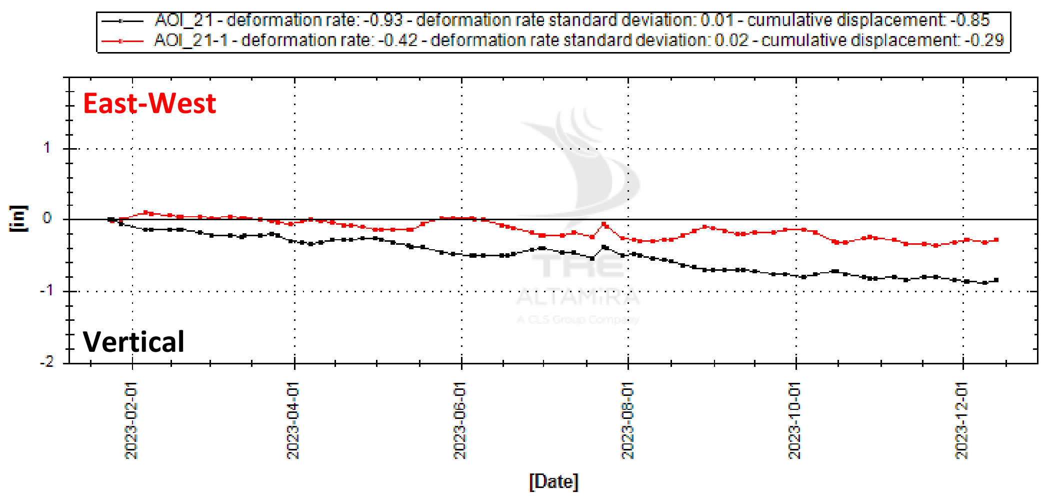

Figure 20: Average time series of the vertical and east-west displacement rates of all measurement points within Lonquist areas of interest.

TRE
ALTAMIRA
A CLS Group Company

TRE ALTAMIRA s.r.l.
Ripa di Porta Ticinese, 79
20143 Milan Italy
Tel: +39 02 4343 121

TRE ALTAMIRA S.L.U.
Carrer de Còrsega, 381-387
08037 Barcelona Spain
Tel.: +34 93 183 57 50

TRE ALTAMIRA Inc.
Suite 410, 475 West Georgia Street
Vancouver, BC V6B 4M9 Canada
Tel: +1 604 331 2512

tre-altamira.com